

Biophysical effects of cold atmospheric plasma on glial tumor cells



**Dissertation der Fakultät für Physik
der
Ludwig-Maximilians-Universität München**

Vorgelegt von Julia Köritzer

München, 2013

1. Gutachter: Prof. Dr. Dr. h. c. Gregor E. Morfill
2. Gutachter: Prof. Dr. Jürgen Schlegel

Datum mündliche Prüfung: 02.10.2013

Inhalt

A. Summary	6
B. Zusammenfassung	7
C. Introduction	9
1. Cold Atmospheric Plasma (CAP)	9
2. Plasma device used in this study	11
3. Plasma chemistry.....	14
3.1 Characteristics of the Plasma Device FlatPlaSter 2.0	17
4. Plasma Liquid Chemistry	18
5. State of the Art/ Tumor Treatment with CAP	19
6. Glioma	20
7. Glioblastoma	20
8. Epidemiology and histology	21
9. Treatment of glioblastoma.....	22
10. Therapy resistance	23
11. Objective.....	24
D. Materials and Methods	26
1. Technical devices.....	26
2. Chemicals, reagents and cytostatics	26
3. Software	28
4. Cell culture.....	28
4.1 Cell culture consumables and additives	28
4.2 Cell culture media.....	29
5. Buffers and solutions.....	29
6. Antibodies.....	30
7. Cultivation and cryopreservation of GBM cell lines	30
8. Primary cell culture	31
9. Cell authentication and Mycoplasma-test	31
10. Protein isolation	31
11. SDS-PAGE and Western blotting	32
12. Cell viability	32
13. Clonogenicity assay	33

14.	Flow cytometry.....	33
15.	Migration.....	34
16.	Organotypic slices cultures (OSCs).....	34
16.1	Cell implantation.....	34
17.	Immunohistochemistry of paraffin slides.....	34
18.	Statistical analysis.....	35
E.	Results.....	36
1.	Effects of CAP on liquids.....	36
1.1	CAP effects on medium.....	36
1.3	Treatment of glioma cells in minimized amounts of medium.....	37
2.	Effects of CAP on TMZ -resistant and -sensitive glioma cell lines.....	39
2.1	CAP treatment inhibits cell proliferation in MGMT positive and MGMT negative glioma cell lines.....	39
2.2	Induction of apoptosis is present to a minor extent after CAP treatment.....	41
2.3	Cytolysis is only induced by long CAP treatment durations.....	42
2.4	Strong induction of cell cycle arrest in MGMT positive and MGMT negative glioma cells by CAP treatment.....	43
2.5	Induction of cell cycle arrest by CAP application is a long lasting effect in glioma cells.....	44
2.6	CAP reduces the clonogenic potential of glioma cells.....	45
2.7	CAP application impairs migration of glioma cells.....	46
3.	Combined treatment with CAP and chemotherapy.....	49
3.1	Concomitant treatment with CAP and TMZ has a synergistic effect on cell viability in MGMT positive and MGMT negative cells.....	49
3.2	Combined therapy induces prolonged G2/ M phase cell cycle arrest.....	50
4.	CAP displays cell selectivity towards tumor cells.....	51
4.1	Cell cycle distribution in primary astrocytes.....	51
4.2	Treatment of LN18pEGFP in organotypic brain slice cultures.....	52
4.3	Staining for p-Cdc25c reveals activation of the ATM/ ATR signaling pathway by CAP application in OSCs.....	55
F.	Discussion.....	56
1.	Effects of CAP on liquids.....	57
2.	Effects of CAP on TMZ -resistant and -sensitive glioma cell lines.....	58
3.	Combined treatment with CAP and chemotherapy.....	60

4.	CAP displays cell selectivity towards tumor cells	61
G.	Assessment and Outlook	65
H.	Supplementary Data	68
I.	References	76
J.	Abbreviations	83
K.	List of publications	85

A. Summary

Cancer still is one of the medical nightmares of manhood, being one of the major causes of death across Europe in this decade. Despite intensive research and multimodal therapy strategies, comprehension of tumor development, behavior and treatment remains challenging.

Cold atmospheric plasma (CAP) offers a tool for both investigation of tumor behavior with regard to the role of radicals in tumor metabolism and in addition a possible therapeutic application in tumor treatment. Glioblastoma (GBM) is the most frequent brain tumor in adults and one of the most lethal and heterogeneous human cancers. Although advances in surgical resection, the use of radiotherapy and concomitant chemotherapy have led to improvements in median survival, few options exist for the management of recurrent or resistant tumor sub – populations of GBMs. In this work, the impact of CAP treatment on human glioma cell biology including proliferation, induction of apoptosis, cell cycle distribution, clonogenicity and migration was examined. CAP application effectively inhibited tumor cell growth, induced a strong cell cycle arrest in G2/ M phase and reduced clonogenicity and migration in chemosensitive and chemoresistant glioma cells in a dose dependent manner. CAP was able to restore the responsiveness of glioma cells with an unfavorable MGMT status towards treatment with the chemotherapeutic temozolomide (TMZ) and revealed synergistic effects. Long term investigation indicated a consistent effect of the CAP application seven days post - treatment. Thus, CAP might be a promising candidate for an intraoperative combination therapy especially for patients suffering from GBMs featuring an unfavorable MGMT status and TMZ resistance. In addition, selective activity of CAP application towards tumor cells was addressed. Murine primary astrocytes treated with CAP showed a delayed cell cycle arrest compared to treated tumor cells, indicating a possible ‘therapeutic window’. To overcome the disadvantages of the cell culture model, an organotypic brain slice culture (OSC) was established. OSCs enable the investigation of tumor treatment by CAP in its microenvironment and simultaneously the investigation of CAP effects on healthy, non-tumorous tissue. Immunohistological staining of the OSCs 14 days after CAP application indicate the activation of the ATM/ATR signaling pathway in tumor cells by CAP treatment. The kinase Cdc25c, a mediator of the G2/ M checkpoint mechanism triggered in response to DNA injury, was found to be activated via phosphorylation upon CAP treatment. This suggest that CAP modulates cell cycle checkpoint response by either inducing genotoxic stress or by creating high intracellular ROS levels leading to DNA damage.

The data of the present work demonstrate that CAP application could be a therapeutic option for glioma treatment in combination with chemotherapy especially in chemoresistant sub – populations. Preliminary data on cell selectivity suggest a selective activity of CAP application on glial tumor cells.

B. Zusammenfassung

Krebs ist immer noch eine der medizinischen Schrecken der Menschheit, da es sich hierbei um eine der häufigsten Todesursachen in Europa in diesem Jahrzehnt handelt. Trotz intensiver Forschung und multimodalen Therapieansätzen stellt das Verständnis der Tumorentstehung, des Tumorverhaltens und der Tumorbehandlung eine Herausforderung dar.

Kaltes atmosphärisches Plasma (KAP) ermöglicht sowohl die Untersuchung des Tumorverhaltens, hierbei insbesondere die Rolle von Radikalen auf den Tumormetabolismus, als auch den Einsatz als therapeutische Anwendung in der Tumorbehandlung. Das Glioblastom (GBM) ist der häufigste Hirntumor bei Erwachsenen und zudem einer der tödlichsten und heterogensten humanen Krebsarten. Obgleich Fortschritte bei der chirurgischen Entfernung des Tumors, dem Einsatz von Bestrahlung und gleichzeitiger Chemotherapie zu einer Verbesserung in der mittleren Überlebenszeit geführt haben, existieren nur wenige therapeutische Ansätze zur Behandlung von wiederkehrenden oder resistenten Tumor-Teilpopulationen des GBMs.

In dieser Arbeit wurde die Bedeutung der KAP-Behandlung auf die Zellbiologie von humanen Gliomen am Beispiel der Auswirkung auf das Proliferationsverhalten, der Induktion von Apoptose, der Zellzyklus Verteilung, der Klonogenizität und des Migrationsverhalten, untersucht. Die KAP-Anwendung konnte effektive das Wachstum der Tumorzellen stoppen, induzierte einen Zellzyklusarrest in der G2/ M Phase und reduzierte die klonogene Kapazität und Migration in chemosensitiven wie auch in chemoresistenten Gliomzellen in einer dosisabhängigen Weise. Zudem konnte KAP die Sensitivität von Gliomazellen mit einem ungünstigen MGMT Status auf eine Behandlung mit dem Chemotherapeutikum Temozolomide (TMZ) wieder herstellen und wies dabei synergistische Effekte auf. Langzeituntersuchungen zeigten einen anhaltenden Effekt der KAP-Anwendung auch nach sieben Tagen. Daher könnte KAP, speziell bei Patienten die an einem GBM mit ungünstigem MGMT Status und einer TMZ-Resistenz leiden, ein erfolgsversprechender Therapieansatz sein. Zusätzlich wurde die selektive Wirksamkeit der KAP-Anwendung auf Tumorzellen untersucht. Murine primäre Astrozyten zeigten eine verzögerte Zellzyklus-Unterbrechung im Vergleich zu behandelten Tumorzellen, was auf ein mögliches „therapeutisches Fenster“ hindeutet. Um die Nachteile eines Zellkultur-Modells zu umgehen, wurden organotypische Kulturen aus Hirnschnitten (OHK) etabliert. OHKs ermöglichen die Untersuchung der KAP-Wirkung einerseits auf den Tumor innerhalb seines Mikromilieus, als auch zugleich auf gesundes, nicht tumorhaftes Gewebe. Immunhistologische Färbungen 14 Tage nach der KAP-Behandlung weisen auf eine Aktivierung des ATM/ ATR Signalweges durch die KAP-Behandlung hin. Die Cdc25c Kinase, eine Vermittlerin des G2/ M Phase Checkpoints die durch DNA Schädigung ausgelöst wird, wurde per Phosphorylierung nach der KAP-Anwendung aktiviert. Dieser Umstand lässt vermuten, dass KAP den Zellzyklus Checkpoint entweder über die Produktion von genotoxischem Stress oder durch die Induktion

eines hohen intrazellulären ROS Spiegels, welcher dann wiederum zu DNA Schäden führt, reguliert.

Die Resultate der hier präsentierten Arbeit zeigen, dass die KAP-Anwendung in Kombination mit Chemotherapie eine therapeutische Option in der Behandlung von Gliomen besonders mit chemoresistenten Teilpopulationen wäre. Vorläufige Daten zur Zellselektivität lassen eine selektive Wirkung der KAP-Behandlung auf gliale Tumorzellen vermuten.

C. Introduction

1. Cold Atmospheric Plasma (CAP)

The fourth fundamental state of matter is named plasma as others being solid, liquid and gas. Sir William Crookes, an English physicist, first described in 1879 what we know today as plasma. In 1929, the term “plasma” was first applied to ionized gas by Dr. Irving Langmuir, an American chemist and physicist [1]. Ionization includes that at least one electron is not bound to an atom or molecule, respectively converting the atoms or molecules into positively charged ions. The plasma state is the most abundant state of all observable matter in our universe. Examples are the sun and the stellar wind. On earth this state of matter can be observed as lightning or as the aurora borealis. Plasma is defined as an ionized gas that contains equal number of negative and positive charged particles, it is quasi-neutral. Neutral particles may well be present. The relative number of ions and atoms (the ratio of density of major charged species to that of neutral gas, $n_i = n_a$) is called the degree of ionization. Both natural and artificially generated plasmas are quasi-neutral, which means that concentrations of positively charged particles (positive ions) and negatively charged particles (electrons and negative ions) are well balanced. The ionization energy, or ionization potential, is typically specified in electron volts (eV) and refers to the energy required to remove a single electron from a single atom or molecule. Usually very high temperatures and high energy input are needed for ionization. Plasma is referred to as being "hot" since at least the electron temperature is high. Sometimes the term "cold plasma" is used when the temperatures of the present ions and neutrals are much lower than the electron temperature, i. e. the particles in the plasma are not in a thermal equilibrium.

Numerous plasmas exist far from the thermodynamic equilibrium and are characterized by multiple temperatures related to different plasma particles and diverse degrees of freedom. It is the electron temperature T_e that often significantly exceeds the temperature of heavy particles T_0 ($T_e \gg T_0$). Ionization and chemical processes in such non-equilibrium plasmas are mainly determined by the electron distribution function, therefore are not as sensitive to thermal processes and temperature of the gas. Plasma in a non-equilibrium state is usually called non-thermal plasma. An example of non-thermal plasma in nature is the aurora borealis. In many non-thermal plasma systems, electron temperature is in order of several eV (1 eV equals to 11,600 K), whereas the temperature of neutrals and ions is close to room temperature. Non-thermal plasmas are usually generated either at low pressures or at lower power levels compared to thermal plasmas, or in different kinds of pulsed discharge systems. The Surface Micro-Discharge (SMD) device used in this study is producing cold, non-thermal plasma at atmospheric pressure by short intervals (in the range of 100 ns) of plasma ignition resulting in only partial ionization of the ambient air. Thereby, electrons are energized and reach temperatures of a few eV while simultaneously the ion temperature remains at room

temperature. The overall temperature of the system does not exceed room temperature since the ionization degree is at its maximum 10^{-7} . Another possibility of reducing the temperature of the plasma system (but not of the electrons) would be to dilute the “hot” plasma components by inducing a gas flow. This was realized for the MicroPlaSter – a microwave driven cold atmospheric plasma device - where a cold argon gas flow leads to a decrease of the temperature of the whole system. The density of the electrons and the ions are quasi neutral

($n_e = n_i; 10^{10} - 10^{11} \text{ cm}^{-3}$) at a bright spot of the electrode.

In a simplified scheme a plasma device is composed of two electrodes, inserted into a chamber, which is filled with air or various other gases. By applying electrical power between two electrodes and increasing of the applied voltage, the current suddenly increases at a certain voltage required for sufficiently intensive electron cascades. If the pressure is low, lower than of the order of a few 100 Pa, a glow discharge develops. This presents a low-current, high-voltage discharge widely used to generate non-thermal plasma. Such glow discharges are used for several semiconductor fabrication processes, such as etching, ashing, deposition.

Cascades of electrons are produced first due to their low mass and high mobility. Subsequently, electrons transmit their energy to all other plasma components, providing energy for ionization, excitation, dissociation, and other plasma-chemical processes (figure 1). Emission of light and heating are by-products of the plasma generation process. The rates of such processes strongly depend on power input and the used gas composition and can often be far from the equilibrium distribution. Chemically active plasmas exhibit multi-component systems that are highly reactive due to large concentrations of charged particles (electrons, negative and positive ions), excited atoms and molecules, reactive species, and UV photons.

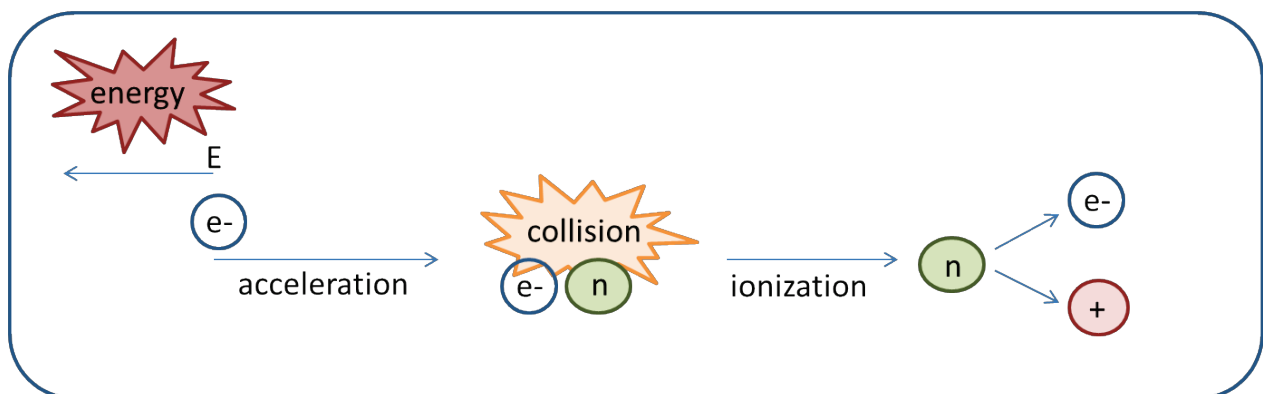


Figure 1: Plasma ignition. Model of plasma production including acceleration of electrons, excitation (with light emission) and dissociation of atoms (after collision with accelerated electrons). Heating which is a by-product is not displayed.

Examples of artificially generated plasmas in application are plasma display panels, fluorescent lamps and component analysis using inductively coupled plasmas together with optical emission spectroscopy and mass spectrometry. Most plasmas of practical significance, however, have electron temperatures of 1 – 10 eV, with electron densities in the range 10^8 – 10^{13} cm⁻³. This high electron temperature gives high reactivity in the system while the whole system can be kept at low temperature.

2. Plasma device used in this study

Currently, several CAP devices with various designations are in use. In general, CAPs relevant for biomedical applications can be classified into three groups of plasma due to their characteristics: direct, indirect and ‘hybrid’ plasma.

Table 1: Characteristics of different atmospheric low temperature plasmas relevant for biomedical applications (modified after Heinlin et al. 2010 [2])

	Direct plasmas	Indirect plasmas	‘Hybrid’ plasmas
<i>Plasma sources</i>	Floating electrode dielectric barrier discharge (FE-DBD)	Plasma jet, plasma bullet, plasma gun, plasma needle, plasma torch (i.e. MicroPlaSter)	Surface micro discharge (SMD), barrier coronal discharges
<i>Mode of production and properties</i>	The sample to be treated functions as the second electrode, current flows through the sample	Plasma is produced in between two electrodes and transported to the sample via gas flow	The mode of production of direct plasmas is coupled with properties of indirect plasmas: ‘Hybrid’ plasmas contain a grounded electrode - i.e. here the sample does not function as the second electrode
<i>Gas</i>	Air	Noble gas/air	Air
<i>Distance between device and treated sample</i>	~ mm	~ mm - cm	~ mm
<i>UV radiation</i>	Relatively weak	Relatively high	Relatively weak
<i>Plasma density on the sample</i>	high	Low (strongly depends on the distance)	Low (strongly depends on the distance)

<i>Site of production of reactive species</i>	RONS are produced in the plasma	RONS are produced by mixing plasma and gas/air	RONS are produced in the plasma
<i>Produced plasma species</i>	Charged particles ↑ Short life time species ↑ Long life time species ↑	Charged particles ↓ Short life time species → Long life time species ↑	Charged particles → Short life time species → Long life time species ↑

Charged particles (i. e. O_2^+ , N_2^+ , Ar^+ , He^+), short life time species (i. e. NO, O, OH) and long life time species (i. e. O_3 , NO_2 , N_2O) are categorized as ↑ dominant, → relatively high and ↓ relatively low

External parameters such as voltage, frequency, surrounding conditions, as well as the distance between the CAP electrode and the biological sample, the treatment time and the carrier gas influence the CAP chemistry and therefore change the composition and concentration of plasma species that reach the sample.

Using a direct plasma device, the samples (skin, cells, etc.) act as a counter electrode and the plasma discharge is produced between the electrode and the sample. A typical example is the Floating Electrode Dielectric Barrier Discharge (FE-DBD) developed and tested by Fridman [3], [4]. Since the plasma is produced just above the sample, the plasma density as well as the density of reactive species is high. Often the ambient air is used for the plasma production and the UV emission is rather low. Fridman and colleagues demonstrated bactericidal properties by membrane lipid peroxidation in *E. coli* [5], as well as blood coagulation [6] and induction of apoptosis in melanoma cells [7] using a FE-DBD.

Devices of indirect plasma contain two electrodes for the plasma production. The plasma created is transported via gas flow to the sample. Often noble gas, e. g. helium or argon, is required as a carrier gas for plasma production. The reactive species are produced by mixing with the ambient air. Several devices with this technology are available from small 'plasma needles' [8], [9] and 'plasma jets' [10], [11], [12] to larger 'plasma torches' [13], [14].

As already mentioned in chapter 1 the FlatPlaSter 2.0 used for the experiments in this study is based on the Surface Micro Discharge (SMD) technology developed and described by Morfill et al. [14]. This device is classified as 'hybrid plasma' due to the combined features of indirect and direct plasmas. The FlatPlaSter 2.0 is a further development of the FlatPlaSter 1, which is a SMD device without housing, thus operating in an open volume. A main characteristic of this technique is relatively high density of reactive species produced by the plasma. In addition, the electrical current does not flow through the sample.

This SMD electrode itself is integrated into a plastic box containing a lid to facilitate a closed volume (figure 2B and C). The size of the housing was manufactured to fit a 96-well - plate, therefore making *in vitro* studies simple. The respective samples to be treated can be located below the electrode and the distance between the electrode and the sample can be adjusted to different heights. The SMD electrode itself is composed of a Teflon plate (insulator of 0.5 mm in thickness) which is sandwiched by a planar metal plate (brass sheet electrode of 1 mm thickness) and a stainless steel mesh grid (6 mesh inch⁻¹) (figure 2A).

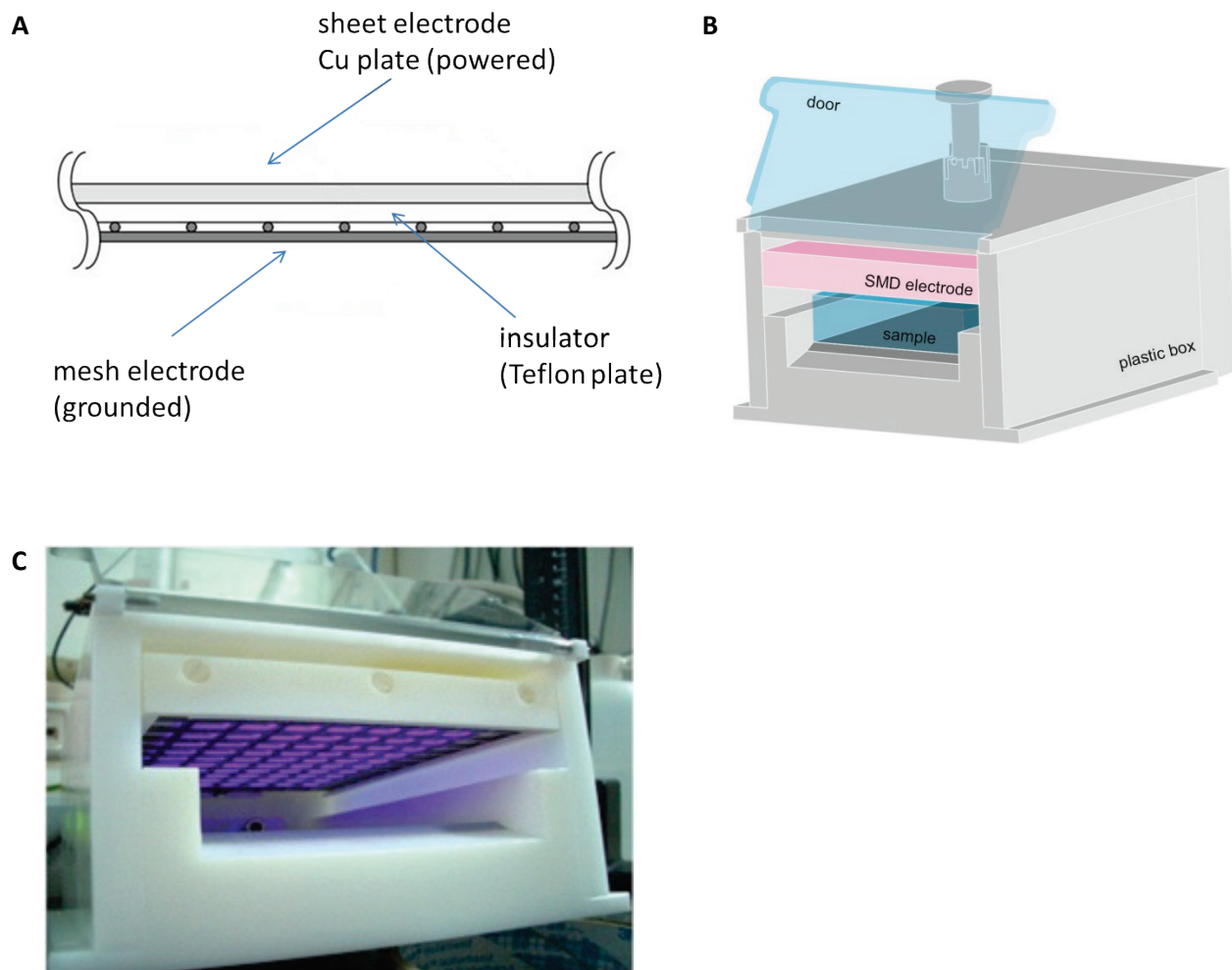


Figure 2: **A** Sketch of the surface micro-discharge electrode (Morfill et al., 2009) and **B** with housing (drawing by T. Shimizu). **C** SMD FlatPlaSter 2.0 during plasma production with an opened lid. Emission of blue light is visible.

By applying high sinusoidal voltage of 8.5 kV_{pp} with a frequency of 10 kHz, micro-discharges are generated homogeneously across the stainless steel mesh grid, thereby initiating a cascade of chemical reactions in the surrounding air. The produced species reach the sample mainly by

diffusion, as no airstream or gas jet was applied. The power consumption for the plasma discharge is 20 mW/ cm^2 and was measured with the Lissajous method using a $0.1 \text{ }\mu\text{F}$ capacitance [15]. For the treatment times used in this study, the temperature increase was measured to 4 degrees above the ambient temperature at maximum. The main ultraviolet (UV) components emitted by the device are in the wavelength range between 280 and 400 nm, corresponding to the N_2 second positive system. Furthermore, negligible intensities of UVC light emission are detected. The UV power density was measured to be 25 nW/ cm^2 . Concerning the production of reactive species of the device mean values of approximately 500 ppm for O_3 , <1 ppm for NO and 3 ppm for NO_2 were measured at the end of the application.

3. Plasma chemistry

Simulations using computational modeling aim to predict distributions of neutral reactive species in plasma at relatively low power density ($< 0.1 \text{ W/ cm}^2$). The model contains more than 600 chemical reactions for the analysis of the plasma discharge.

Table 2: Chemical components included in the modulation (Y. Sakiyama et al., 2012 [16])

Positively charged particles	$\text{N}^+, \text{N}_2^+, \text{N}_3^+, \text{N}_4^+, \text{O}^+, \text{O}_2^+, \text{O}_4^+, \text{NO}^+, \text{N}_2\text{O}^+, \text{NO}_2^+, \text{H}^+, \text{H}_2^+, \text{H}_3^+, \text{OH}^+, \text{H}_2\text{O}^+, \text{H}_3\text{O}^+$
Negatively charged particles	$\text{e}, \text{O}^-, \text{O}_2^-, \text{O}_3^-, \text{O}_4^-, \text{NO}^-, \text{N}_2\text{O}^-, \text{NO}_2^-, \text{NO}_3^-, \text{H}^-, \text{OH}^-$
Neutral species	
Group (a)	$\text{N}(^2D), \text{N}_2(A^3\Sigma), \text{N}_2(B^3\Pi), \text{O}(^1D), \text{H}$
Group (b)	$\text{N}, \text{O}, \text{O}_2(a^1\Delta), \text{O}_3, \text{NO}, \text{N}_2\text{O}, \text{NO}_2, \text{NO}_3, \text{N}_2\text{O}_3, \text{N}_2\text{O}_4, \text{N}_2\text{O}_5, \text{H}_2, \text{OH}, \text{HO}_2, \text{H}_2\text{O}_2, \text{HNO}, \text{HNO}_2, \text{HNO}_3, \text{N}_2, \text{O}_2, \text{H}_2\text{O}$

In this modulation a SMD device similar to the FlatPlaSter 2.0 described in chapter 2 was modeled as two coupled zero-dimensional models with a discharge layer and an afterglow region [16]. The applied voltage frequency equalled 10 kHz, the power density in the discharge layer was 0.05 W/ cm^{-2} and the distance between the discharge layer and the treated surface was 10 mm. The system was assumed to be closed processing a gas temperature of 300 K, i. e. the plasma gas was confined in a closed volume. The lifetime of the produced charged particles ($< 100 \text{ }\mu\text{s}$) is relatively short since the plasma discharge consists of numerous micro discharges

whose duration is typically ~ 100 ns. The neutral species in the reactive mix are classified into short-lived species which are confined to the discharge layer and long-lived species which diffuse into the afterglow region. Considering all possible reactions, including electron excitation, ionization, dissociation, recombination, attachment and detachment, charge transfer, ion recombination and reactions between neutrals, the air plasma and most of its chemical components revert back to their original state after a short time period of seconds to minutes.

The modulation showed that most charged particles are quenched within a single cycle (100 μ s), except NO_2^+ and NO_3^- which possess relatively long lifetimes. Neutral species are dominant over charged particles. The most abundant species is O_3 , with roughly 90% being delivered in the afterglow by diffusion from the discharge layer, whereas 10% of O_3 is locally generated by reactions between O, O_2 and a third body. Highly reactive neutral species (N, O, OH, NO, O_2 and HO_2) are mainly confined in the discharge layer (around 1 ppm), whereas they are rarely available in the afterglow region (less than 0.01 ppm), indicating a quenching of these species in the discharge layer [16].

Time dependent ozone generation of the SMD device for different power consumptions (ranging from 9.5×10^{-4} W/ cm^2 to 2.6 W/ cm^2) was measured using UV absorption spectroscopy at 254 nm in a closed volume. The UV light, emitted by an argon/ mercury lamp, was passing through the two diaphragms and collected by an optical fiber. The measurements indicated that the ozone density increased monotonically within the first tens of seconds and reached a steady state afterwards for input power lower than 0.1 W/ cm^2 . At higher input power (> 0.1 W/ cm^2) the average ozone density dropped within 10 seconds after plasma ignition [17](figure **3A** and **B**).

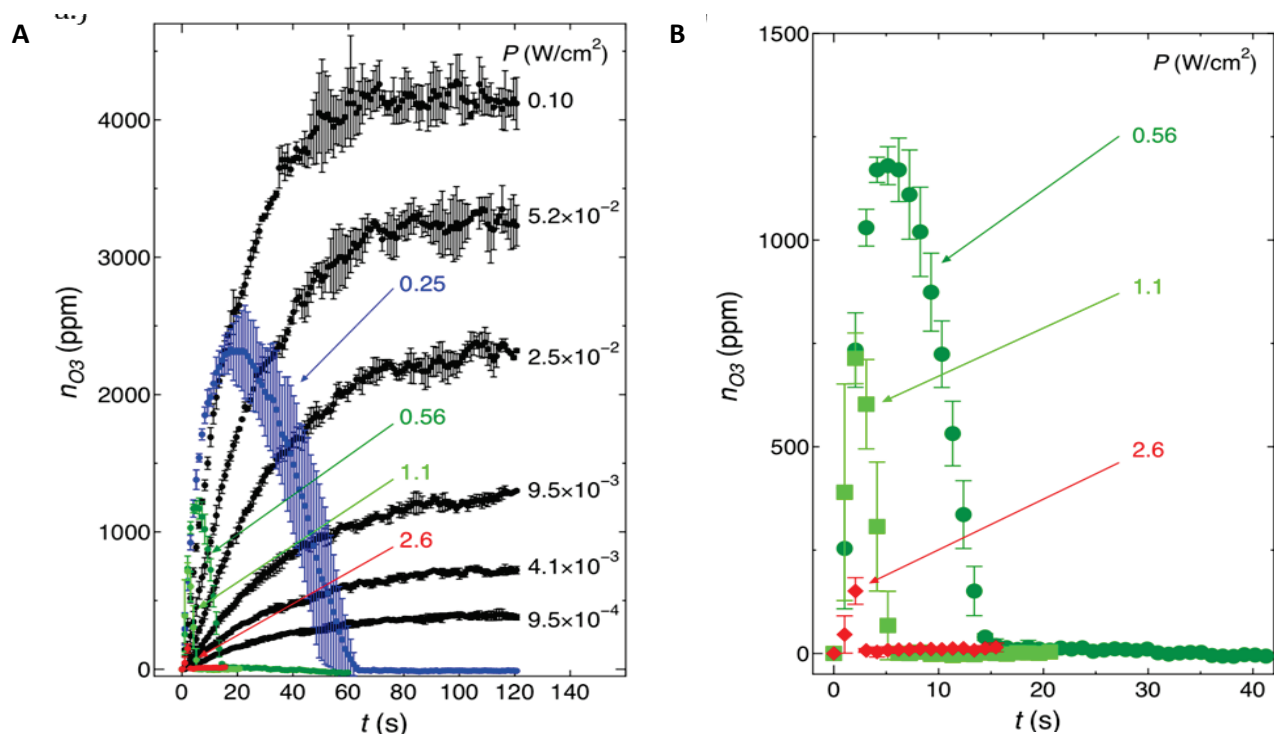


Figure 3: Time dependent ozone production of the SMD device in air. A Time evolution of the ozone density (n_{O_3}) produced by the SMD electrode (in a confined volume of 5 cm³) for different power consumptions measured with UV absorption spectroscopy at 254 nm [17]. **B** Time evolution of the ozone density with power consumptions of 0.56 W/cm² and higher. The applied voltage was 15 kVpp. (The graphs were taken from Shimizu et al., 2012).

Model calculations suggest that the observed ozone depletion at higher power densities is caused by quenching reaction with nitrogen oxides [16]. They are in turn created by vibrational excited nitrogen molecules reacting with O atoms. This mode transition from predominately ozone (generated at low power consumptions) to nitrogen oxides (produced at high power consumptions) displays how SMD plasma can be selected to favor either oxygen or nitrogen based chemistry by changing the external parameters.

Further characteristics of SMD plasmas were estimated in collaboration with the Chemical and Biomolecular Engineering Faculty of the University of Berkeley. Fourier transformation infrared spectroscopy (FTIR) measurements of a SMD electrode with a power consumption of 0.3 W/cm² identified species such as N₂O, NO₂ and HNO₃ (figure 4A). Obviously, the experimental set up influences the produced plasma chemistry of the SMD electrode, i. e. a thin film of liquid gives a reduced decline rate of O₃ (figure 4B).

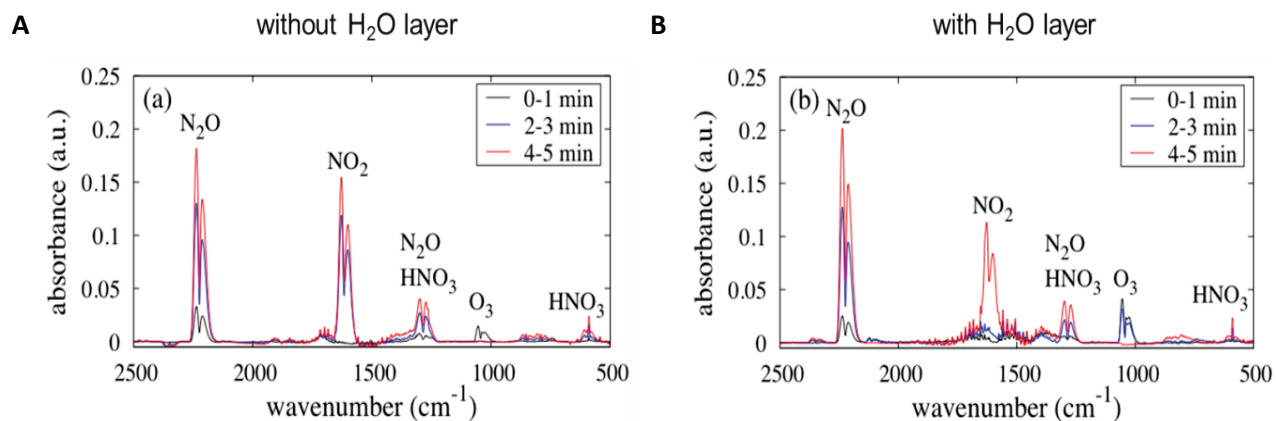


Figure 4: Liquid phase chemistry of the SMD changes with power. **A** IR absorption spectrum of the plasma gas (power consumption 0.3 W/ cm^2) in the absence of H_2O and **B** in the presence of a H_2O layer (manuscript in preparation by Shimizu et al.).

3.1 Characteristics of the Plasma Device FlatPlaSter 2.0

As described in chapter 2 the used plasma device FlatPlaSter 2.0 is operated at a power consumption of 20 mW/ cm^2 – i.e. in the low power mode - predominantly producing reactive oxygen species (ROS). Detailed measurements confirmed this revealed mean values of approximately 500 ppm for O_3 , <1 ppm for NO and 3 ppm for NO_2 at the end of the application. The temperature increase for the treatment times applied in this study was measured to 4 degrees above the ambient temperature at maximum. Main UV components emitted by the device are in the wavelength range between 280 and 400 nm and correspond to the N_2 second positive system (figure 5). Furthermore, negligible intensities of UVC light emission can be detected. The UV power density was measured to be 25 nW/ cm^2 .

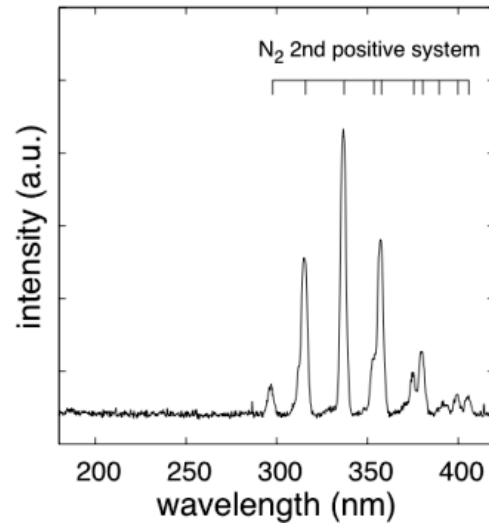


Figure 5: Optical emission spectroscopy in the low power mode in air. No emission of UVC light, only low dose emission of UVB and UVA light could be detected (manuscript in preparation by Shimizu et al.).

Which species reach the sample and therefore induce the specific effects of the SMD device depends on the input power, the treatment time and the distance between the electrode and the sample.

4. Plasma Liquid Chemistry

As the studies carried out within this thesis mainly include the analysis of eukaryotic cells covered by a thin liquid film, it is mandatory to also understand the chemistry/ composition of CAP - induced species in liquids following CAP treatment.

Pavlovich and colleagues therefore measured the key chemical species in CAP treated aqueous buffer (PBS) using a SMD device similar to the FlatPlaSter 2.0 [18]. The results revealed that the aqueous chemistry corresponds to the air plasma chemistry – i.e. a transition from the ozone mode to the nitrogen mode can be observed as the discharge power density increases (figure 6 **A** and **B**).

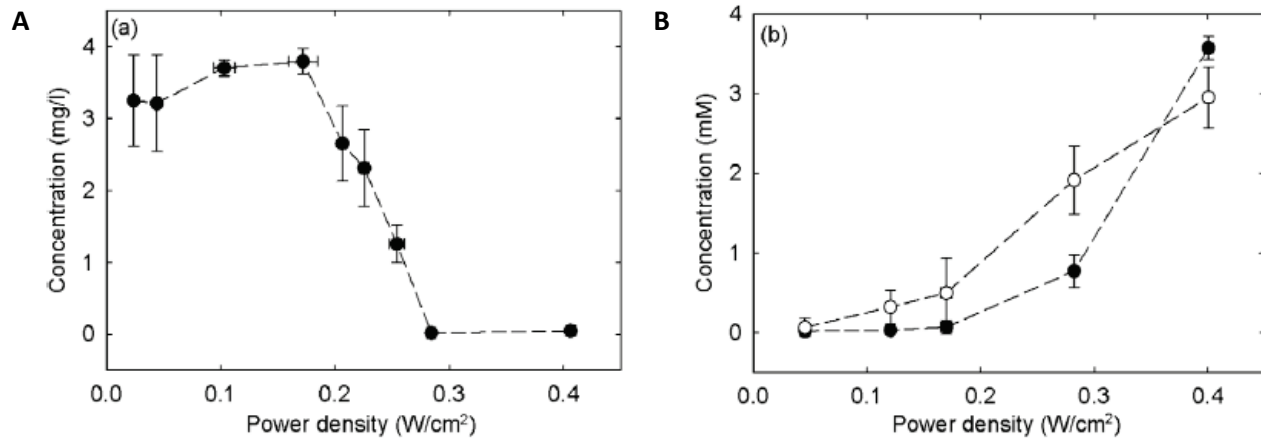


Figure 6: Liquid phase chemistry of the SMD changes with power density. Measurement of ozone (A) and nitrate/nitrite (B) present at different power densities (Pavlovich et al., 2013).

5. State of the Art/ Tumor Treatment with CAP

A new research field was established in the 1980s when plasma medicine emerged. Since then, several developed CAP sources have proven to successfully inactivate bacteria, fungi, viruses and spores in a dose-dependent manner [14], [19], [20], [21], [22]. First therapeutic approaches in plasma medicine were established in dermatology [23], [24] and wound disinfection [25], [2]. Different plasma devices, ranging from plasma jets driven with argon gas to devices using the biological sample as a second electrode, were investigated in medical science and also showed anti-cancer properties. Clearly, a comparison of the diverse devices is difficult, as the experimental setting as well as the used cells vary. A rough overview of the development in cancer application of CAP is given as followed.

In 2009 first results investigating the effects of different CAPs on cancer cells *in vitro* were published [26], [27]. Advanced publications addressing cancers of breast, brain, colon, lung, skin and pancreas followed. The main focus in these studies was set on the analysis of growth inhibition [28], [29], the inhibition of migration and invasion [30], the induction of cell cycle arrest [31], [32] and the induction of apoptosis in a dose dependent manner [33], [34], [35], [36], [37], [38], [39]. Recent experiments on melanoma verified the induction of apoptosis with high CAP treatment times, whereas low treatment times were able to induce senescence [40]. Successful treatment with CAP of cancers of melanoma and bladder *in vivo* were achieved by Keidar et al. [35]. In addition, a subcutaneous model of glioma using U87MG cells was CAP treated. Here, a reduced tumor size after CAP treatment conducted by induction of apoptosis and cell cycle arrest was demonstrated [41], [31]. The latest publications on tumor treatment with CAP revealed synergistic effects in a combined therapy with gemcitabine chemotherapy *in*

vivo in the case of pancreas carcinoma [42] as well as both *in vitro* and *in vivo* efficacy for tumor ablation in a murine neuroblastoma model [43].

6. Glioma

Gliomas encompass all brain tumors arising from glial cells. They are classified according to their histopathology into astrocytomas (referring to astrocytes), oligodendrogliomas (referring to oligodendrocytes), oligoastrocytomas (mixed gliomas, contains several types of glial cells) and ependymomas (referring to ependymal cells). Astrocytomas are the most common brain tumors in adults, accounting for more than 75% of gliomas [44]. The world health organization (WHO) grading of CNS tumors established a malignancy scale based on histologic features, i.e. infiltration of surrounding tissue, genetic markers of the tumor and disease progression, defining four different categories of astrocytomas: grade I is assigned to the more circumscribed pilocytic astrocytoma, whereas diffusely infiltrative astrocytic tumors with cytological atypia are defined as grade II (diffuse astrocytoma). Those also showing anaplasia and mitotic activity are defined as grade III (anaplastic astrocytoma), and tumors additionally showing microvascular proliferation and necrosis as WHO grade IV [45]. Glioblastomas, but also embryonal neoplasms and gliosarcomas are examples of grade IV neoplasms. Patients suffering from glioblastoma, particularly the elderly succumb to the disease within a short time, approximately within 15 months.

7. Glioblastoma

Glioblastoma (GBM) is the most common, aggressive and lethal brain tumor in adults. The incidence is 3 to 4 per 100,000 people in the United States and Europe. GBM accounts for 12% to 15% of all intracranial tumors and more than 50% of astrocytic tumors [44]. This deadly disease occurs more frequently in elderly, with a median age of 64 years at diagnosis [46]. The incidence rate of GBM cases is 1.6 fold higher in male than in female. Despite new insights into glioblastoma pathophysiology, the prognosis for patients diagnosed with this highly aggressive tumor remains unfavorable. Current treatment regimens combine surgical resection and radio- and chemotherapy, providing an increase in median overall survival of 14.6 months post-diagnosis [47]. The five – year survival rates are less than 5% for glioblastomas [44]. Despite intensive epidemiological studies risk factors for GBM remain unknown. To date, the only environmental risk factor linked to glioblastoma is the exposure to ionizing radiation, typically during radiation therapy. Several recent studies could not show a significant correlation between higher risk of glioblastoma and cell phone use or chemicals like polyvinyl chloride. Various rare genetic disorders as Li-Fraumeni syndrome and neurofibromatosis 1 and 2 are

associated with increased incidence of glial tumors. Besides these rare inherited syndromes, no familiar genetic susceptibility for malignant gliomas could be found [46].

8. Epidemiology and histology

Histopathologically, GBMs are heterogeneous, infiltrative and proliferative neoplasms showing neovascularization and necrosis within the tumor mass. Approximately 95% of all GBMs develop de novo (primary glioblastomas), while 5% emerge from WHO grade II or III astrocytomas (secondary glioblastomas) [48]. Regarding histology, primary and secondary GBMs can hardly be distinguished. Present studies suggest that both forms develop through different genetic alterations. Mutation of isocitrate dehydrogenase 1 and 2 (IDH1/ 2) is rare in primary GBMs (5 - 10%), while it is found frequently in secondary GBMs (> 80%). Genetic alterations that are prevalent in primary glioblastomas are loss of heterozygosity (LOH) 10p, epidermal growth factor receptor (EGFR) gene amplification and the phosphatase and tensin homolog (PTEN) mutations. TP53 mutations, LOH 19q and LOH 22q are prevalent in secondary GBMs, while LOH 10p and p16INK4a occur equally in primary and secondary neoplasms [49], [48]. At the present time the loss of 10p/19q is to be regarded as a prognostic rather than a predictive factor. Furthermore, the determination of the promoter methylation of the DNA repair enzyme O6-methylguanine-DNA methyltransferase (MGMT) has gained clinical importance and is the only established prognostic and predictive marker in GBM.

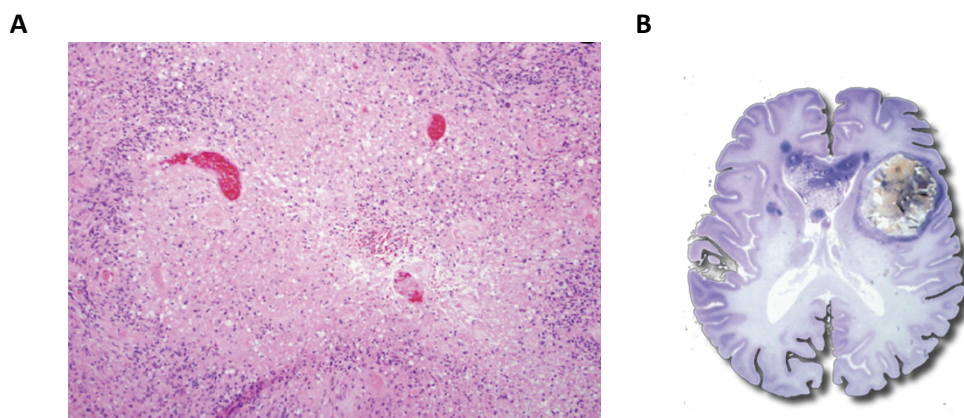


Figure 7: Histology of glioblastoma. **A** Hematoxylin-eosin staining of a glioblastoma showing necrosis and vascularization [50]. **B** Nissl stained axial brain-section feature a large necrotic area in the right cerebral hemisphere and vital Nissl-positive tumor cells infiltrating the surrounding brain tissue. Alterations in the left hemisphere are first evidence for a secondary tumor.

9. Treatment of glioblastoma

Standard therapy of GBMs includes complete resection or biopsy of the tumor followed, if feasible, by combined radio- and chemotherapy according to Stupp [51]. Despite this intensive therapy, relapse occurs regularly (figure 8). For the treatment of relapse resection followed by radio- or chemotherapy with Temozolomide (TMZ) is proposed. TMZ, a DNA alkylating agent, is the most successful anti-glioma drug and has added several months to the life expectancy of malignant glioma patients. However, for this reason glioblastoma care remains largely palliative.

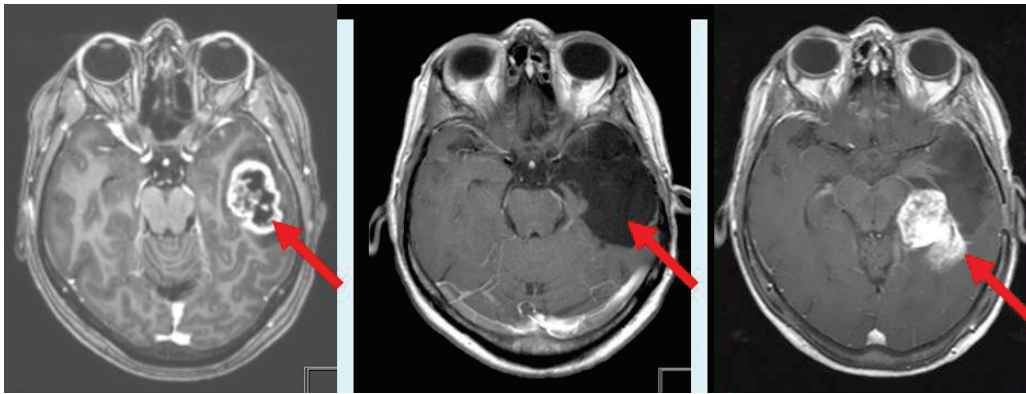


Figure 8: Magnetic resonance imaging (MRI) scans of a patient suffering from glioblastoma. Pre-operative (left), 10 months post-operative (middle) and recurrent one year after the surgery (right)(Neurosurgery department TUM, C. Zimmer, 2010).

TMZ is a pro-drug that undergoes spontaneous hydrolysis and is converted to the active metabolite 5-(3-methyl)-1-triazene-1-yl-imidazole-4-carboximide (MTIC) [52], [53]. TMZ is efficiently absorbed after oral administration, has a schedule-dependent antitumor activity and crosses the blood–brain barrier [54]. Conversion of TMZ to MTIC results in the formation of a reactive DNA-methylating agent, which is capable of transferring methyl groups to the N7 and O6 position of guanine and the O3 position of adenine. Formation of O6-methylguanine (O6-MG) is believed to initiate futile cycles of mismatch repair (MMR) and double strand breaks [55], [56]. Prolonged G2/ M arrest, cellular senescence or induction of apoptosis are possible results of O6-MG lesions [57].

10. Therapy resistance

The enzyme O6-methylguanine-DNA methyltransferase (MGMT) is capable of counteracting the cytotoxicity induced by chemotherapy [58], [59], [60] - thus tumors expressing high levels of MGMT (MGMT positive) are more resistant to alkylating agents than those in which the enzyme has become silenced by promoter methylation (MGMT negative). MGMT promoter methylation is associated with a favorable outcome and predicts a benefit from alkylating agent chemotherapy in patients with newly diagnosed glioblastoma [61], [62], [63], [64], [65] (figure 9).

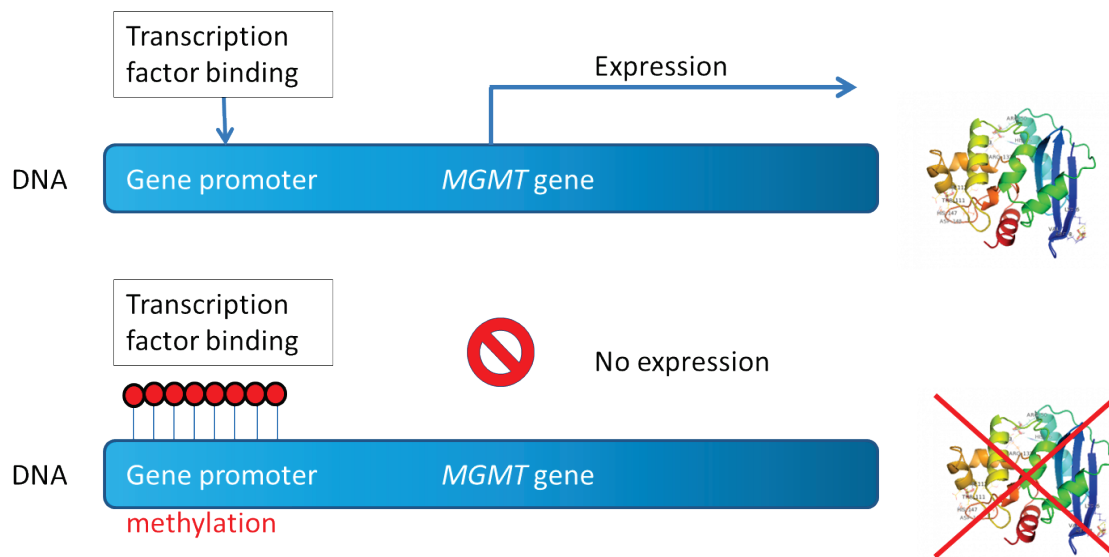


Figure 9: Promoter methylation of the *MGMT* gene suppresses protein expression. Model of MGMT promoter methylation resulting in the blockage of transcription factor binding to the promoter.

Hegi et al. demonstrated that in 45% of newly diagnosed glioblastoma patients with tumor promoter hypermethylation (and therefore MGMT gene silencing), TMZ was effective when administered concurrently or sequentially, with an improvement in median survival (21 versus 12 months) and 2-year survival (48% versus 10%) compared with patients with unmethylated tumor MGMT (figure 10) [62]. Nevertheless, there are patients profiting from TMZ treatment despite expression of MGMT as well as patients with an epigenetically silenced MGMT promoter showing no response to therapy with TMZ [62], [66].

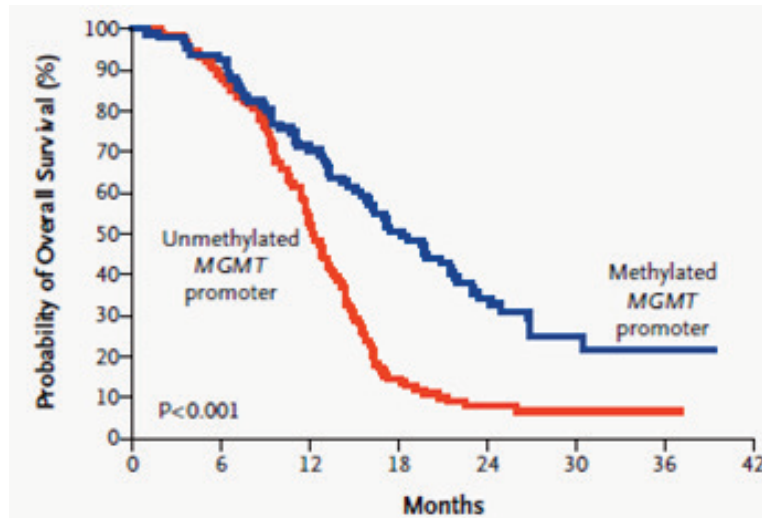


Figure 10: Patient overall survival according to *MGMT* promoter methylation status. Kaplan-Meier plot estimates the differences in survival and evaluates the prognostic value of *MGMT* promoter methylation status (Hegi et al., 2005).

Consequently, 55% of all newly diagnosed glioblastoma cases do not benefit from the addition of TMZ [67]. In addition, most tumors acquire resistance towards chemotherapy during treatment, accompanied by a change of the methylation status from methylated to unfavorable unmethylated *MGMT* [68], [69].

Further, a limitation to the established treatment protocol is the tumor's location within the brain. The resistance to therapy is largely a result of the considerable cellular and phenotypical heterogeneity that characterizes this particular tumor. The discovery of a subpopulation of cells exhibiting stem cell properties within the tumor bulk has profound implications for therapy. These so called brain tumor stem cells (bTSC) are thought to be responsible for the origin, maintenance and recurrence of glioblastomas [70], [71]. As a result, novel strategies are continually being established to improve patient prognosis, quality of life, and overall outcome.

11. Objective

Plasma medicine is an emerging research field that lately attracted a lot of interest. Cold atmospheric plasma (CAP) has proven its effectiveness in various medical applications such as sterilization of surgical instruments and wound disinfection. Recently, possible appliance of CAP in cancer treatment with modified devices aroused interest.

Despite intensive multimodal treatments including surgery, radiation and chemotherapy with temozolomide, the prognosis for patients suffering from glioblastoma remains poor. Especially

patients with an unmethylated MGMT promoter do not benefit from treatment with chemotherapy, making new treatment options a need.

The present investigation aimed to characterize the effects of CAP on human glioma cells. Cell growth, the induction of apoptosis, clonogenicity, migration and the cell cycle distribution were analyzed after CAP application. Special emphasis was placed on the effects of CAP on chemo-resistant glioma cells, as these cell populations are believed to give rise to the recurrent tumor. Thus, combined treatment of glioma cells with CAP and the chemotherapeutic TMZ *in vitro* was evaluated. A further aim of the present study was to analyze a possible selectivity of CAP towards tumor cells compared to non-tumorous cells. Therefore the cell cycle distribution of primary murine astrocytes after CAP application was compared to the cell cycle distribution of glioma cells after treatment. An orthotopic brain slice culture model for investigation of CAP application on tumor tissue and cell selective properties of CAP was established and preliminary data *ex vivo* on CAP effects in tissue were achieved.

D. Materials and Methods

1. Technical devices

Device	Model	Producer
Cell counter	Casy 1 [®]	SchärfeSystem, Reutlingen Germany
Centrifuges	5471R	Eppendorf AG, Hamburg, Germany
	4K15	Sigma, Deisenhofen, Germany
CO ₂ incubator	HERAcell [®]	Thermo Fisher Scientific Inc, Waltham, MA, USA
Electrophoresis cell	Mini-Protean [®] tetra cell	Bio-Rad Laboratories, Inc., Munich, Germany
Flow cytometer	FACS Calibur TM	Becton Dickinson GmbH, Heidelberg, Germany
Magnetic stirrer	RCT basic	IKA [®] -Werke GmbH & Co. KG, Staufen, Germany
Microplate reader	Asys Expert plus	Biochrom AG, Berlin, Germany
	Infinite F200 PRO	Tecan Group Ltd., Männedorf, Switzerland
Microscopes	Axiovert 25	Carl Zeiss AG, Jena, Germany
	Axiolmager Z.1	Carl Zeiss AG, Jena, Germany
	AxioObserver.A1	Carl Zeiss AG, Jena, Germany
	AxioCam ICm1	Carl Zeiss AG, Jena, Germany
	ApoTome	Carl Zeiss AG, Jena, Germany
	Eclipse TS100	Nikon, Düsseldorf, Germany
Microtome	Microm HM 355	Thermo Fisher Scientific Inc, Waltham, MA, USA
pH-meter	EL-30	Mettler-Toledo GmbH, Giessen, Germany
Power Supply	PowerPAC HC	Bio-Rad Laboratories, Inc., Munich, Germany
Semi-dry transfer cell	Trans-Blot [®] SD	Bio-Rad Laboratories, Inc., Munich, Germany
Shaker	Minishaker MS1	IKA [®] -Werke GmbH & Co. KG, Staufen, Germany
Spectrophotometer	NanoDrop TM 2000c	Thermo Fisher Scientific Inc, Waltham, MA, USA
Vibratom	VT 1200S	Leica GmbH, Wetzlar, Germany
Water bath	WD 14	Memmert GmbH, Schwabach, Germany
X-ray film processor	Konica SRX-101A	Konica Minolta GmbH, Langenhagen, Germany

2. Chemicals, reagents and cytostatics

Substances	Abbreviation	Producer
Acetic acid		Carl Roth GmbH + Co. KG, Karlsruhe, Germany
Agarose		Biozym Scientific GmbH, Hessisch Oldendorf, Germany
Amino-n-caprioic-acid		Sigma-Aldrich, Munich, Germany

Materials and Methods

Ammonium chlorid	NH ₄ Cl	Carl Roth GmbH + Co. KG, Karlsruhe, Germany
Ammoniumperoxosulphate	APS	Carl Roth GmbH + Co. KG, Karlsruhe, Germany
Bovineserumalbumin	BSA	Bio-Rad Laboratories, Munich, Germany
Bromphenol-blue		Sigma-Aldrich, Munich, Germany
Chemiluminescence detection film		GE Healthcare, Munich, Germany
Chemiluminescence HRP substrate	ECL	Millipore, Billerica, MA, USA
Diamidino-phenylindole	DAPI	Roche Diagnostics, Mannheim, Germany
Dimethylsulfoxide	DMSO	Carl Roth GmbH + Co. KG, Karlsruhe, Germany
Dithiothreitol	DTT	Sigma-Aldrich, Munich, Germany
Ethanol		Carl Roth GmbH + Co. KG, Karlsruhe, Germany
Ethidium bromide		Sigma-Aldrich, Munich, Germany
Formaldehyde		Carl Roth GmbH + Co. KG, Karlsruhe, Germany
Glycerol		Carl Roth GmbH + Co. KG, Karlsruhe, Germany
Hämatoxylin-Eosin	HE	Carl Roth GmbH + Co. KG, Karlsruhe, Germany
Hydrochloricacid	HCl	Carl Roth GmbH + Co. KG, Karlsruhe, Germany
Hydrogen peroxide	H ₂ O ₂	Carl Roth GmbH + Co. KG, Karlsruhe, Germany
Isopropanol		Carl Roth GmbH + Co. KG, Karlsruhe, Germany
Lysis buffer (10x)		New England Biolabs, Ipswich, MA, USA
Magnesium chloride	MgCl ₂	Carl Roth GmbH + Co. KG, Karlsruhe, Germany
Methanol		Carl Roth GmbH + Co. KG, Karlsruhe, Germany
Meyer's hemalaun		Carl Roth GmbH + Co. KG, Karlsruhe, Germany
N-Acetyl-L-cysteine	NAC	Sigma-Aldrich, Munich, Germany
Nocodazole		Sigma-Aldrich, Munich, Germany
Nonident P-40		Sigma-Aldrich, Munich, Germany
Phenylmethylsulfonylfluoride	PMSF	Sigma-Aldrich, Munich, Germany
Phosphate buffered saline	PBS	PAA, Pasching, Austria
Phosphatase Inhibitor Cocktail	PhosSTOP	Roche Diagnostics, Mannheim, Germany
Propidiumiodid	PI	Sigma-Aldrich, Munich, Germany
Rotiphorese® NF-acrylamide/ bis-acrylamide solution		Carl Roth GmbH + Co. KG, Karlsruhe, Germany
Skimmed milk powder		Merck KG, Darmstadt, Germany
Sodium chloride	NaCl ₂	Carl Roth GmbH + Co. KG, Karlsruhe, Germany
Sodium dodecyl sulfate	SDS	Carl Roth GmbH + Co. KG, Karlsruhe, Germany
Sodium hydroxide	NaOH	Carl Roth GmbH + Co. KG, Karlsruhe, Germany
Sodium hydrogen carbonate	NaHCO ₃	Merck KG, Darmstadt, Germany
Temozolomide	TMZ	Sigma-Aldrich, Munich, Germany
Tetramethylethylendiamine	TEMED	Carl Roth GmbH + Co. KG, Karlsruhe, Germany

Transfer membrane Immobilon-P	PVDF	Millipore, Billerica, MA, USA
Tris		Carl Roth GmbH + Co. KG, Karlsruhe, Germany
Triton X-100		Sigma-Aldrich, Munich, Germany
Trypan blue solution		Carl Roth GmbH + Co. KG, Karlsruhe, Germany
Tween-20		Carl Roth GmbH + Co. KG, Karlsruhe, Germany
Xylol		Carl Roth GmbH + Co. KG, Karlsruhe, Germany

3. Software

Software	Software producer
Adobe® Photoshop® CS5, Adobe® Acrobat® X Suite	Adobe Systems incorporated, San Jose, CA, USA
Axiovision Rel. 4.8.	Carl Zeiss Microscopy, LLC, Thornwood, NY, USA
EndNote X5	Thomson ISI Research Soft, NY, USA
FlowJo analysis software	Tree Star, Inc., Ashland, OR, USA
GraphPad Prism®	GraphPad Software, La Jolla, CA, USA
NIS Elements F 3.2	Nikon Instruments Inc., Melville, NY, USA

4. Cell culture

4.1 Cell culture consumables and additives

Substances/Materials	Abbreviation	Producer
Accutase		PAA, Pasching, Austria
B-27® Supplement	B27	Life Technologies, Darmstadt, Germany
Basic Fibroblast Growth Factor, human recombinant	bFGF	Life Technologies, Darmstadt, Germany
Cell culture inserts for live cell analysis		ibidi, Munich, Germany
Cell culture inserts membrane		Millipore, Billerica, MA, USA
Collagen Type I		Biochrom AG, Berlin, Germany
Dulbecco's Modified Eagle Medium GlutaMAX-I, high Glucose	DMEM	Life Technologies, Darmstadt, Germany
DMEM/nutrient mixture F-12 ham powder	DMEM/F-12	Sigma Aldrich, Munich, Germany
D-(+)-Glucose Solution (45%)	Gluc	Sigma Aldrich, Munich, Germany
Epidermal growth factor	EGF	Millipore, Billerica, MA, USA
Fetal bovine serum	FCS	Biochrom AG, Berlin, Germany
Geneticin	G418	Biochrom AG, Berlin, Germany
Ham's F-12 NutrientMixture	Ham's F-12	Life Technologies, Darmstadt, Germany

Horse serum	HS	Sigma Aldrich, Munich, Germany
Minimum Essential Medium	MEM	Life Technologies, Darmstadt, Germany
Mitomycin C from <i>S. caespitosus</i>		Sigma Aldrich, Munich, Germany
N-2 Supplement	N2	Life Technologies, Darmstadt, Germany
Neubauer hemocytometer		VWR International GmbH, Darmstadt, Germany
Penicillin/Streptomycin	P/S	Biochrom AG, Berlin, Germany
Phosphate buffered saline	PBS	PAA, Pasching, Austria
Serological pipettes, cell scraper, centrifuge tubes		SARSTEDT AG & Co., Nümbrecht, Germany
Temozolomide	TMZ	Sigma Aldrich, Munich, Germany
Tissue culture dishes/flasks/test plates		TPP Techno Plastic Products AG, Trasadingen, Switzerland
Dissection instruments		Carl Roth GmbH + Co. KG, Karlsruhe, Germany

4.2 Cell culture media

Media	Components
Astrocyte medium	DMEM/F12 supplemented with 2% (v/v) B27, , 100U/ml penicillin, 100µg/ml streptomycin, 20ng/ml basic FGF, 50ng/ml EGF
Cell freezing medium	95% FBS, 5% DMSO
Dissection medium	7.8g DMEM/F-12 powder, 0.6g NaHCO ₃ , 1.45g glucose diluted in 495ml qH ₂ O, supplemented with, 100U/ml penicillin, 100µg/ml streptomycin, sterile filtered, aerated with 95% O ₂ and 5% CO ₂ for 20min before use
DMEM + FBS	DMEM supplemented with 10% (v/v) FBS, 100U/ml penicillin and 100µg/ml streptomycin
MEM + FBS	MEM supplemented with 15% (v/v) FBS, 100 U/ml penicillin and 100µg/ml streptomycin
Slice medium	Dissection medium supplemented with 5% (v/v) HS, 5% (v/v) FCS, , 100U/ml penicillin, 100µg/ml streptomycin, 1% (v/v) N2 and 2% (v/v) B-27

5. Buffers and solutions

Buffer	Components
5x SDS protein sample buffer	312.5mM Tris-Cl pH 6.8, 10% (w/v) SDS, 50% (v/v) glycerol, 250mM DTT, 0.05% (w/v) bromphenol-blue, ad 10ml H ₂ O
10x SDS running buffer	250mM Tris, 1.92M glycine, 1% (w/v) SDS, ad 500ml H ₂ O
10x TBS buffer	24.2g Tris, 80.0g NaCl, pH 7.6 with acetic acid, ad 1000ml H ₂ O
Blocking buffer	1xTTBS + 5% (w/v) skimmed milk powder

Membrane stripping solution	100ml methanol, 100ml acetic acid, ad 1000ml H ₂ O
Primary antibody solution	1xTTBS
Secondary antibody solution	1xTTBS + 5% (w/v) skimmed milk powder
Transfer buffers	anode I: 300mM Tris, 20% (v/v) methanol, ad 500ml H ₂ O anode II: 25mM Tris, 20% (v/v) methanol, ad 500ml H ₂ O cathode: 25mM Tris, 20% (v/v) methanol, 40mM amino-n-caprioric-acid ad 500ml H ₂ O
Washing buffer (TTBS)	1xTBS, 0.1% (v/v) Tween20

6. Antibodies

Antibody	Dilution	Producer
Anti-mouse HRP-linked pAb	1:10000	New England Biolabs, Frankfurt, Germany
Anti-rabbit HRP-linked pAb	1:10000	New England Biolabs, Frankfurt, Germany
ChK1, rabbit pAb	1:200	New England Biolabs, Frankfurt, Germany
Cleaved Caspase 3, rabbit pAb	1:2000	New England Biolabs, Frankfurt, Germany
Cleaved Caspase 9, rabbit pAb	1:2000	New England Biolabs, Frankfurt, Germany
Cleaved PARP1 (Asp214), rabbit pAb	1:1000	New England Biolabs, Frankfurt, Germany
Caspase 3, full length, rabbit pAb	1:5000	New England Biolabs, Frankfurt, Germany
Caspase 9, full length, rabbit pAb	1:5000	New England Biolabs, Frankfurt, Germany
GAPDH (clone GAPDH-71.1), mouse mAb	1:50000	Sigma-Aldrich, Munich, Germany
GFAP, rabbit pAb	1:100	Dako, Jena, Germany
MGMT, rabbit pAb	1:2500	New England Biolabs, Frankfurt, Germany
MIB 1, mouse mAb	1:50	Dianova, Hamburg, Germany
mt p53, mAb	1:200	Dako, Jena, Germany
PARP1 rabbit, pAb	1:1000	New England Biolabs, Frankfurt, Germany
Phospho-Cdc25c (S216), rabbit pAb	1:200	New England Biolabs, Frankfurt, Germany
Phospho-Histone H2A.X (Ser139), rabbit pAb	1:1000	New England Biolabs, Frankfurt, Germany

7. Cultivation and cryopreservation of GBM cell lines

The human glioblastoma cell lines LN18 (mtp53) [72], LN18pEGFP (transfected in-house with pEGFP-N2 vector by Anne Rapp), LN229 (mtp53) [72] and U87MG [73] were maintained in Dulbecco's modified Eagle's medium (DMEM) with 10% (v/v) FBS and antibiotics under standard cell culture conditions at 37°C and 5% CO₂. T98G (mtp53) [74] glioblastoma cells were provided by Dr. Inge Tinhofer (Charité University Hospital, Berlin, Germany) and were maintained in Minimum essential medium (MEM) supplemented with 15% (v/v) FBS and antibiotics. Adherent

GBM cells were passaged twice weekly. Therefore, cells were washed with PBS, accutase was applied for cell detachment and cells were seeded in fresh media.

For cryopreservation, cells were harvested at 70% confluence and dissolved in freezing medium. After gradual freezing for 2 days at -80°C, cells were stored at -180°C in liquid nitrogen.

8. Primary cell culture

Primary astrocytes were provided by the group of Prof Magdalena Götz, HelmholtzZentrum, Munich. Primary cells were isolated from fetal mice brain according to Heins [75] and cultivated as a single cell suspension. Single cells were cultured in astrocyte media under standard cell culture conditions at 37°C and 5% CO₂.

9. Cell authentication and Mycoplasma-test

Authentication of the human cell lines LN18, LN229, U87MG and T98G was performed prior to the experiments by analyzing microsatellites with Cell ID™ Systems (Promega Corporation, Madison, USA). Therefore genomic DNA was isolated with QIAamp® DNA Mini Kit (Qiagen, Hilden, Germany). Following purification, 2 ng DNA was used as template with Cell ID™ SystemPCR Master Mix. After DNA amplification, nine human loci, including D21S11, TH01, TPOX, vWA, Amelogenin, CSF1PO, D16S539, D7S820, D13S317 and D5S818 were analyzed as described by the manufacturer with capillary electrophoresis. STR (short tandem repeat) genotype was evaluated with GeneMapper® ID software and compared to data available on the ATCC-LGC Standards homepage (LGC Standards, Wesel, Germany).

Regularly all used cell lines were tested by a nested PCR for mycoplasma infections. Therefore 100 µl of the cell culture supernatant was boiled for 5 minutes at 95°C. Following brief centrifugation, 5 µl of the supernatant served as template for the first PCR. The primers, which detect 11 species of mycoplasma (*M. fermentans*, *M. hyorhinitis*, *M. arginini*, *M. orale*, *M. salivarium*, *M. hominis*, *M. pulmonis*, *M. arthritidis*, *M. neurolyticum*, *M. hyopneumoniae*, *M. capricolum*) and one species ureaplasma (*U. urealyticum*) were from PCR mycoplasma detection set (TAKARA, Otsu, Japan). The product of the first PCR served as template for the second PCR.

10. Protein isolation

For cell lysis, 10x lysis buffer was diluted in H₂O and supplemented with 1 mM PMSF and 1x PhosSTOP Phosphatase Inhibitor Cocktail. Adherent cells were harvested with a cell scraper

after rinsing with PBS. Following 5 minutes incubation with lysis buffer on ice, cell debris was pelleted by centrifugation at 13,000 rpm for 10 minutes. The supernatant was transferred to a fresh tube and protein amount was determined by NanoDrop™ UV-Vis spectrophotometer with an absorption measurement at 595 nm.

11. SDS-PAGE and Western blotting

Equal amounts of protein (20 µg) were separated by size performing a SDS-PAGE (sodium dodecyl sulfate polyacrylamide gel electrophoresis). The negatively charged SDS binds proteins in a constant weight ratio, resulting in fractionation by size. Disulfide bonds are reduced by dithiothreitol (DTT). Heating the samples for 5 minutes at 96°C with SDS sample buffer further promotes protein denaturation. The stacking gel (5%) contains tris-glycine at pH 6.8 and the running gel (12.5%) resolves at a pH 8.8. PageRuler™ plus prestained protein ladder (Fermentas, St. Leon-Rot, Germany) was used as molecular weight marker. Gels for PAGE were purchased (Mini-PROTEAN TGX Precast Gels; Bio-Rad Laboratories). Separation was done at 200 V for 45 min with precast gels and at 120 V for 1.5 h with freshly prepared gels. Afterwards, proteins were transferred to a methanol-activated PVDF membrane in a semi-dry blot system at 225 mA for 40 – 60 min, depending on the molecular weight of the protein of interest. Blotting paper (Sartorius blotting paper; VWR International, Darmstadt, Germany) was soaked with transfer buffers. Unspecific binding sites were blocked with 5 % skim milk powder in PBS for 1 h at room temperature on a shaking device. Incubation with primary antibodies was carried out over night at 4°C in the respective dilution. The membrane was washed thrice in TPBS for 10 min each on the shaker at room temperature before applying the corresponding secondary antibodies on a shaker for 45 min at room temperature. Immunoreactivity was visualized by addition of HRP substrate (Immobilon Western Chemiluminescent HRP substrate; Millipore) and exposure to chemiluminescence detection film. For an additional detection of the transferred proteins, bound antibodies were removed from the membrane by incubation with stripping buffer under shaking for 15 min at room temperature. Afterwards the western blot steps were repeated starting with the blocking of unspecific binding sites with 5 % skim milk powder.

12. Cell viability

For the investigation of cell viability after the treatment with cold atmospheric plasma (CAP) and/or temozolomide (TMZ), 5×10^3 cells were seeded on a 96-well plate and grown over night until they reached 80% confluence. Cells were CAP treated with or without medium covering them (than fresh medium (DMEM) with 1% FCS was added immediately afterwards). TMZ treatment (50 µM, 100 µM and 200 µM), if applied in a combined therapy, was carried out

immediately after a single CAP treatment. Medium was changed every 24 h and fresh TMZ was added for three days consecutively. Controls were kept without medium for the same duration as CAP treatment and/ or were DMSO treated in equal concentrations as TMZ. Cells were incubated for 48 h at 37°C and 5% CO₂ before cytotoxicity of various treatments was estimated with colorimetric Cell Proliferation Kit I (MTT) according to manufacturer's instructions (Roche, Basel, Switzerland). The color change was quantified at 595 nm using a scanning multi-well spectrophotometer and correlated to the number of viable cells.

13. Clonogenicity assay

Cells were seeded in 6 cm dishes and treated with CAP without medium and/or with TMZ (50 µM, 100 µM, and 200 µM) afterwards. As described earlier fresh medium was added immediately after the CAP treatment. Controls were treated equally. Cells were seeded into 6-well plates with a total of 150 viable cells per well 24 h after the CAP treatment and allowed to form colonies over a time period of 12 days. Fixation and staining of the colonies was performed using the DiffQuik Kit (Medion Diagnostics, Düringen, Switzerland). Colonies of more than 50 cells were counted.

14. Flow cytometry

Cell cycle analysis was carried out by flow cytometry. Cell nuclei containing different amounts of DNA in the cell cycle phases were stained with propidiumiodid (PI). The G1 phase is featured by two complete sets of chromosomes (2N). During S phase, DNA is synthesized and the DNA amount is intermediate between G1 and G2. In G2 phase, doubled DNA content defines a tetraploid stage (4N). Following RNA and protein synthesis, G2 phase culminates in mitosis (M phase). Regarding DNA amount, G2 and M phase are indistinguishable. Apoptotic cells with fragmented DNA appear as subG1 population.

Cells were seeded in 100 mm² tissue culture dishes (1× 10⁶ cells/ dish), allowed to attach overnight, and CAP and/or TMZ treated for the indicated times and indicated concentrations. Controls were treated equally. For FACS analysis cells were washed twice in phosphate buffered saline (PBS) and fixed in ice-cold 70% methanol at 4°C for at least 2 h. Afterwards cells were washed with PBS and then incubated with 100 µg/ ml of RNase A (Sigma-Aldrich, Hamburg, Germany) for 20 min at 37°C and stained with PI (50 µg/ ml). Cell cycle distribution was analyzed using the BD FACS Calibur (Becton and Dickinson, Heidelberg, Germany) counting 10,000 events per determination. Doublet discrimination and analysis of cell cycle distribution was performed with FlowJo analysis software.

15. Migration

Cells were plated on 6-well dishes in cell culture inserts (ibidi) to obtain a defined cell free gap suitable for migration assays. Inserts were removed 24 h after cell seeding and CAP treatment was applied for indicated times without medium. Fresh medium was added and gap size was measured at three randomized positions 4 h, 24 h and 48 h after CAP treatment.

16. Organotypic slices cultures (OSCs)

Organotypic cultures of brains were obtained from newborn C57BL/6 mice (P1 - P3). After decapitation, the brains were rapidly removed and placed into ice-cold dissection medium, which was aerated with 95% O₂ and 5% CO₂ prior to use and the olfactory bulb and the cerebellum were removed. The remaining desired parts of the brain were embedded in 1% low-melting agarose. The brains were cut out in cubes from the agarose and glued onto the support of the vibratom using Roti Coll I (Carl Roth GmbH + Co. KG, Karlsruhe, Germany), in proper orientation. Brains were cut in 300 µm-thick coronal slices using a vibratom (amplitude setting was 0.3mm with a speed of no faster than 0.5 mm/sec) and transferred onto membranes filters in a collagen mix (320 µl cell matrix type I-A mixed with 120 µl 5x DMEM mixed with 60 µl reconstitution buffer). Collagen was removed from the slices as much as possible and slice cultures were incubated at 37°C and 5% CO₂ for 15 min to allowed attachment of the slices to the membrane. Afterwards slice culture medium was provided and membranes were put above omitting the formation of bubbles. Medium was changed after 2 h and every second day afterwards (serum free slice medium).

16.1 Cell implantation

Injection of LN18pEGFP cells into the cortex of the OSCs were performed using a Hamilton syringe under the microscope. Cells were trypsinized, centrifuged and resuspended in serum free medium to obtain 1×10^5 cells/ µl. 0.5 µl of the cell suspension was applied over 1.5 minutes. 24 h after implantation slices images were taken and CAP was applied afterwards four times within the next 48 h without medium. Further images were taken 14 days after CAP treatment and slices were fixed in 4% formalin and embedded in paraffin using HistoGel (Thermo Fisher, Waltham, MA).

17. Immunohistochemistry of paraffin slides

Paraffin embedded tissue was cut in 3 µm sections and mounted on glass slides for incubation at 50°C. For immunohistochemistry the Dako REAL™ Detection System Peroxidase/DAB+ Kit (K

5001) (Dako, Jena, Germany) was used according to the protocol with slight modifications. Briefly, paraffin slices were de-paraffinized by incubation twice in xylol (15 min each). Rehydration of the slides in 100%, 95%, 85%, 60%, 30% ethanol (4 min each) was carried out and subsequently slides were thoroughly washed in 1x PBS. For heat-mediated antigen retrieval, slides were placed in 1x sodium citrate buffer, pH 6.0 and heated to 95°C. Total heating time in the citrate buffer in the steamer was seven minutes. Slides were allowed to cool down for 30 min at room temperature. Three additional washing steps in 1x PBS for a total of 15 min followed by an incubation for further 15 min in 3% H₂O₂ at room temperature. After further washing steps with 1x PBS, samples were blocked with Avidin/ Biotin for 15 min. Pre - incubation with 5% normal goat serum for 30 min at room temperature occurred before the slices were incubated overnight at 4°C with the desired primary antibody in 1x PBS containing 5% normal goat serum. The following day, each slide was washed in 1x PBS and incubated in secondary antibodies (antibody A and complex B) for 30 min at 37°C. Slides were washed in 1x PBS and DAB (3,3'-Diaminobenzidin, concentrations according to the Dako protocol) was mounted onto the slides for 5 to 10 min. Afterwards the slides were washed with tap water followed by nuclei staining with haemalaun. Slides were covered with glass coverslips and images were taken.

18. Statistical analysis

All statistical significances were evaluated using one or two factor analysis of variance (ANOVA) followed by Bonferroni post-test. Differences were considered significant at $p < 0.001$. Experiments were repeated thrice if not stated otherwise.

E. Results

1. Effects of CAP on liquids

1.1 CAP effects on medium

First, the effects of CAP and its components on liquids were investigated. Among others, pH change during CAP application was verified (supplementary data S26). No significant change in pH was observed for treatment times up to 320 seconds in DMEM supplemented with 1% FCS. Effects on FCS alone or in medium were not found (supplementary data S27). From publications and experiments previously carried out by our and other groups it is known that the height of the liquid has an effect on the CAP impact on the respective cells. To analyze the effects of CAP treated medium on glioma cells, LN18 cells were CAP treated for different time durations in 100 μ l/well of a 96-well plate and medium was either filled up to 200 μ l (figure 11A) or medium was removed completely after CAP treatment and fresh medium was added (figure 11B). Effects of respective CAP treatment on the proliferation of glioma cells were examined using the MTT assay. When the medium was filled up, the proliferation was strongly reduced independently of the CAP treatment time (figure 11A). In comparison, the medium change led to a dose dependent effect of CAP treatment on the proliferation of the cells (figure 11B).

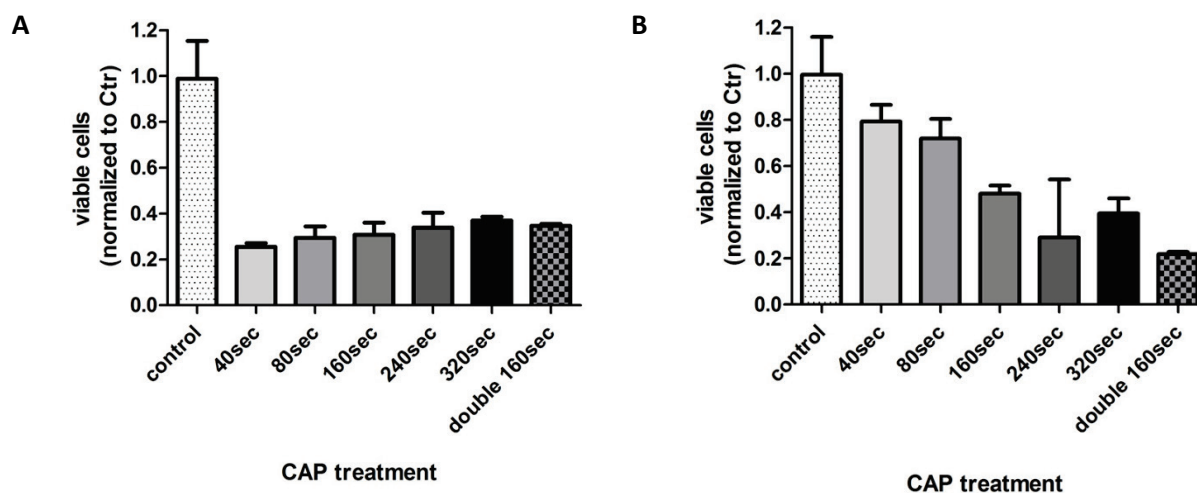


Figure 11: CAP effects on medium. **A** LN18 glioma cells were CAP treated for the indicated times in medium and afterwards the well was filled up with fresh medium to double the amount of medium. MTT assay was performed 48 h later. **B** After CAP was applied on LN18 cells in medium, the medium was completely changed to fresh medium and cell viability was measured using a MTT assay. Double 160 sec: twice applications of 160 seconds of CAP with a 1 min pause in between.

1.2 Storage of pre-treated medium reduces the CAP efficacy

To further distinguish the effects of CAP on medium, 100 μ l/ 96-well DMEM was pre - treated with CAP and kept at 37°C and 5% CO₂ for 1 h, 12 h and 24 h, before applying solely the pre-treated medium to the cells. Effects of the pre - treated medium with incubation time on cell proliferation were compared to the treatment of cells with medium which was exposed to CAP immediately before applying to the cells (figure 12). The results show that cell viability of glioma cells is reduced if the cells are incubated with pre - treated medium. Furthermore, the data confirms that CAP “activated” medium reveals effects on cancer cells upon storage, nevertheless reduced effects of CAP on the cell viability were observed for storage times of 12 h and 24 h.

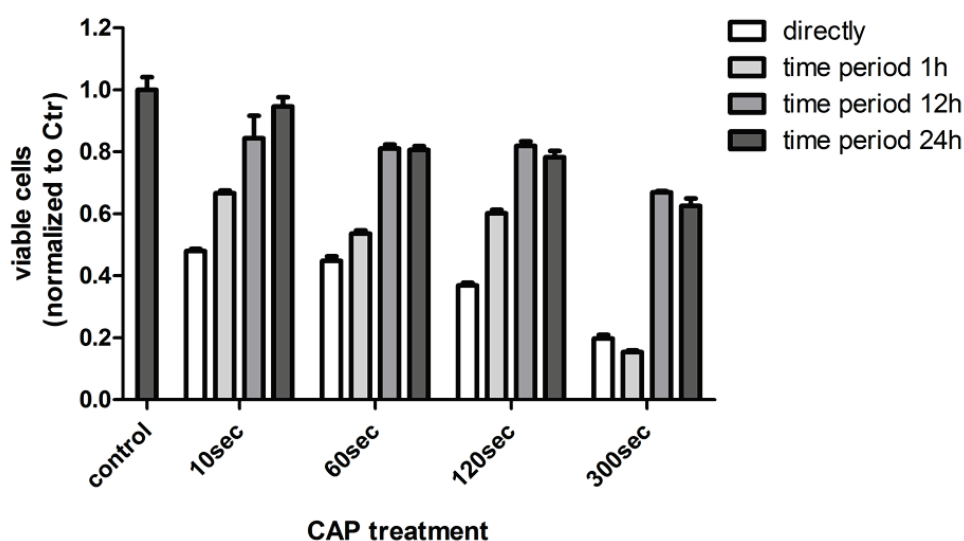


Figure 12: Pre-treated medium is effective in reducing cell proliferation. DMEM supplemented with 1% FCS was pre-treated with CAP without cells. Pre - treated medium was either immediately applied to LN18 cells (“directly”), or stored at 37°C for 1 h, 12 h or 24 h and afterwards applied to the cells. Viability was detected using MTT assay.

1.3 Treatment of glioma cells in minimized amounts of medium

To decline of the CAP effects on liquids and to resemble the situation in the patient, LN18 glioma cells were treated with only a thin film of liquid covering them (referred to as w/o medium). Keeping the cells with only a thin film of medium for time durations of up to 240 seconds did not significantly change the viability of the cells (figure 13A). Upon treatment between 10 seconds and 240 seconds with CAP w/o medium, a strong reduction of cell viability was achieved when normalized to the control which was kept w/o medium for the indicated times. Henceforth the treatment with CAP was performed after sucking off the medium from

the cells followed by addition of fresh medium immediately after the treatment. Comparison of the effects of CAP on the viability of LN229 (figure 13B) and LN18 (data not shown) glioma cells indicated that CAP was effective in reducing the proliferation either for treatment with or without medium, nonetheless the CAP effect was less pronounced when treated in medium (figure 13B).

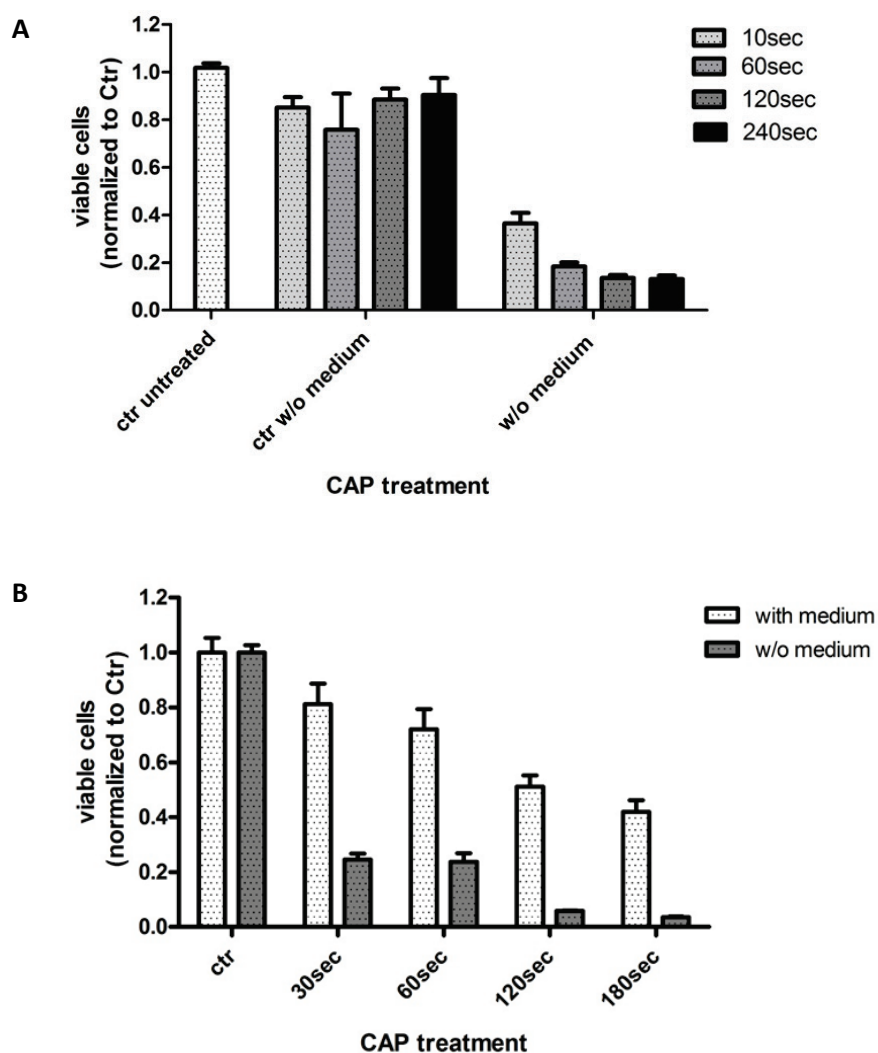


Figure13: A LN18 glioma cells were kept without medium to investigate differences in proliferation by only having a thin film of liquid on the cells for up to 240 seconds. Cells were CAP treated without medium for the indicated times and cell viability was measured 48 h afterwards. **B** LN229 cells were either CAP treated in 100 μ l medium or treated while the medium was sucked off and fresh medium was added to the cells subsequently after treatment. Proliferation was detected using the MTT assay.

2. Effects of CAP on TMZ -resistant and -sensitive glioma cell lines

2.1 *CAP treatment inhibits cell proliferation in MGMT positive and MGMT negative glioma cell lines*

Several tumor biology studies identified the prognostic role of O6-methylguanine-DNA methyltransferase (MGMT) status in patients with newly diagnosed glioblastoma. Thus, newly diagnosed glioblastoma can be stratified into two prognostic groups based upon *MGMT* promoter methylation status. Promoter methylation of the *MGMT* gene predicts benefit from chemotherapy with the standard chemotherapeutic temozolomide (TMZ), whereas patients with an unmethylated promoter status do not benefit from chemotherapy. The expression of the MGMT protein of the cell lines U87MG, LN229, LN18 and T98G under standard culture conditions was illustrated by antibody detection (figure 14A). GAPDH served as a loading control. The cell lines U87MG and LN229 that do not express MGMT (MGMT negative, favorable) and the cell lines LN18 and T98G that express MGMT (MGMT positive, unfavorable) were treated with TMZ for three days consecutively and cell viability was measured afterwards (figure 14B). Treatment with TMZ was able to reduce the viability of the MGMT negative cell lines by about 20 - 25%, whereas the viability of the MGMT positive cell lines was only reduced to a minor content (T98G) or remained unreduced (LN18). These MGMT positive and MGMT negative cell lines were CAP treated with one single application and viability was detected 48 h later (figure 14C). A dose dependent inhibition of proliferation by CAP treatment for all cell lines was observed. Treatment times of 60 seconds and longer achieved a significant reduction of proliferation in the resistant as well as in the sensitive cell lines.

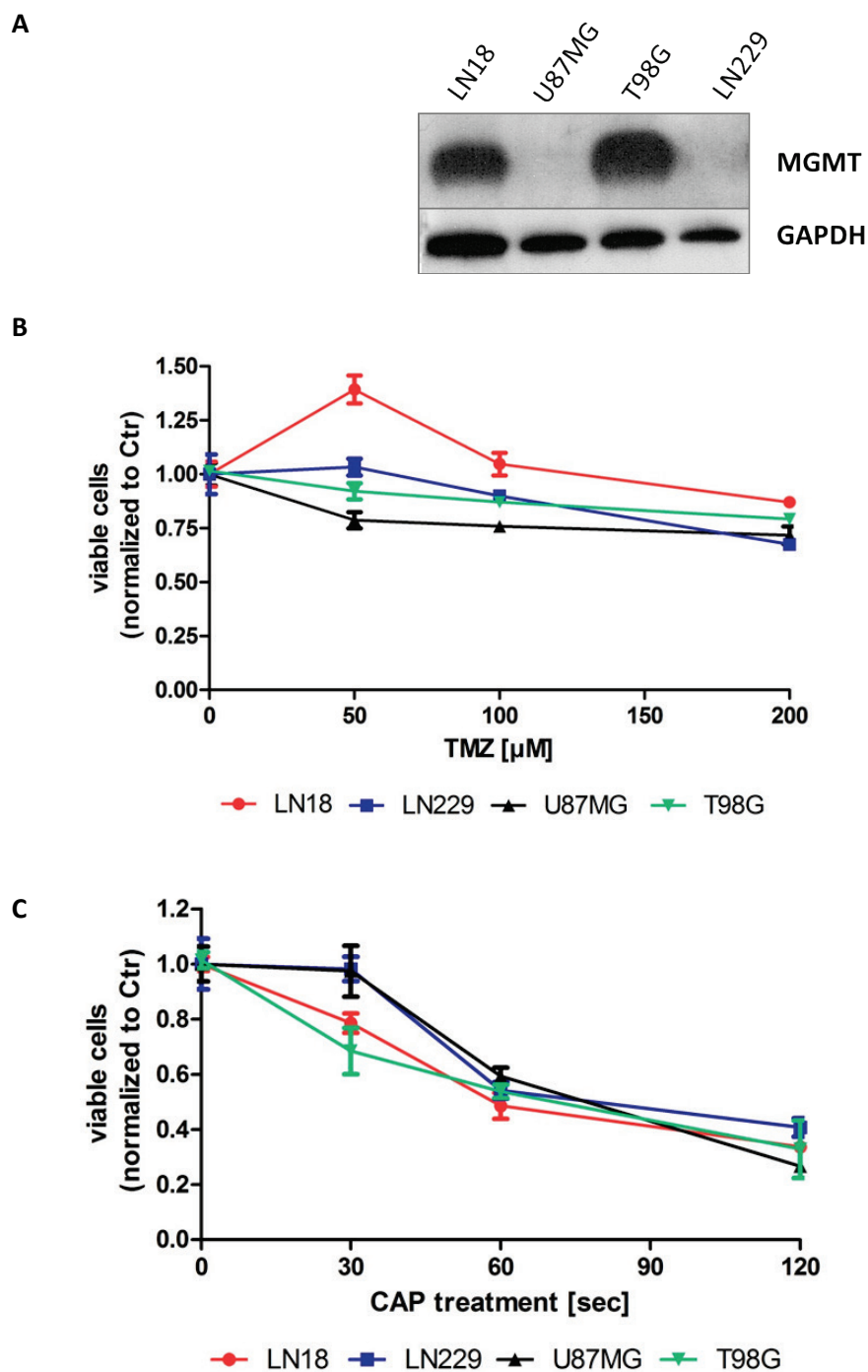


Figure14: MGMT promoter methylation predicts response to chemotherapy but does not affect the response to CAP. A Immunoblotting of cell lysates for the expression of MGMT protein under normal culture conditions. GAPDH served as a loading control. **B** TMZ was administered in several concentrations to glioma cells for three days consecutively and cell viability was detected. **C** Glioma cells were CAP treated once for 30 seconds to 120 seconds and viability was detected 48 h afterwards.

2.2 *Induction of apoptosis is present to a minor extent after CAP treatment*

The perceived reduction of proliferation in all tested cell lines was conducted by minor induction of apoptosis. Immunoblotting of protein lysates gained from LN18 (MGMT positive, unfavorable)(figure 15) and LN229 (MGMT negative, favorable) (supplementary data S28) cells with antibodies against γ H2AX, cleaved PARP1 (figure 15A), Caspase 3 (figure 15B) and Caspase 9 (figure 15C) as marker for DNA damage was performed. Cleavage of PARP1 was detected 48 h and 72 h post - treatment for 120 seconds of CAP treatment and longer, but not after 4 h and 12 h (data not shown). Phosphorylation of H2AX was demonstrated for a treatment time of 180 seconds after 72 h, but not after 4 h, 12 h (data not shown) and 48 h. Cleavage of Caspase 9 was observed to a minor extent after treatment for 120 seconds and 180 seconds only after 48 h, while cleavage of Caspase 3 was detected at none of the mentioned time points. Additionally, DNA damage including single strand breaks (ssb), double strand breaks (dsb) and cross linking sites at the level of single cells was observable by the comet assay to a minor content 1 h after CAP treatment in LN229 cells, but was repaired 24 h afterwards (supplementary data S29). Taken these results into account, apoptosis was induced in glioma by CAP treatment only to a minor extent, primarily in the first hour(s) after application of CAP.

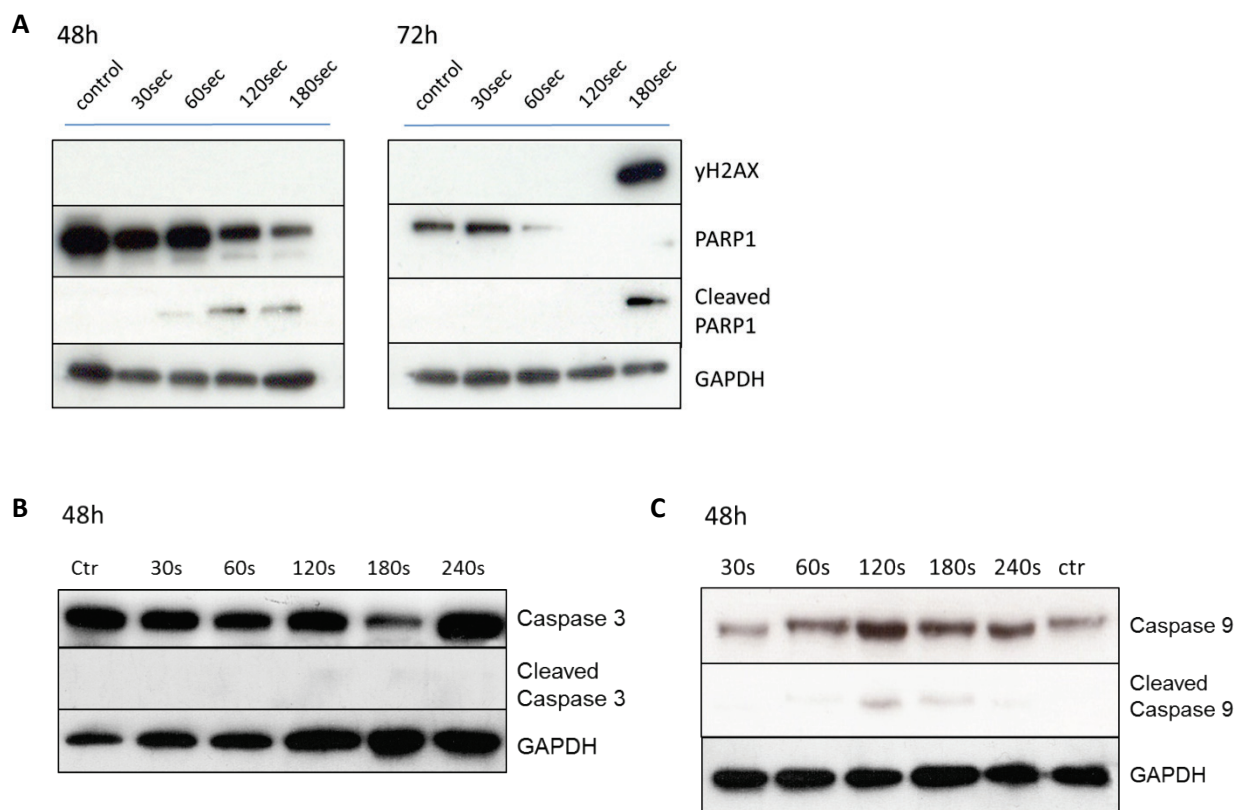


Figure 15: Severe apoptosis is not an early feature of CAP treatment in glioma cells. **A** Immunoblotting of LN18 cell lysates taken 48 h and 72 h after CAP treatment with antibodies for PARP1, cleaved PARP1 and γ H2AX. GAPDH served as a loading control. **B** Caspase 3 full length was detectable by immunoblotting in LN18 cell lysates 48 h after CAP treatment but not the cleaved and therefore activated Caspase 3. **C** Cleavage of Caspase 9 as a marker for induction of apoptosis was not found in LN18 cell lysates after CAP treatment.

2.3 Cytolysis is only induced by long CAP treatment durations

Measurement of released lactate dehydrogenase (LDH) in the medium for the detection of cytolysis was performed 2 h, 24 h and 48 h after CAP treatment (figure 16). This assay is based on measurement of LDH which is a stable enzyme normally found in the cytosol of all cells but is rapidly released into the supernatant upon damage of the plasma membrane. Treatment of cells with 1% Triton x-100 served as a positive control. No increased release of LDH after treatment for up to 180 seconds was displayed, whereas treatment for 10 minutes resulted in about 50 percent increase of released LDH in the medium.

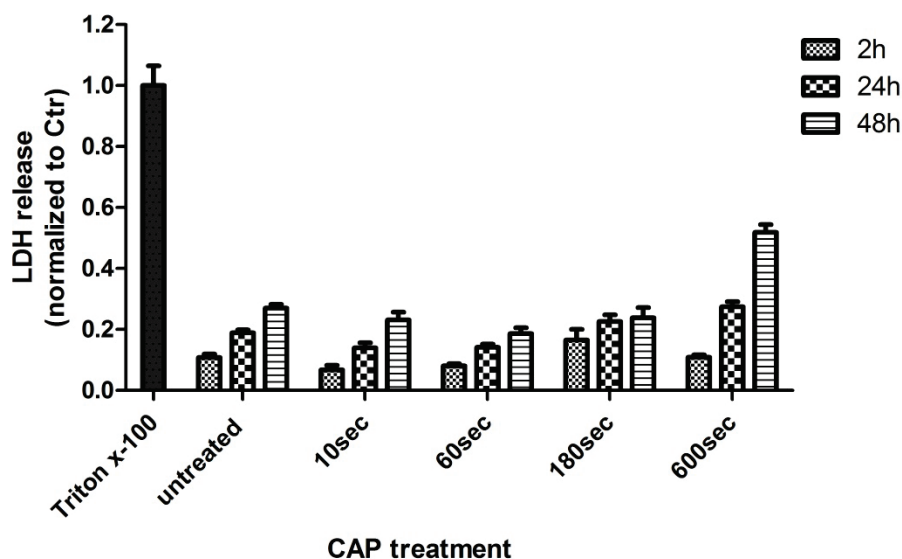


Figure 16: Cytolysis is not promoted by CAP treatment in LN18 glioma cells. The release of LDH from the cells in the medium 2 h, 24 h and 48 h after CAP exposure up to 600 seconds was assessed. Treatment with 1% Triton x-100 served as a positive control.

2.4 Strong induction of cell cycle arrest in MGMT positive and MGMT negative glioma cells by CAP treatment

Based on these findings, we assumed that CAP has an influence on the regulation of the cell cycle progression. Thus, cell cycle progression of the MGMT positive and MGMT negative cell lines was analyzed 24 h, 48 h and 72 h after CAP exposure (figure 17 and supplementary data S30). Treatment times of 120 seconds and longer resulted in a significant arrest in the G2/ M phase of the cell cycle in the U87MG (figure 17A), LN229 and T98G (supplementary data S30B and S30C) cells. A factor two to four higher amount of cells in the G2/ M phase was found for the CAP treated cells compared to the control cells. For the LN18 cell line with an unfavorable MGMT status, the arrest was achieved after treatment for 60 seconds (supplementary data S30A). The arrest achieved in the tested cell lines U87MG, LN18 and LN229 persisted for at least 72 h and was independent of the MGMT status. Statistical analysis revealed a significant arrest in the U87MG cells (figure 17B) after 120 seconds and longer, whereas the cell cycle progression of the LN18 cells (figure 17C) and LN229 cells (supplementary data S30D) was significantly inhibited after 60 seconds and longer of CAP treatment.

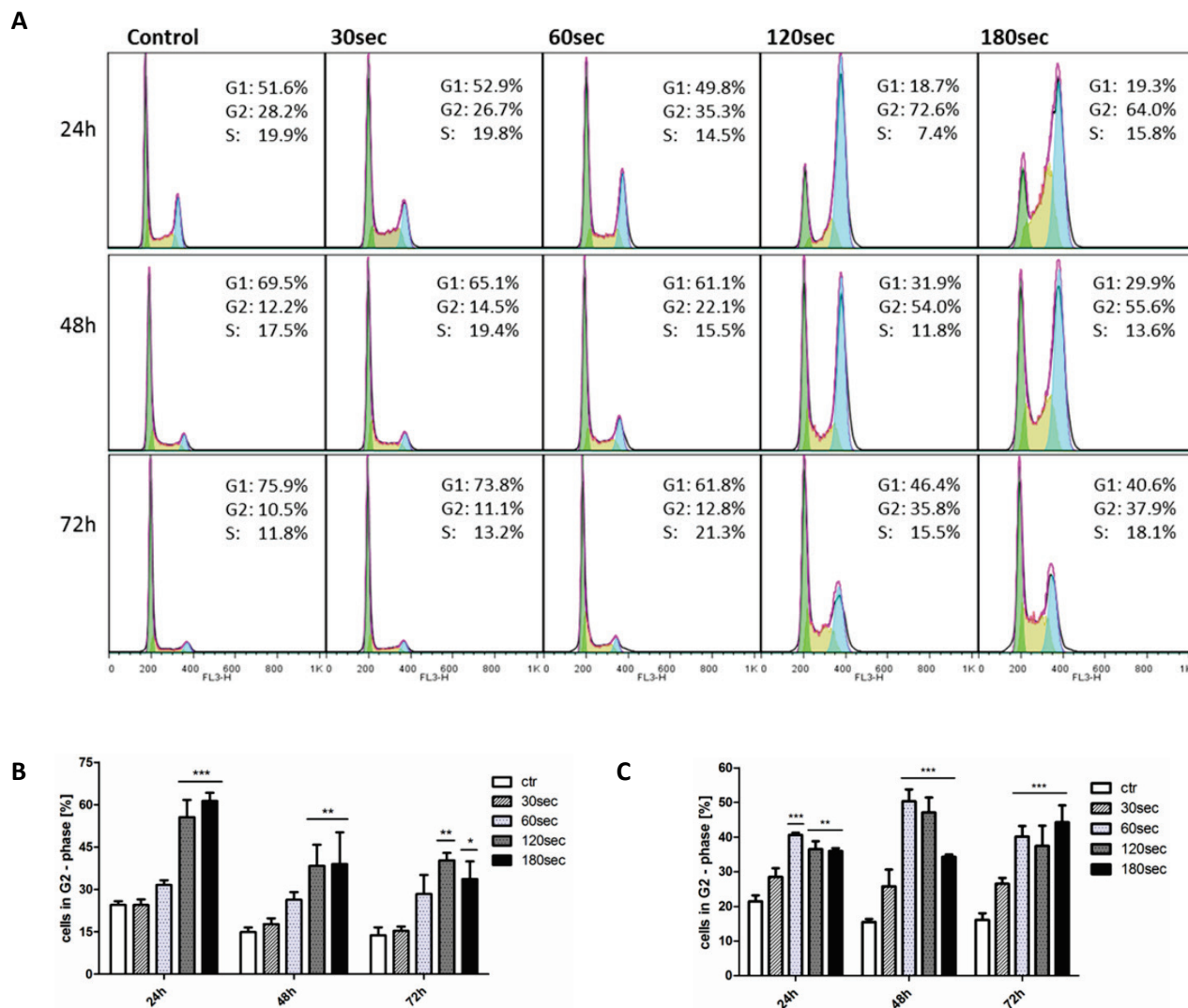


Figure 17: CAP treatment induces G2/ M phase cell cycle arrest in glioma cells. **A** Representative cell cycle distribution of U87MG glioma cells after CAP treatment. Treatment was performed only with a thin film of liquid covering the cells. Cell cycle distribution was analyzed using flow cytometry. Similar results were observed for the LN229 (MGMT negative) and LN18 (MGMT positive) cells (supplementary results S5). **B** Statistical significances of the observed arrest in the G2/ M phase in U87MG and **C** in LN18 cells. P-value *** <0.001

2.5 Induction of cell cycle arrest by CAP application is a long lasting effect in glioma cells

Long term investigation of the cell cycle progression in LN18 and U87MG cells was conducted 7 days post - treatment, as an extended duration of the CAP effects on cell cycle regulation would represent a benefit regarding the application in a combined therapy with chemotherapeutics. Therefore, LN18 and U87MG cells were CAP treated once without medium and cultured for 7

days. Cell cycle analysis was performed using flow cytometry. A significant cell cycle arrest in G2/ M phase 7 days post - treatment was demonstrated in the resistant cell line LN18 by CAP treatment for 120 seconds (figure 18A). Noticeably, the sensitive cell line U87MG featured a significant arrest 7 days post - treatment by 120 seconds of CAP application in the S phase of the cell cycle (figure 18B).

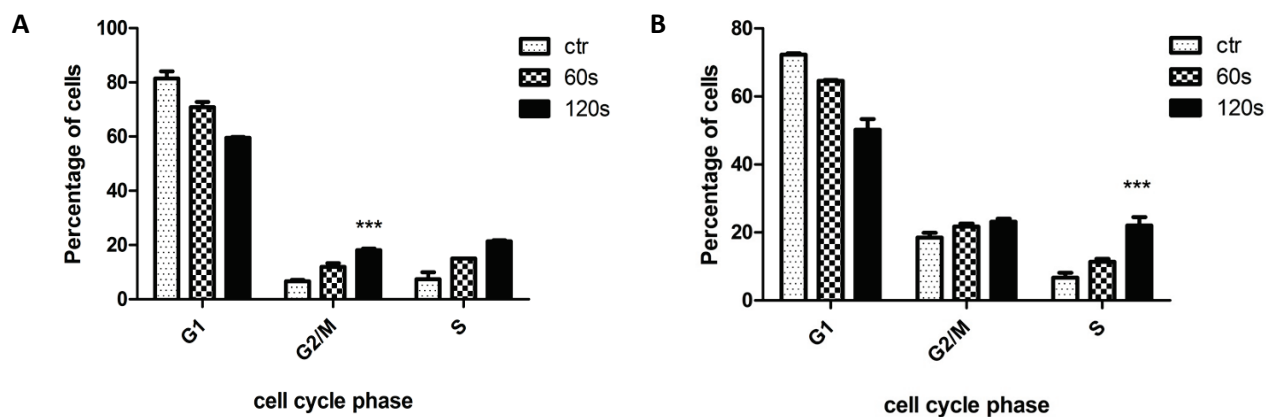


Figure 18: Extended cell cycle arrest was observed post-treatment with CAP. A LN18 and **B** U87MG cells were CAP treated for the indicated times and cell cycle progression was examined 7 days afterwards. P-value < 0.001.

2.6 CAP reduces the clonogenic potential of glioma cells

The ability of cells to form clones after treatment with the chemotherapeutic temozolomide (TMZ) or CAP was verified (figure 19). Therefore, glioma cells were either TMZ or CAP treated and 24 h later 150 cells were seeded and allowed to form colonies over 12 days. Treatment with TMZ was able to reduce the clonogenicity in LN18 cells (MGMT positive, unfavorable) only to a minor content up to concentrations of 500 μ M (figure 19B). The MGMT negative cell line (favorable) LN229 was sensitive to treatment with 50 μ M TMZ, resulting in a significant reduction of clonogenicity. In contrast, a significantly reduced clonogenicity was found after CAP treatment for both cell lines independent of their MGMT status (figure 19C). CAP treatment of 120 seconds strikingly culminated in a complete loss of the clonogenic capacity of the LN18 cells.

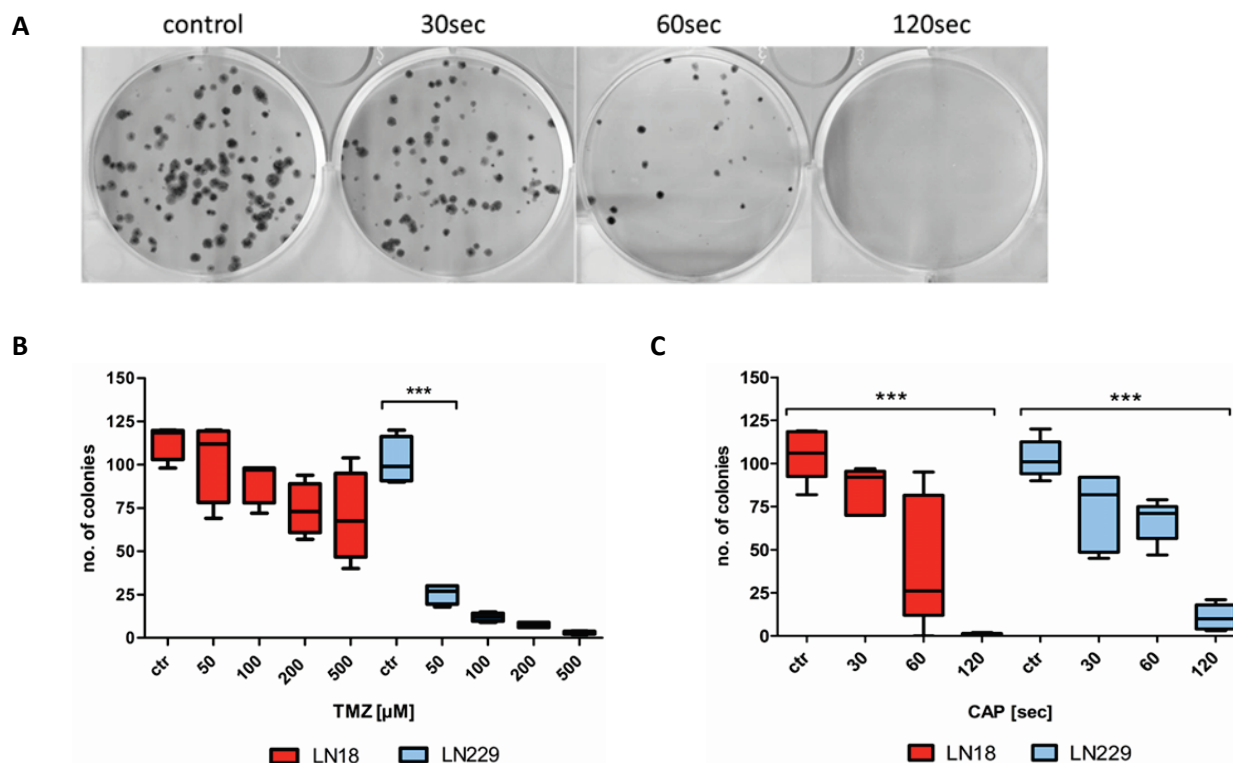
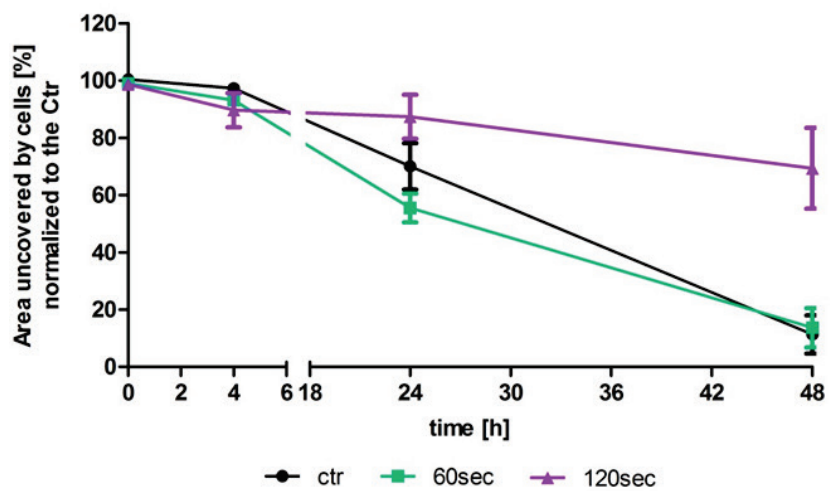


Figure 19: Reduced clonogenic capacity of glioma cells treated with TMZ or CAP. Glioma cells were either TMZ or CAP treated and 24 h later 150 cells/ well were seeded on a 6-well plate. Colonies formed after 12 days were stained and counted. P values *** <0.001. **A** Picture of the LN18 (MGMT positive, unfavorable) cells treated with CAP for 30 seconds, 60 seconds and 120 seconds. Afterwards the formed colonies were stained. **B** Results of the colony formation assay for MGMT positive and negative glioma cells (LN18 and LN229) treated with TMZ with concentrations of up to 500 μ M. **C** CAP treatment followed by the colony formation assay in either MGMT positive or MGMT negative cells.

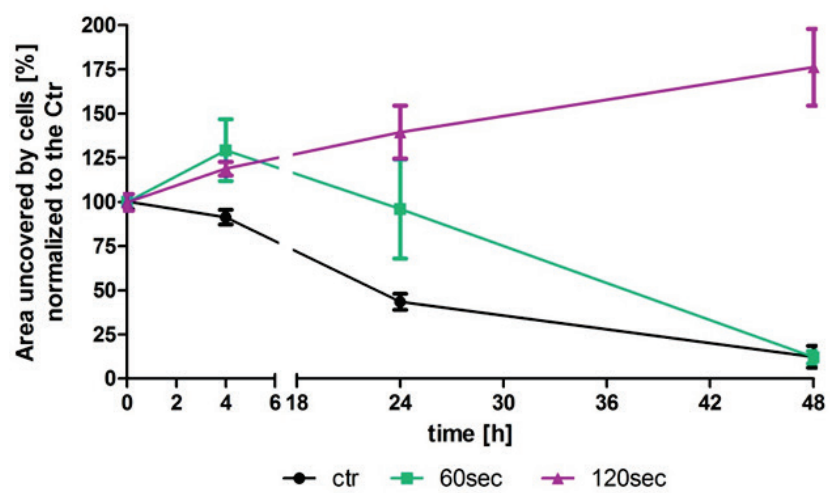
2.7 CAP application impairs migration of glioma cells

To further address the effects of CAP application on glioma cells, the migration ability after CAP treatment in LN18 and LN229 cells was investigated. A gap was originated by a cell culture insert and cells were CAP treated. Migration of the cells was monitored for 48 h under the microscope.

A



B



C

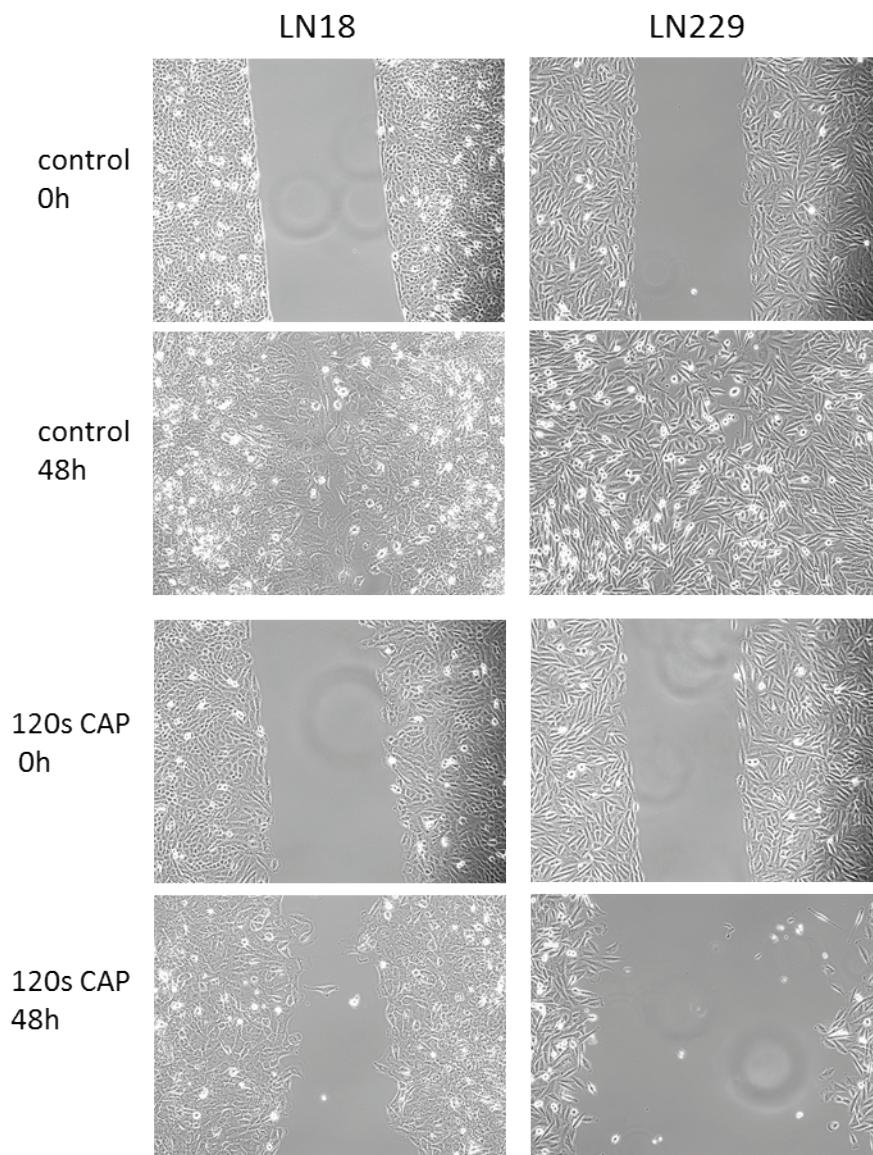


Figure 20: Inhibition of migration in glioma cells after CAP treatment. A LN18 cells and B LN229 cells were CAP treated and migration of the cells was monitored over 48 h. Gap size was measured after 4 h, 24 h and 48 h. C Pictures illustrating the gap directly after the treatment in CAP treated cells or in control cells, compared to migration in CAP treated and control cells after 48 h.

Migration was reduced in LN18 cells (figure 20A) after 120 seconds of CAP, but not after 60 seconds of treatment. A noticeable enlargement of the gap was observed 4 h after CAP treatment for both 60 and 120 seconds in the LN229 cell line (figure 20B). Strikingly, the gap was even more distinct 24 h and 48 h post - treatment for 120 seconds possibly due to detachment of cells. Migration of LN229 cells with 60 seconds of CAP treatment recovered after

48 h. Reduced migration rate and de-attachment of cells was visible in LN18 and LN229 cells which were CAP treated for 120 seconds on the pictures taken directly after CAP treatment (0 h) and after 48h of incubation after treatment (figure 20C).

3. Combined treatment with CAP and chemotherapy

3.1 Concomitant treatment with CAP and TMZ has a synergistic effect on cell viability in MGMT positive and MGMT negative cells

To investigate the effects of a combined therapy consisting of CAP and the chemotherapeutic TMZ in glioma cells, both sensitive as well as both resistant cell lines were CAP treated once followed by a consecutively TMZ application for three days. Proliferation of the cells was quantified using the MTT assay. Combined treatment with CAP and TMZ leads to a significant stronger inhibition of proliferation in the sensitive U87MG (figure 21A) and LN229 (supplementary data S31) cells, as well as the resistant LN18 (figure 21B) and T98G (supplementary data S31) cells compared to separate treatment with CAP or TMZ alone. Furthermore, combined treatment with low dose of TMZ (50 μ M) and short treatment times of CAP (30 seconds in U87MG and LN18, 60 seconds in LN229 and T98G cells) caused significant higher suppression of cellular growth as compared to a high dose of TMZ (100 μ M) alone. As displayed in figure 21, combined therapy revealed a synergistic effect on cell viability in the treated TMZ -sensitive and -resistant glioma cells. Especially low dose TMZ (50 μ M) combined with short CAP treatment times (30 seconds) clearly showed a synergistic effect rather than an additive effect.

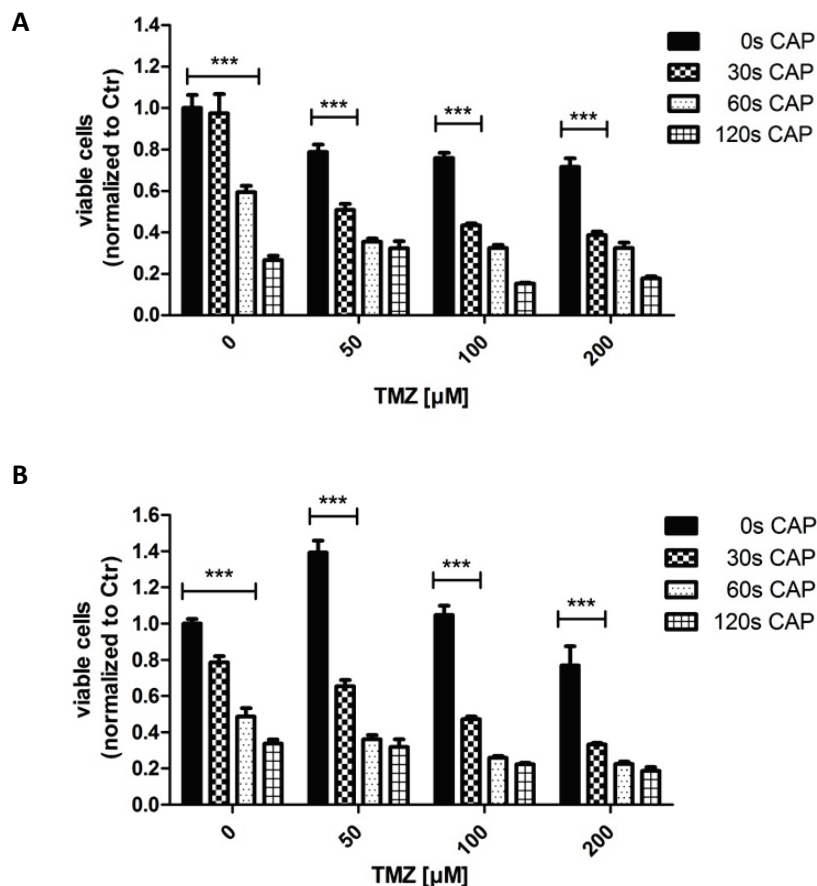


Figure 21: Concomitant therapy with TMZ and CAP re-sensitizes glioma cells. A U87MG cells were CAP treated once and TMZ was applied consecutively afterwards for three days. MTT assay for evaluating the cell viability was performed at day four. Controls were kept without medium and/or DMSO treated. **B** The same approach was carried out for LN18 cells, which were CAP treated once and TMZ was applied afterwards consecutively for three days. P-value *** <0.001

3.2 Combined therapy induces prolonged G2/ M phase cell cycle arrest

The LN18 and T98G cell lines, which are known to be fairly resistant to therapy with TMZ, were exposed to various TMZ concentrations repeatedly (figure 22 and supplementary data S32). Remarkably, only the highest concentration of 500 μ M was able to induce a G2/ M phase arrest. In contrast, combined treatment of CAP for 60 seconds (single treatment) and TMZ (50 μ M, 100 μ M, 200 μ M for three days consecutively) indicated a significant cell cycle arrest (figure 22A). Especially a combination of 60 seconds CAP and 100 μ M TMZ or 200 μ M TMZ, respectively, turned out to be strongly effective in inhibition of the cell cycle progression (figure 22B).

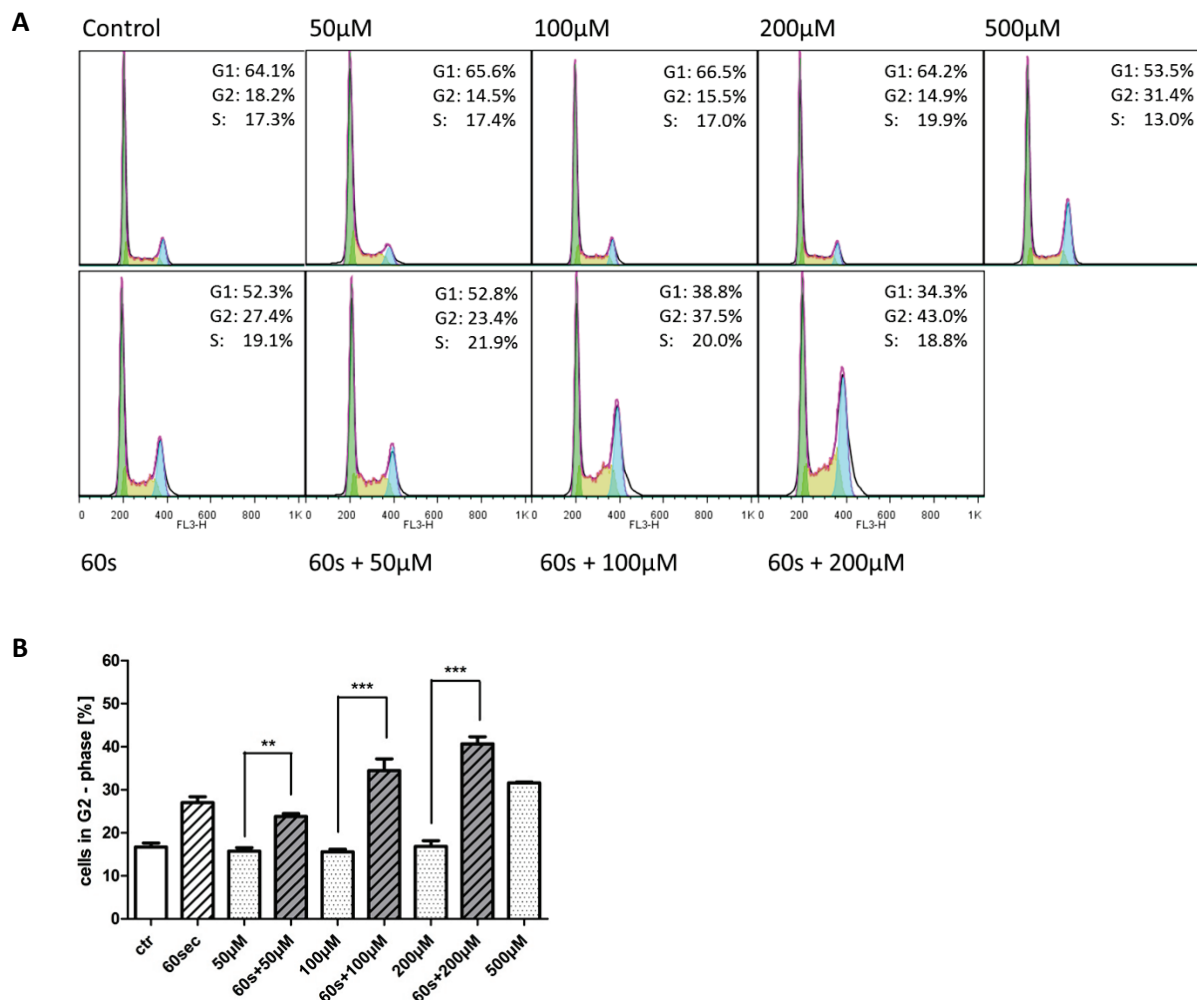


Figure 22: TMZ resistant cells respond with cell cycle arrest to concomitant treatment. **A** LN18 glioma cells were TMZ treated for three days consecutively with 50 µM, 100 µM, 200 µM and 500 µM and cell cycle analysis was performed afterwards. In comparison, CAP treatment for 60 seconds was applied once to LN18 glioma cells, followed by TMZ treatment with 50 µM, 100 µM and 200 µM for three days consecutively. Cell cycle distribution was determined afterwards. **B** Analysis of the percentage of cells in the G2/ M phase after treatment with TMZ and combined treatment with CAP. P-value *** <0.001.

4. CAP displays cell selectivity towards tumor cells

4.1 Cell cycle distribution in primary astrocytes

As CAP treatment was effective in glioma cells, the influence of CAP on healthy, non-tumorous cells and brain tissue was investigated. Therefore, primary astrocytes were isolated from newborn mice and exposed to CAP similar to the tumor cells before (figure 23). Treatment occurred with only a thin film of medium covering the cells. The experiment was performed

twice. Using flow cytometry the cell cycle progression was determined 48 h after CAP treatment. Primary astrocytes did not respond to CAP application with a cell cycle arrest in the G2/ M phase, even not when treated for up to 180 seconds. A shift towards the S phase was observable for CAP times of 180 seconds, but not for shorter treatment times (figure 23). These results indicate that CAP treatment induces different effects in non-tumorous compared to the effects induced in tumor cells. Furthermore, the treatment time needed to induce a change on cell cycle progression in non-tumorous cells is longer than in tumor cells, suggesting a 'therapeutic window' for the CAP application.

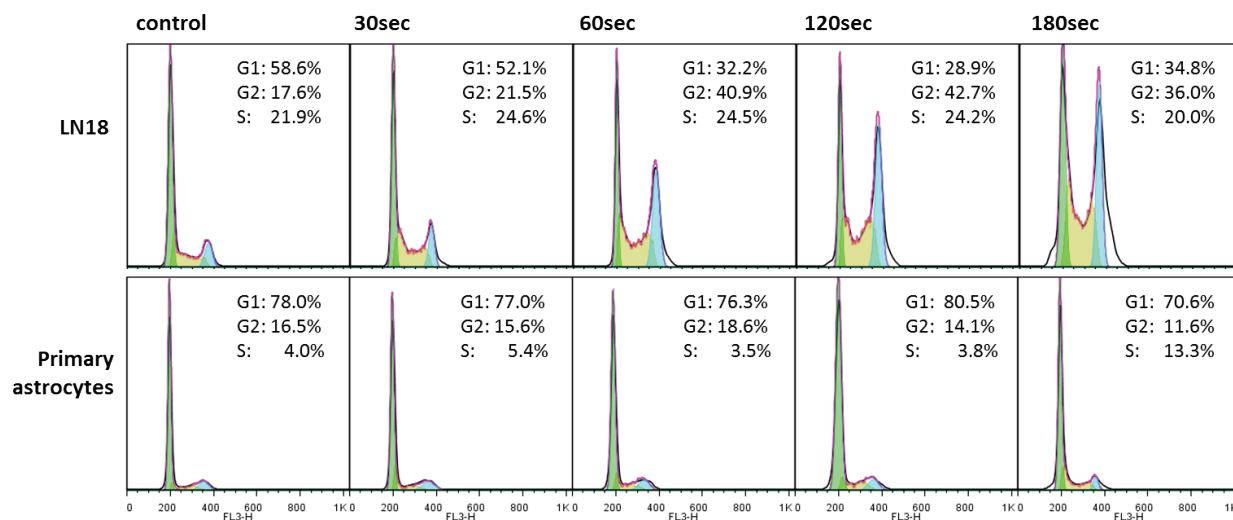


Figure 23: CAP demonstrates cell selective properties. Primary astrocytes isolated from newborn mice were CAP treated and cell cycle progression was analyzed 48 h later. In comparison the cell cycle distribution for CAP treated LN18 glioma cells is shown.

4.2 Treatment of LN18pEGFP in organotypic brain slice cultures

To further explore the impact of CAP on cell selectivity, LN18pEGFP tumor cells were implanted in organotypic brain slices cultures (OSCs) from newborn mice and cultured for 14 days. CAP was applied twice 24 h and 48 h after implantation. Tumor progression was monitored via fluorescence before and 14 days after CAP treatment (figure 24 and supplementary data S34). LN18pEGFP revealed similar proliferation behavior towards CAP as LN18 wt cells did *in vitro* (supplementary data S33). Tracking of the LN18 cells via GFP fluorescence revealed that the tumor cells were migrated through the OSCs up to a depth of 80 – 160 μ m in the slides after 14 days. CAP treated OSCs seem to express a reduced fluorescence area for treatment times between 60 seconds and 180 seconds, even so CAP treatment did not diminish fluorescence *in vitro* (data not shown). There was a remarkable morphological change on the surface of the

tissue 14 days after CAP application exclusively in the tumor area, even though CAP was applied overall onto the OSCs (figure 24).

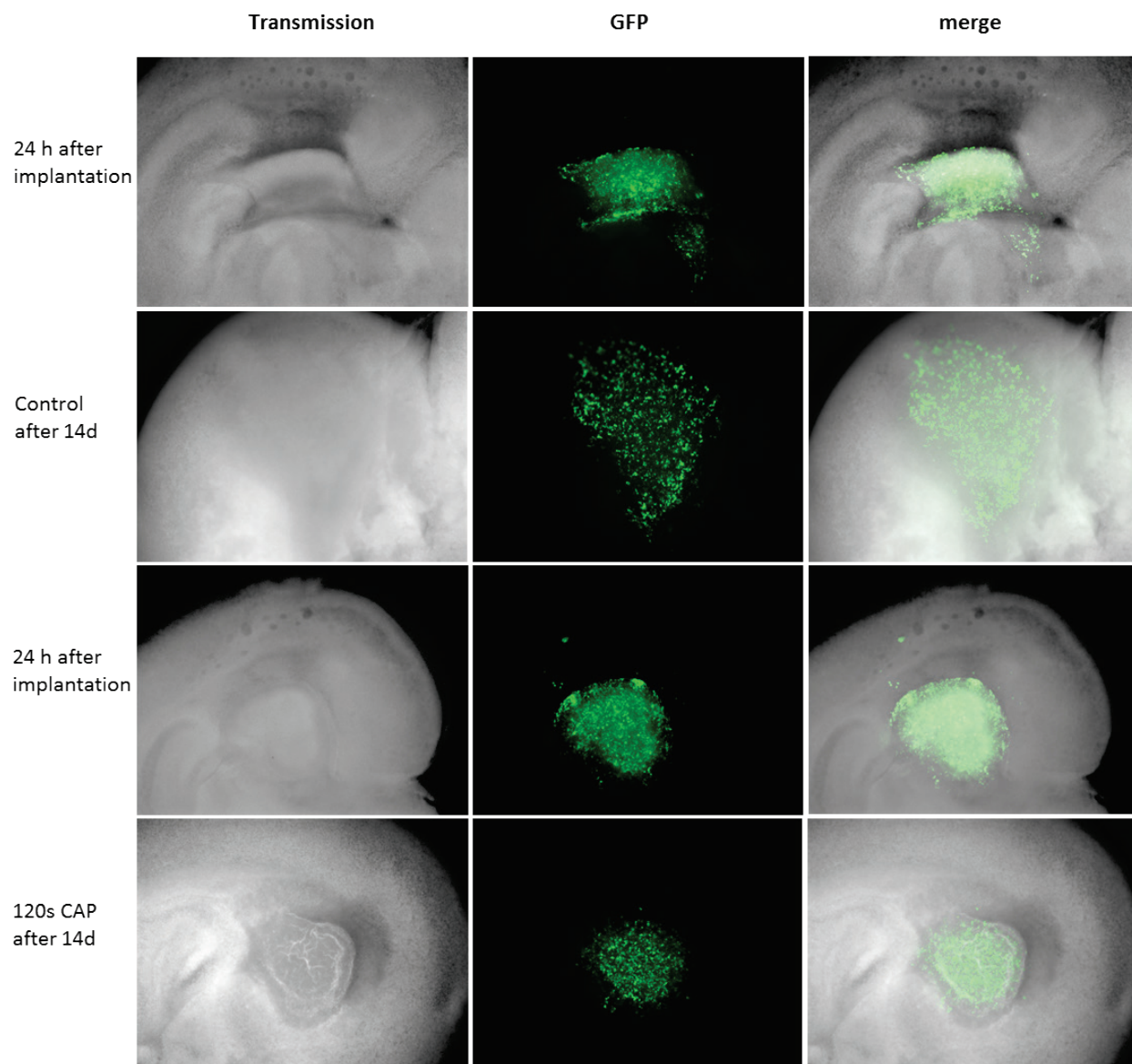


Figure 11: CAP treatment of LN18pEGFP cells in a murine brain slice model. LN18 cells expressing EGFP were implanted in freshly prepared brain slices from newborn mice. CAP was applied 24 h after implantation of the cells for four times within 48 h and cells were monitored over 14 days.

For immunohistological analyzes of effects on brain tissue and tumor cells slices were fixed 14 days after four times of CAP application and stained with hematoxylin - eosin (HE), mut p53, Glial fibrillary acidic protein (GFAP) and Mib-1 (figure 25A). A precise discrimination between normal tissue and tumor cells can be made based upon these staining. p53 is mutated in

LN18pEGFP cells, whereas non-tumorous cells express wt p53. GFAP is exclusively expressed in astrocytes in the central nervous system, and is not present in LN18 tumor cells (ATCC® CRL-2610™). The proliferation marker Mib-1 (also known as Ki-67) is solely expressed in the periphery of the tumor, demonstrating a marginal growth of the tumor.

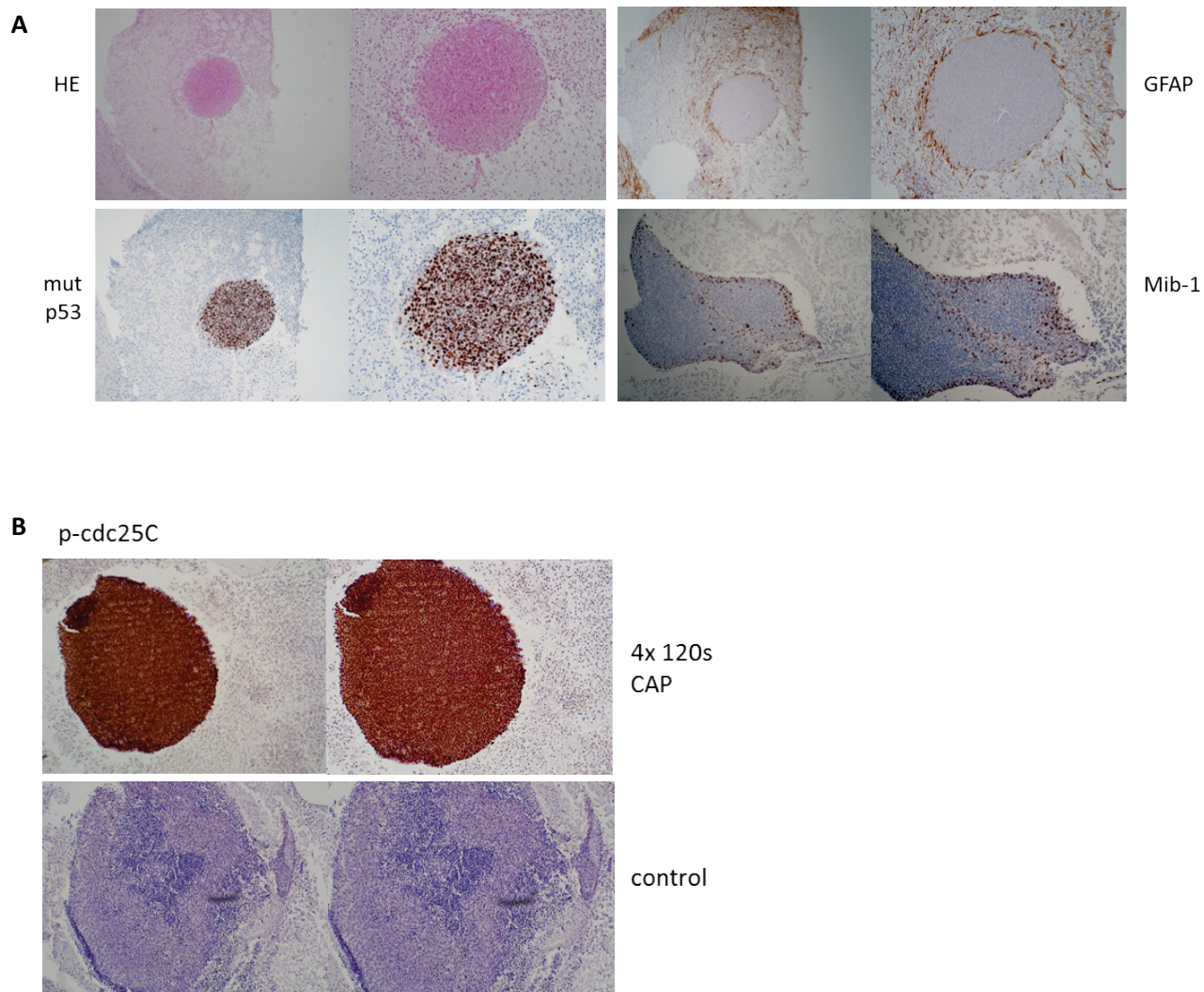


Figure 25: Staining of the OSC revealed tumor formation after implantation of LN18pEGFP glioma cells.

A Immunohistological staining of OSCs with hemotoxylin-eosin (HE), mut p53, GFAP and Mib-1. **B** The activated checkpoint kinase Chk1 can inactivate Cdc25C via phosphorylation at Ser216, thereby blocking the transition into mitosis. The control slice presented no phosphorylation of Chk1.

4.3 Staining for p-Cdc25c reveals activation of the ATM/ ATR signaling pathway by CAP application in OSCs

OSCs were stained for the phosphorylation of Cdc25c (figure 25B), a key regulator of the cell cycle. Cdc25c plays a role in promoting progression from G2 phase to mitosis. The checkpoint kinases Chk1 and Chk2 phosphorylate Cdc25c at Ser216 in response to DNA damage or unreplicated DNA, thus delaying progression of the cell cycle to provide time to repair the damaged DNA or to complete replication. Slices that were CAP treated four times for 120 seconds demonstrated phosphorylation of the Cdc25c phosphatase in the tumor, whereas phosphorylation was not detectable in the tumor of the untreated control slices. Notably, the phosphorylation at Ser216 does not occur in mouse cells as mouse Cdc25c does not have an equivalent to this residue.

F. Discussion

Over the past decade, cold atmospheric plasmas (CAPs) attracted a lot of interest not only from physicists but also from biologists and medical scientist. Cold or non-thermal plasmas offer the opportunity of a new, exceeding treatment technology in many fields, such as sterilization of medical instruments, disinfection of surfaces, tooth bleaching and application on the skin. Newest research gives hope to successful application of CAP in cancer therapy. The present work focuses on glioblastoma, as patients suffering from this aggressive tumor still have a poor prognosis despite multimodal treatment options including surgical resection, chemotherapy and radiotherapy. Temozolomide (TMZ), as the standard chemotherapeutic, in combination with surgery and radiation has added several months to the overall survival (from 12.1 to 14.6 months [51], but is restricted to a subpopulation of tumors with a methylated MGMT promoter status [76], [47]. Glioblastomas, which exhibit an unmethylated MGMT promoter and thus express the DNA repair enzyme MGMT, are resistant to therapy with alkylating agents like TMZ. Treatment options for this resistant subpopulation are of high clinical interest.

Plasma application on human cells has been investigated since the late nineties. First, the effects of so called plasma needles which use helium as a carrier gas were investigated. Often cell detachment and cell death were induced [77], [78], [79]. Inspired by these findings, the possible application of plasma on cancer cells came into focus. Fridman and colleagues marked the beginning of plasma application on tumor cells as they treated human melanoma cells *in vitro* with a FE-DBD device (Floating Electrode Dielectric Barrier Discharge), which produces CAP in the surrounding air and furthermore uses the target – in this case melanoma cells - as a second electrode [7]. Other publications followed including treatment of cancer cells derived from colon, liver and skin. The main focus was set on the analysis of growth inhibition [28], [29], cell death [26], [80] and the inhibition of migration and invasion [30] by the usage of various plasma devices.

In the present work we were able to determine the inhibitory effect of CAP produced by a SMD electrode on glioma cells *in vitro*. CAP accomplished a decrease in viability (figure 14), a reduced clonogenicity (figure 19) and a robust cell cycle arrest in G2/ M phase (figure 17) in TMZ - resistant and TMZ - sensitive cells thus independent of their MGMT status. Moreover, sensitivity of resistant glioma cells towards treatment with TMZ was restored by pre - treatment with CAP, as indicated by reduced proliferation and a significant cell cycle arrest in G2/ M phase in these cells (figure 21 and 22). Besides CAP efficacy in tumor cells and the mechanism(s) of CAP - cell interaction, one issue of CAP application in cancer treatment is the selectivity of CAP. First results on cell selectivity of CAP in primary astrocytes *in vitro* disclose an induction of an S phase arrest after treatment with CAP for longer treatment times of up to 180 seconds (figure 23). No induction of a G2/ M phase arrest was observed even with treatment up to 180 seconds. In

contrast glioma cell lines showed a high induction of G2/ M phase arrest already for CAP treatment times of 60 seconds to 120 seconds (figure 17 and 23). To further address cell selective characteristics of CAP a novel suitable model for glioma was established. Organotypic murine brain culture slices implanted with LN18pEGFP cells represent an orthotopic *ex vivo* model for CAP application in a tumor - bearing tissue, providing the possibility to study CAP effects on tumor and non-tumorous cells within their histological microenvironment (figure 24 and 25).

1. Effects of CAP on liquids

The influence of liquids on the CAP effect on cells is under discussion since the first experiments with CAP and cells were performed. The device used in the present investigation had no influence on the pH of the medium or on the FCS, suggesting that protein modifications may not play a major role (supplementary data S26 and S27). In fact, the effect of plasma irradiation is depending on depth of the liquid phase (figure 13B) as well as the composition of the medium itself for the treatment of bacteria [81], [82]. We made similar observations for the effects on cells. Medium change after CAP treatment presented dose dependent effects on cell viability (figure 11B), whereas keeping the medium plus adding some fresh medium strongly reduced the proliferation for all treatment times (figure 11A). This is probably due to the fact that reactive species produced by CAP dissolve into the medium, react further there and the newly generated species themselves interact with the cells. For example, the dissolved ozone initiates a reaction with the hydroxyl radical (OH^\cdot), resulting in the production of HO_2 and the superoxide radical (O_2^-) [83]. Furthermore, O_2^- is converted to hydroxyl radical (OH^\cdot) and nitrogen dioxide (NO_2) in the presence of the nitrosyl cation (NO^+). Once the RONS reach the cell, they might activate cell surface receptor and propagate opening of pores and membrane channels. In case RONS gain access to different cell compartments, the levels of RONS attained in the cell are crucial for their influence on cell fate. At physiological low levels, RONS functions as 'redox messengers' in cellular signaling and regulation, whereas excess ROS induce various oxidative damage to proteins, lipids and DNA. In turn these alterations inactivate metabolic enzymes, ionic pumps, and structural proteins, disrupt cell membranes and break nucleic acids, resulting in the dysfunction of multiple cellular processes [84], [85], [86].

Due to the short life time of radicals, this process seems to be time dependent, as pre - treatment of the medium and storage of the medium for over an hour before applying it onto the cells reduced the effect of CAP on cell proliferation (figure 12). Applying pre - treated medium immediately to LN18 cells showed only minor reduction of proliferation compared to treatment of cells in medium (figure 12), as also issued by Vandamme and co-workers for U98MG cells treated with plasma floating electrode dielectric barrier discharge (FE - DBD) [87], [34]. To minimize the influence of medium on the CAP effects on cells, further experiments

were carried out with as less liquid as possible without damaging the cells (figure 13A). This composition resembles the situation in the patient/ tissue, where cells are enclosed by a thin film of liquid.

2. Effects of CAP on TMZ -resistant and -sensitive glioma cell lines

Up to now the methylation status of the MGMT promoter is the only predictive marker in glioblastoma. Patients with an epigenetically silenced MGMT promoter (MGMT negative) have an improved median overall survival when treated with TMZ [88]. No alternative therapy exists for patients with an unfavorable MGMT promoter methylation status (MGMT positive). Therefore both MGMT negative and positive cell lines (figure 14A) were analyzed concerning their response to TMZ and CAP. TMZ offered only minor effects on the proliferation of glioma cell lines, especially on the cell lines with an unmethylated MGMT promoter (figure 14B). Noteworthy, the inhibition of cell proliferation by TMZ was less than published by others before, who showed a reduction of 20 - 40 percent by similar TMZ concentrations. CAP treatment, however, had a distinct effect on proliferation, as it reduced the viability by 50 – 80 percent independent of the MGMT status of the cells (figure 14C). Together with the reduced clonogenic potential observed in both TMZ -resistant and -sensitive cell lines (figure 19), the present data indicate that CAP might be a novel treatment option in TMZ -resistant cell.

Nevertheless, it was not possible to detect induction of severe apoptosis by immunoblotting for the apoptosis marker Caspase 3 and Caspase 9 between 4 h and 72 h after CAP treatment (figure 15B and 15C). Using a plasma jet device other groups were able to show apoptosis by Annexin V staining and TUNEL in neuroblastoma [43], in melanoma cells [89] and pancreatic cells [39]. The DNA damage markers γ H2AX and cleaved PARP1 were only present 48 h and 72 h, respectively, after CAP treatment using the SMD device (figure 15A), indicating that primary CAP effect on glioma cells might not be the induction of apoptosis but may ultimately lead to severe damage of the cells.

The robust induction of a cell cycle arrest in the G2/ M phase rather than induction of apoptosis (no sub-G1 DNA content present) after CAP application is in line with observations of TMZ effects in glioblastoma (figure 17). It is known that DNA lesions induced by TMZ lead to cell cycle arrest in S or G2/ M phase and senescence instead of direct apoptosis [90], [91], [92]. Glioma cells often feature DNA modifications of genes that are important for efficient DNA repair and cell fate. The role of p53 was described by Hirose, demonstrating that in p53 - proficient human glioma cells TMZ did not induced apoptosis but rather a prolonged, p53 - associated G2/ M arrest and senescence [93]. Only a small fraction of cells underwent apoptosis. p53 is not necessary for this G2/ M arrest to occur but is important for the duration of G2/ M arrest and the ultimate fate of TMZ - treated cells. In addition, DNA lesions induced by TMZ activate the p53 - controlled DNA damage response pathway. Activation of p53 suppresses MGMT gene

activity after TMZ exposure. Consequently, tumors containing wild-type p53 are more responsive to TMZ than tumors containing mutant p53 [94], [95]. In the present investigation, most cell lines used in cell cycle experiments had mutated p53 (LN18, LN229, T98G). Hirose and colleagues demonstrated that the p53 wild type cell line U87MG underwent G2/ M arrest associated with Chk1 activation and phosphorylation of both Cdc25 and Cdc2 when treated with TMZ [92].

Our findings were supported by the publication on successful CAP treatment of glioma cells in a subcutaneous mouse model [96]. Here the authors could demonstrate potential antitumor effects of FE-DBD plasma on U87MG-Luc cells *in vitro* and in glioma xenografts by repeated treatments (five days 6 min each). They confirmed a power input dependent cell cycle arrest in S phase (low and high power) or G2/ M phase (only low power), leading to cell death especially for the high power mode. An increase in DNA damage was observed for both power settings 1 h after treatment (20 and 40 percent, respectively). *In vivo* CAP treatment of subcutaneous implanted U87MG cells for 5 days/ 6 minutes consecutively revealed a significant lower tumor volume compared to untreated tumors. Vandamme and colleagues speculate that plasma components act either by penetrating in the tissue or by inducing ROS releases in the tumor. Recent publications demonstrated beneficial effects of CAP in various *in vivo* models of tumors, among melanoma, pancreas carcinoma and neuroblastoma [35], [39], [43].

One of the most important hallmarks of malignant gliomas is their ability to infiltrate diffusely into the normal brain parenchyma. At the clinical level, the diffuse nature of GBMs can be illustrated by the fact that after surgical resection, a residual pool of invasive cells gives rise to a recurrent tumor. More than 90% of the cases develop immediately adjacent to the resection margin or within several centimeters of the resection cavity, but satellite lesions may also occur at a distance from the resection cavity and even in the contralateral hemisphere. Thus, migration and invasive behavior is a critical issue to therapy success. Cell adhesion, motility and invasion require receptor turnover (adhesion) and the reorganization of cytoskeleton elements (motility) creating an intercellular space in which invading cells can migrate (invasion) [97]. Using a wound healing assay we found reduced migration in glioma cells after CAP treatment in both TMZ -resistant and -sensitive cell lines when treated for 120 seconds and longer (figure 20). It is well known that CAP is capable of modifying surfaces, which is i.e. utilized for surface sterilization. The observed disruption of migration therefore might be due to alterations on the dish surface leading to detachment of the cells and/ or the inability of cells to (re-) attach. Moreover, CAP might be able to alter cell - cell interactions and adhesive abilities of cells with specific extracellular matrix (ECM) components. The induction of large openings of tight junctions by plasma jet treated medium [98] and loss of adhesion by treatment with a plasma needle [99], [100] are still under discussion.

3. Combined treatment with CAP and chemotherapy

The present results indicate that CAP is capable of restoring the sensitivity of TMZ -resistant cells towards chemotherapy. Concomitant treatment with a single application of CAP and repeated administration of TMZ revealed synergistic effects even in resistant cells (figure 21 and 22). Cells treated with a combined therapy comprising 30 seconds (LN18, T98G, U87MG) or 60 seconds (LN229) of CAP and concomitant TMZ administration (50 μ M, 100 μ M or 200 μ M) for three days displayed a significant reduction of cell viability (figure 21). Combined therapy was not only more effective compared to exclusive treatment with TMZ or CAP, but it revealed synergistic effects. Notably, combined treatment with 30 seconds plus 50 μ M of TMZ and combination of 30 seconds of CAP plus 100 μ M of TMZ, respectively, revealed stronger inhibition compared to higher dosage of TMZ (200 μ M and 100 μ M, respectively) in the LN18 and U87MG cell lines. Thus, concomitant therapy with CAP and TMZ significantly increases the effectiveness of TMZ both in cells with favorable and unfavorable MGMT status.

Furthermore, cell cycle arrest after CAP treatment was found to be prominent in glioma cells that are unsusceptible towards treatment with TMZ for up to 200 μ M *in vitro* (figure 22). A remarkable induction of a cell cycle arrest in the G2/ M phase in the TMZ -resistant cell line LN18 after CAP treatment of 60 seconds and longer or, 120 seconds and longer, respectively in the T98G cells was noticed. Only administration of high dosage of 500 μ M of TMZ could induce a similar cell cycle arrest in these resistant cell lines. In contrast, a combined treatment of 60 seconds of CAP and 50 μ M TMZ led to a cell cycle arrest, the combination of 60 seconds of CAP with 100 μ M or 200 μ M achieved an even more distinct arrest.

Keeping in mind that achievable TMZ levels in glioblastoma patients do not exceed 50 μ M in the blood plasma and 5 - 10 μ M in the cerebrospinal fluid [101], [102], an efficacy of a combined reduced dosage of TMZ with an additive therapy is desirable. In order to compare *in vitro* concentrations and efficacy of treatment with clinical practice, determination of MTIC levels would be more reasonable as TMZ, a pro-drug, which is rapidly hydrolyzed to its reactive methylating agent MTIC after oral administration. In publications addressing cell culture experiments various TMZ concentrations ranging from 10 μ M to 1000 μ M are applied. Low dosage of 50 μ M TMZ are often efficient to inhibit MGMT negative human GBM cells [103], while for inhibition of MGMT positive cells typically more than 10 fold higher concentrations are necessary [104].

A mechanism, comparable to the one described by Hirose for the concomitant treatment with TMZ and radiation, is conceivable for the observed synergistic effects of TMZ and CAP. They demonstrated that TMZ induces G2/ M cell cycle arrest, thereby increasing the potential for radiation - induced injury because radiotherapy has maximum cytotoxic effect during this phase of the cell cycle [93]. A study in glioblastoma cell lines by van Rijn et al. showed that the application of TMZ either led to an additive or supra-additive effect when combined with

radiotherapy, with an altered effect depending on the particular cell line [105]. CAP therefore might act in synergy with TMZ and possibly by multiple mechanisms, including impairment in DNA repair processes or via imbalance of reactive species in the cells. In fact, it was demonstrated by Laval and co-workers, that nitric oxide has an inhibitory dose- and time-dependent effect on DNA repair enzyme MGMT [106].

Our results on synergistic effects in combined therapy with CAP and a chemotherapeutic is in line with the findings by Brullé and colleagues, who observed an induction of inhibition in MIA PaCa2-Luc pancreatic cell proliferation *in vitro* and *in vivo* in orthotopic xenografts by application of a “plasma gun” DBD. This effect could be improved by association with gemcitabine [42], as tumors treated with combined therapy (three times plasma for 10 min plus 6 times gemcitabine) revealed a reduced tumor mass (33 percent reduction).

4. CAP displays cell selectivity towards tumor cells

A critical issue concerning CAP application is the selectivity of the treatment towards tumor cells. First insights into a possible cell selectivity by CAP was gained by treatment of non-tumorous primary astrocytes and an *ex vivo* murine brain slice model containing implanted glioma cells. The significant cell cycle arrest in G2/ M phase achieved in tumor cells by 60 seconds and longer was not detectable in primary murine astrocytes by CAP treatment times of up to 180 seconds (figure 23). However, an increase of cells residing in the S phase of the cell cycle after 180 seconds of CAP was observed. These results indicate that a “therapeutic window” - where tumor cells are affected but non-tumorous, healthy cells persist unharmed - might be found. It remains speculative why primary astrocytes are less prone to CAP treatment, however one hypothesis is that brain cells proliferate less than tumor cells and thus have a reduced uptake of reactive species produced by CAP. Furthermore, non-tumorous cells have lower ROS levels compared to tumor cells which exhibit a high energy metabolism. ROS amounts in tumor cells will reach cytotoxic levels earlier than the ones in non-tumorous cells, an outcome that is enforced by an insufficient anti-oxidant system in tumor cells.

In 2010, Georgescu and Lupu were among the first to address possible selectivity of CAP towards cancer cells using macrophages and colon cancer cells or melanoma cells, respectively [107]. Other publications corroborated these findings comparing effects of CAP on melanoma cells and keratinocytes [108], ovarian cancer cells and fibroblasts [109], human lung cancer cell lines and human lung normal cell lines [110] as well as glioma cells and human embryonic kidney (HEK) cells [111]. The disadvantages of these approaches are the lack of comparability between the used cell lines and used plasma devices (e.g. glioma compared with kidney cells and plasma jet compared with DBD) and that the cell culture experimental settings are highly artificial, as the origin of the cells as well the microenvironment might be crucial for the specific

response to CAP. Furthermore, equal distribution of CAP as a gas is assured in cell culture settings where cells are exposed as a monolayer, but CAP might induce different effects in connective tissue.

Therefore, we established an *ex vivo* murine organotypic brain slice culture (OSC) model where slices of newborn mice brain were maintained. Glioma cells expressing GFP were injected and proliferation and spreading of the cells was monitored for 14 days via fluorescence (figure 24). An advantage of the OSCs are the comparability of CAP effects on healthy and tumorous cells of the same origin plus the possibility to investigate CAP effects on tumor cells in tissue eliminating the influence of liquids on the effect(s). An *in vivo* subcutaneous mouse model as utilized by Vandamme et al. [41], [96] also lacks the desirable microenvironment of the tumor and leaves the open - ended question how plasma could reach the tumor through the skin as the penetration depth for DBD and Plasma jet devices was found to be $\sim 50 \mu\text{m}$ [112], [39]. An intracranial animal model on the other hand would require a particularly small and flexible plasma device featuring the same characteristics as the FlatPlaSter, which was not available by the time.

Fluorescence microscopy of the OSCs containing LN18pEGFP 14 days after implantation retained cells migrated within the slice thickness rather than on the surface of the slice (figure 24), which is in line with the observation made by Bouïard et al. [113] and Ohnishi et al. [114]. GFP expressing tumor cells were located 80 - 160 μm within the slices, illustrating migration and viability of the cells after 14 days. These results corroborate OSCs as a promising model for investigating the CAP effects on cancer cell proliferation, migration and cell selectivity. Noteworthy, four times of CAP application of 60 seconds and longer reduced the external diameter of the grown tumor consistent of LN18 glioma cells in the OSCs, but did not significantly reduce the migration depth within the tissue. Histological analyzes of the tissue after 14 days clearly demonstrated tumor formation shown by staining with HE, GFAP, Mib-1 and mut p53 (figure 25A). Unfortunately, large necrotic areas even within the untreated slices hamper a distinct statement on cell selectivity. Nevertheless, preliminary data on staining with p-Cdc25c suggest a possible induction of cell cycle arrest in the CAP treated tumor cells compared to the control (figure 25B). Cell division cycle 25 (Cdc25a, b and c) phosphatases regulate key transitions between cell cycle phases during normal cell division, and in the event of DNA damage or genotoxic stress they are main targets of the checkpoint machinery that ensures genetic stability. The dysregulation of Cdc25 phosphatases is often involved in malignant transformation while overexpression is correlated with poor prognosis in many diverse cancers. The inhibition of these proteins therefore represents an attractive therapeutic target in oncology. In eukaryotic cells the three major checkpoints are the transition from G1 to S phase, the intra - S phase and the transition from G2 phase to mitosis. Replication errors, stalled replication forks or damaged DNA by extracellular factors such as UV light or ionizing radiation is sensed by the ataxia-telangiectasia mutated (ATM) and ATM and Rad3-related (ATR)

kinase families. Activation of ATM and/ or ATR is necessary to coordinate cell cycle arrest, to stabilize the replication fork and for mediating DNA repair. Cell cycle arrest is imposed by activation of two downstream kinases, Chk1 and Chk2. Chk1 is activated by DNA damage during interphase, whereas Chk2 is activated in response to stalled replication forks during S phase. In human cells, Chk1 and Chk2 phosphorylate the N-terminal region of Cdc25c on Ser216. Phosphorylation of Cdc25c leads to 14-3-3-mediated sequestration of the phosphatases away from their substrates and consequential maintenance of CDK1/ cyclin B in the phosphorylated and inhibited state (figure 26).

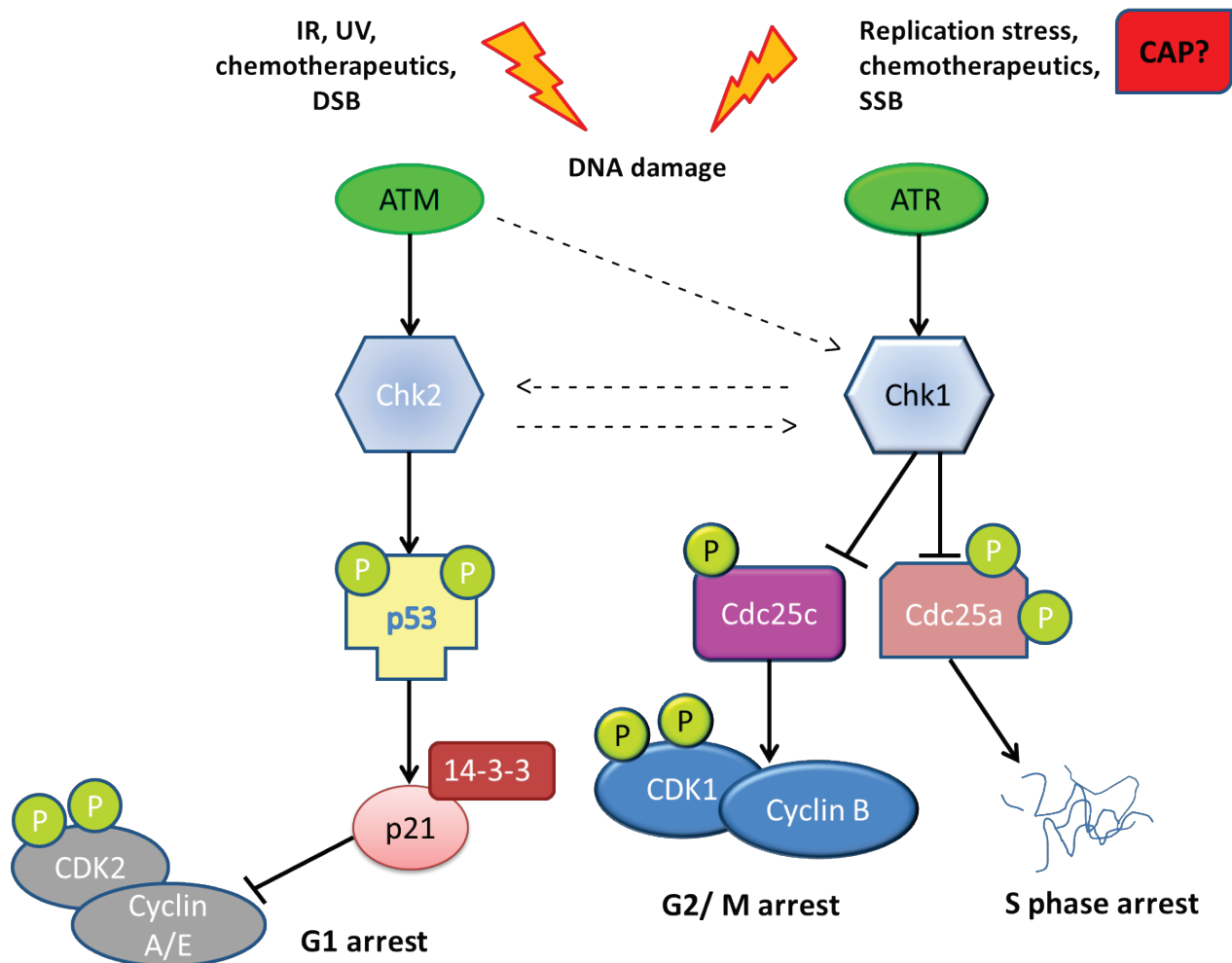


Figure 26: Signaling pathways of the cell cycle control. Cells exposed to ionizing radiation (IR), ultraviolet light (UV), chemotherapy resulting in dsb or cells with ssb as a result from stalled replication forks respond by activating kinases of the ataxia-telangiectasia mutated (ATM) protein family. ATM and ATM related (ATR) phosphorylate and activate the checkpoint kinases Chk1 and Chk2. The checkpoint kinases

are transducers of the DNA damage signal and both phosphorylate a number of substrates involved in the DNA damage response. Chk1 phosphorylates, among others, Cdc25c at Ser 216, creating a binding site for 14-3-3 proteins, which then act by excluding Cdc25c from the nucleus. Cytoplasmic delocalization of Cdc25c prevents cyclin-dependent kinase 1 (CDK1)/ cyclin B from dephosphorylation, thereby suppressing the promitotic activity of this complex. The G2/ M checkpoint prevents entry into mitosis with unrepaired DNA lesions (modified after Ashwell and Zabludoff [115]).

CAP seems to act either as an external stimulus inducing genotoxic stress and activating the cell cycle checkpoints via phosphorylation of Cdc25c or by generating high intracellular ROS levels hence taking action in signaling cascades. ROS are known to influence cell cycle progression via phosphorylation and ubiquitination of CDKs and cell cycle regulatory molecules [116], [117]. Brisson et al could establish that ROS exert their effect on Cdc25 activity via enhancing phosphorylation of Cdc25 or alternatively through inactivation of Cdc25 by sulfonation of cysteine in the active site [118]. Evidence is given that intracellular formation of ROS by CAP is a mediator of CAP efficiency in eukaryotic cells [87], [119]. Kalghatgi and colleagues presented that usage of the ROS scavenger NAC completely blocked phosphorylation of H2AX after DBD plasma treatment of MCF10A cells, which was supported by direct measurement of intracellular ROS and by the formation of malondialdehyde (MDA), a lipid peroxidation product [119]. However, they found that DBD plasma - induced lipid peroxidation is not responsible for the observed DNA damage which points towards different mechanisms of CAP produced by a DBD compared to a SMD device. We could not observe strong induction of phosphorylation of H2AX nor was the ROS scavenger NAC able to block SMD induced CAP effects (data not shown). Lipid peroxidation, in our experimental setting, likewise was not responsible for the reduced cell viability and cell cycle arrest. Stable knockdown of ALDH1A1, an enzyme able to detoxify reactive aldehydes as MDA or 4-hydroxynonenal (4-HNE) [120], in LN18 cells treated with CAP did not reveal a re-established viability (supplementary data S35A) or cell cycle progression (supplementary data S35B). Thus, lipid peroxidation might not be the main target in glioma cells by CAP. Kalghatgi further proposed an ATR dependent phosphorylation of H2AX following plasma treatment, suggesting that CAP may lead to replication arrest or formation of single-stranded DNA breaks [119]. This is in line with the phosphorylation of Cdc25c in OSCs which we found after repeated CAP treatment. Cdc25c is a key mediator of G2/ M phase arrest downstream of the ATM/ ATR signaling pathway, which seems to be involved in mediating CAP effects in tumor cells. Further experiments need to be done to elucidate whether CAP itself activates this pathway by directly producing genotoxic stress or if DNA damage is induced by creating high intracellular ROS levels. Adjustments on OSCs and investigation of the signaling pathways involved in mediation of the CAP effects on eukaryotic cells are necessary and of high scientific interest.

G. Assessment and Outlook

Application of CAP in the medical field gained a lot of interest, ranging from inactivation of various bacterial strains relevant in hospital hygiene, inactivation of spores and viruses to clinical phase II studies on the treatment of chronic wounds. In addition, CAP is a new auspicious candidate in cancer treatment. CAP application in the context of a broad spectrum of different tumor entities has been explored. Besides applied research investigating the application of CAP in cancer therapy, CAP treatment provides the opportunity of a deeper understanding of the tumor behavior regarding the role of radicals and tumor metabolism. Modification of the plasma chemistry produced by the device discriminating between oxygen and nitrogen based chemistry and investigation of the specific effects induced thereby, might provide new insights into tumor behavior and tumor progression. In non-tumorous tissue and cells, oxidative phosphorylation (OxPhos) couples ATP production to the flow of electrons through the electron transport chain (ETC) within the mitochondrial energy metabolism. In contrast, most cancer cells instead rely on aerobic glycolysis, a phenomenon known as the 'Warburg effect' [121], [122]. Based on their results with TMZ -resistant and TMZ -sensitive glioma cells, Oliva and colleagues proposed a new mechanism of adaptive chemoresistance in glioma cells linking both oxidative stress and drug resistance in cancer cells leading to a suppressed apoptotic signaling [123]. Low electron flux through the ETC can promote increased generation of superoxide radicals in cancer cells, while TMZ -resistant glioma cells under conditions of oxidative stress generate less ROS probably due to an increased capacity for electron flux through the ETC. Experiments with ρ^0 cells lacking a functional ETC and which are incapable of generating ATP and ROS at the mitochondrial level, indicate that TMZ sensitivity arises from enhanced ROS production of the mitochondrial ETC. TMZ -resistant cells were found to have a significant reduced ROS production which was associated with enhanced chemoresistance. CAP efficacy in TMZ -resistant glioma cells might therefore result from mitochondrial - independent ROS production or uptake of extracellular ROS produced by CAP.

Three main issues in cancer application of CAP are still under discussion: The topic which is investigated best refers to the interaction of tumors/ tumor cells with CAP. In summary, most investigators found a cell cycle arrest and senescence induced by low concentrations of reactive species (driven by low power input), whereas high density flux (high power input) led to apoptosis or yet necrosis. The plasma device used in the present study is working in the reactive oxygen species rich mode, inducing an inhibition of proliferation and a prolonged cell cycle arrest in the G2/ M phase. The FlatPlaSter 2.0 was operated with low power input (10 mW/cm²). In contrast to devices mentioned above, the power input of the SMD device does not influence the density of total reactive species. The key characteristic using the low power input is the production of mainly reactive oxygen species, like ozone. As stated in the introduction, high power input generates nitrogen based chemistry and less oxygen based species.

Differences in cell fate seem to be dependent on the type of tumor cell as well as the plasma device and the produced plasma chemistry. Outstanding is the observed efficacy of CAP treatment in TMZ -sensitive and -resistant glioma cells *in vitro*, which withstand most therapeutic modalities so far. Combined therapy of CAP and TMZ discovered synergistic effects in resistant glioma cells, restoring sensitivity of chemoresistant cells towards therapy with the alkylating agent TMZ.

The second main topic concerning CAP in cancer treatment is the mechanism that promotes CAP effects on tumor cells. A raising number of publications propose the produced reactive oxygen and nitrogen species (ROS and RNS) to induce anti-cancer effects separately or in conjunction with the UV light or the electrical field produced. Interactions on the cell surface are believed to play an important role, as formation of “nanoholes” or pore opening by lipid peroxidation of the membrane could mediate CAP effects [124], [125]. Yet, the composition of produce species by CAP is not defined completely. The characterization of the FlatPlaSter 2.0 in the low input power mode revealed mainly the production of oxygen - based species. The work presented here did not focus on these aspects of CAP application, as the characterization of the device was conducted simultaneously with the experiments on cells. Moreover, it remains unsettled which reactive species and components effectively reach the desired cells/ tissue. The distance between electrode and cells/ tissue as well as the quantity and nature of interphase(s) are crucial. The distance between the electrode and the sample was set as 14 mm, thus electrons, ions and neutral species (long and short life time) could reach the sample. Treatment was carried out with only a thin film of medium covering the cells to reduce medium induced effects on the cells. Transport of reactive species out of discharge region, through the gas phase into the liquid phase clearly alters the composition of the RONS. Moreover, the presence of liquid can modify both the reactive oxygen and nitrogen species generated in the gas phase due to evaporation of water molecules. Estimation of how the produced species dissolve and react in liquid is important, as the amount of species dissolves in liquid depends on the kind of species produced. While using a SMD device, no electrical current flows through the sample in contrast to DBD devices which use the sample as the second electrode. Obviously, substantial modifications and standardized settings will be necessary to compare relevant publications.

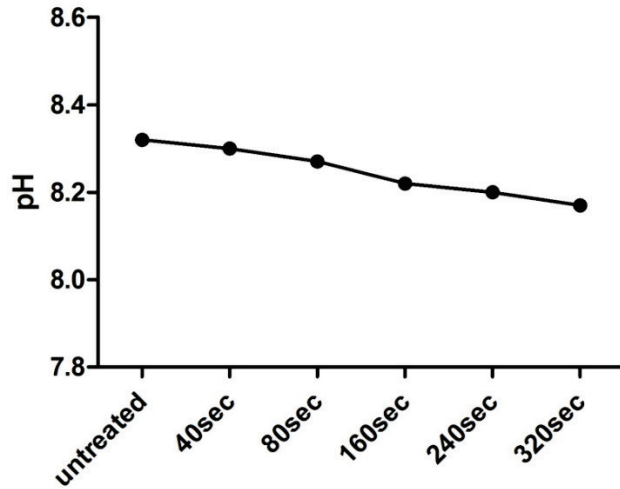
The third issue discussed is the cell selective property of CAP. Whereas most of the literature compares CAP effects on tumor cells with immortalized cell lines, additionally often derived from a different origin, we related the effects of CAP on glioma cells to the effects on freshly prepared primary astrocytes. Primary astrocytes showed a delay of induction of cell cycle arrest in the S phase after 180 seconds of CAP treatment. In comparison CAP treated tumor cells exhibited a strong cell cycle arrest in the G2/ M phase already after 60 seconds. These results indicated a possible ‘therapeutic window’ for the treatment of glioma cells by this SMD device. Advancement was made by establishing an orthotopic *ex vivo* model of murine brain slice

cultures. This model enables addressing both efficacy of tumor inhibition and cell selectivity of CAP in the appropriate microenvironment of the tumor.

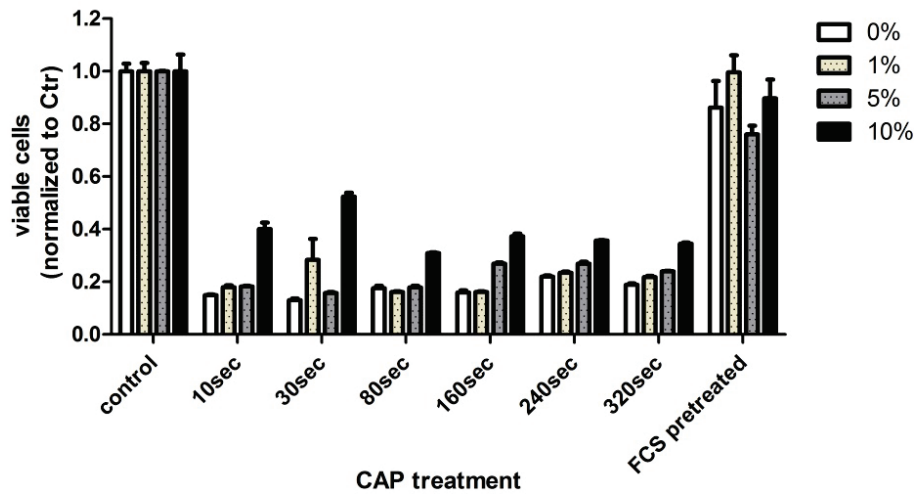
A possible proposal regarding clinical applications of this technology would be an “endoscopic” device, which is flexible and would be applicable in difficult to access regions. Following primary resection CAP application of the surgical cavity would be beneficial in eliminating microscopic residues of the tumor, thereby limiting recurrent disease. CAP would synergize best with an intra - operative chemotherapy such as Gliadel, as the CAP effect on cell cycle inhibition persists on the order of days (figure 18) [126]. We are hopeful that delivery of CAP will be feasible during surgery, permitting treatment of tumor beds and novel localization beyond superficial treatment. Obviously, significant modifications and improvements to the technology will be necessary to realize this ambition.

H. Supplementary Data

Supplementary figure S26: PH change of DMEM supplemented with 1% FCS after CAP



Supplementary figure S27: CAP effects on FCS



Supplementary figure S28: Western blot detection of DNA damage and induction of apoptosis in LN229 cells treated with CAP

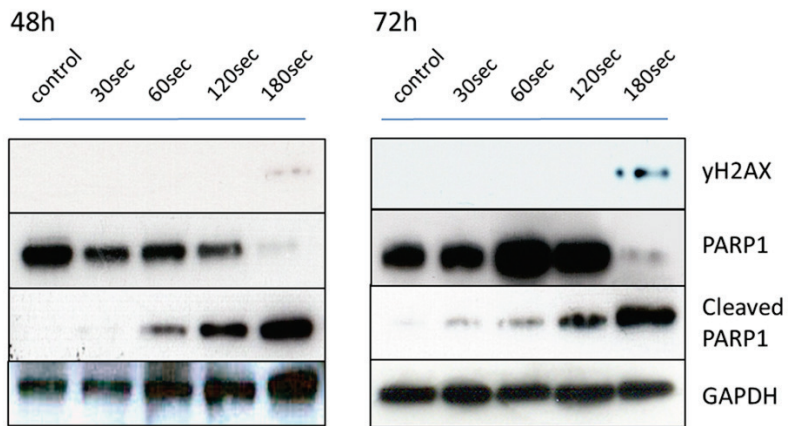
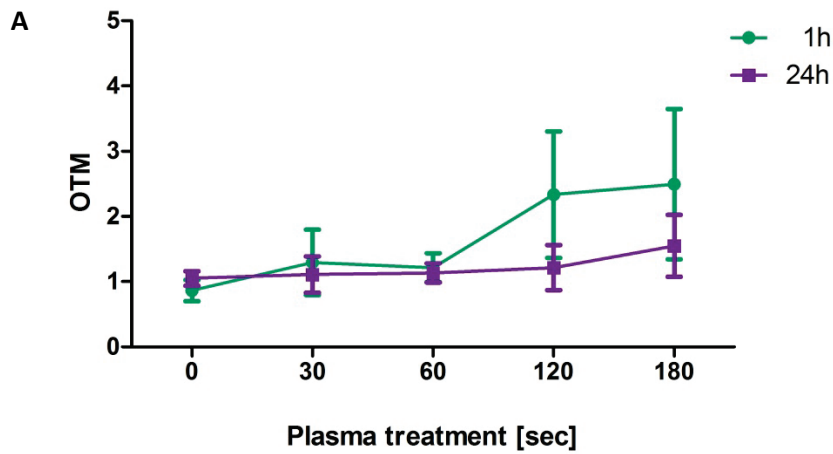


Figure S28: Immunoblotting revealed cleavage of PARP1 and activation of H2AX after 48 and 72 h in LN229 glioma cells.

Supplementary figure S29: Comet assay of LN229 glioma cells after CAP



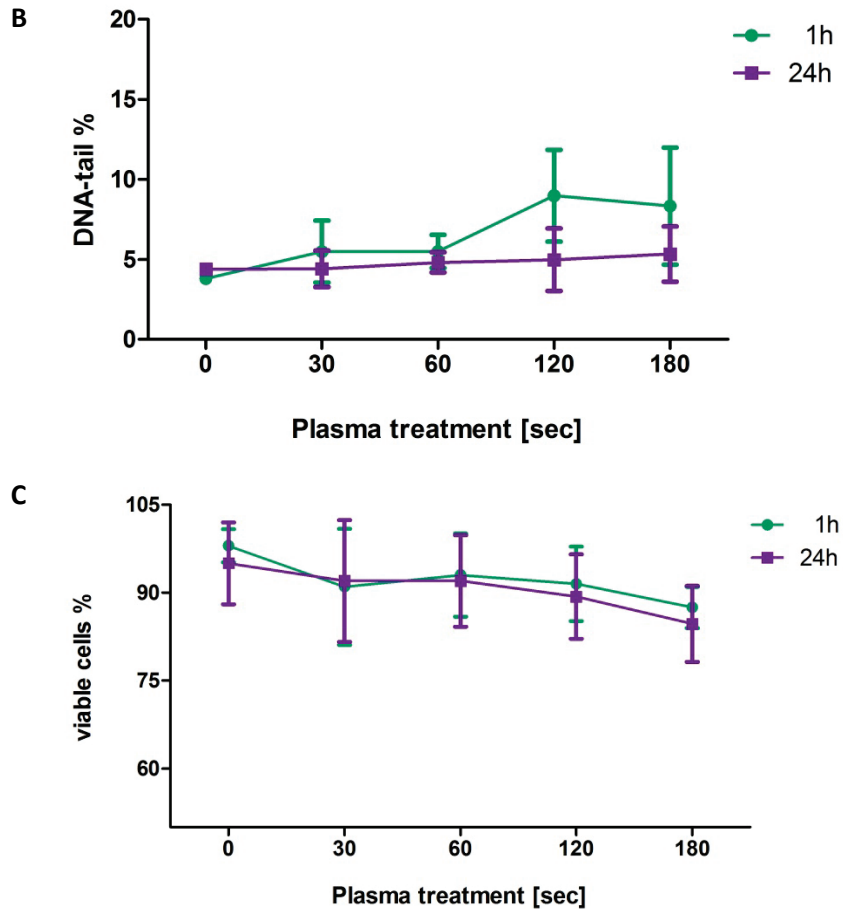
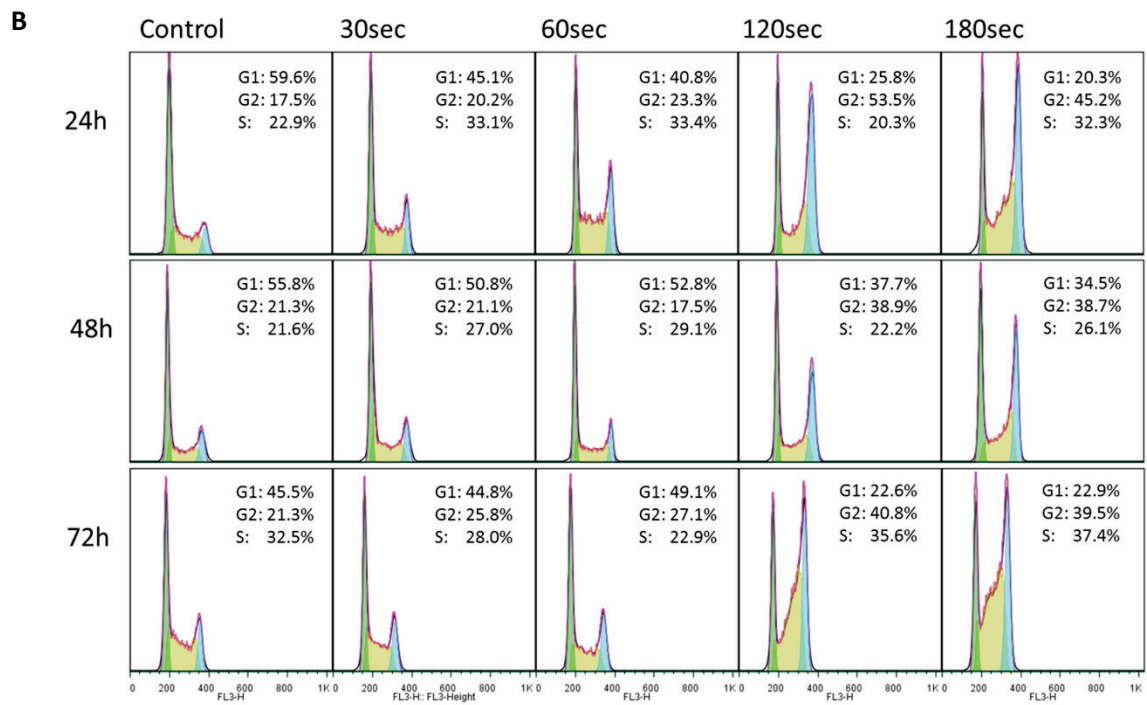
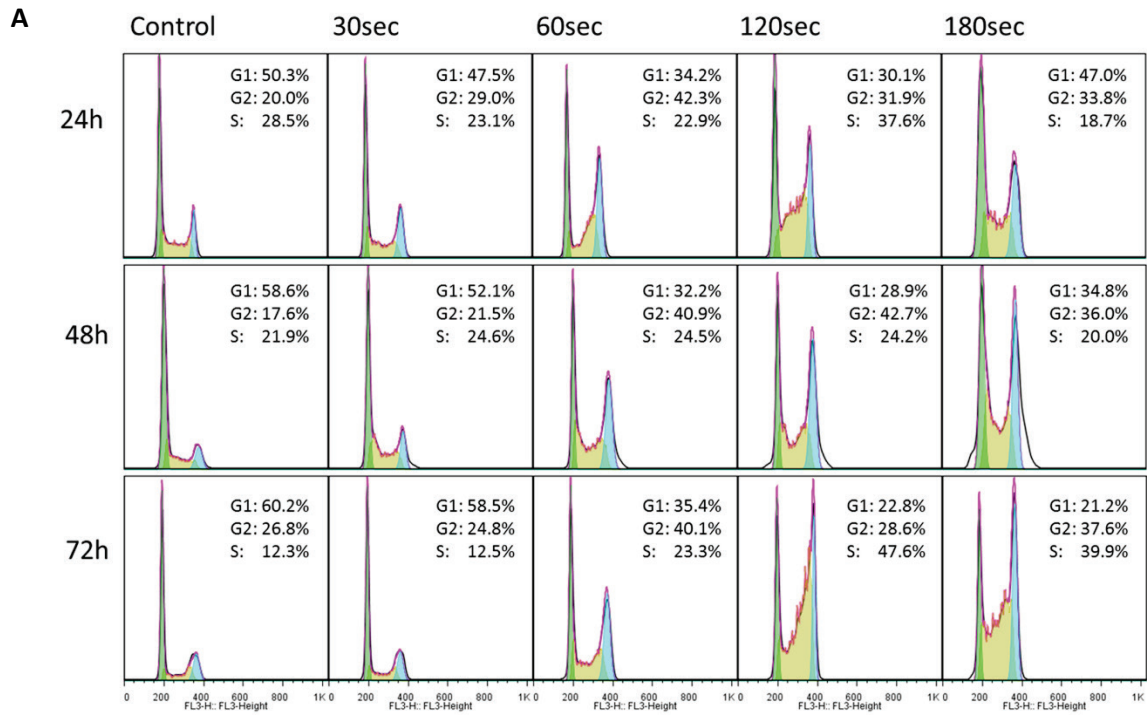


Figure S29: Comet assay analyzing OTM (A), percentage of DNA in tail (B) and testing for viability of the cells. Cell pellets from LN229 cells were resuspended 0.7 % low-melting agarose and applied to slides frosted at the edges and covered with 0.5 % normal melting agarose. For cell lysis slides were placed in alkali solution for 1 h. Prior to electrophoresis, the slides were placed in a horizontal gel electrophoresis chamber and incubated with alkaline buffer solution at pH 13.2. After 20 min of DNA unwinding, electrophoresis was started. Following neutralization fluorescent DNA staining was performed with ethidium bromide. Slides were analyzed and 80 cell nuclei per slide (2 slides per each CAP treatment) were selected with random pattern and digitized with the monochrome CCD camera (Cohu Inc., San Diego, CA, USA). Migration was measured by the image analysis software Komet++ (Kinetic Imaging, Liverpool, UK) using the % of DNA in tail and the Olive Tail Moments (OTM). The OTM represents the multiplication of the relative amount of DNA in the tail with the median migration distance. The % tail DNA is a measure of the relative fluorescent intensity in the head and tail. An OTM above 2 is widely accepted as DNA damage.

Supplementary figure S30: Cell cycle arrest is induced after CAP



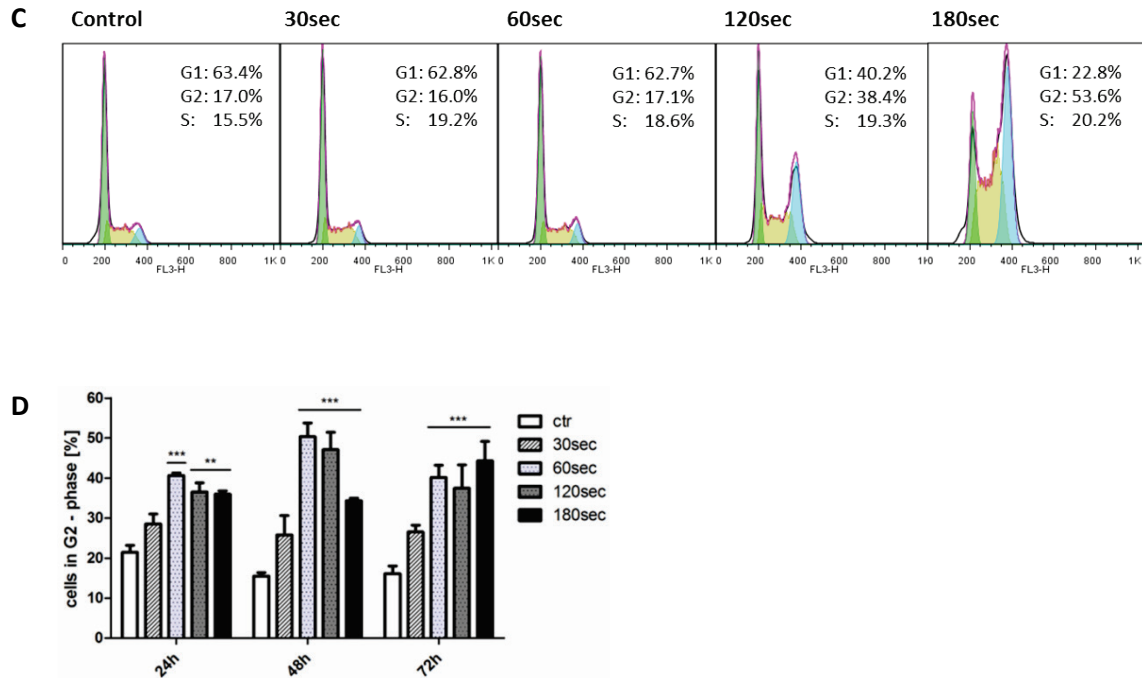


Figure S30: Cell cycle distribution of glioma cells after CAP application. **A** LN18 cells (TMZ-resistant) were CAP treated and flow cytometry was performed 24 h, 48 h and 72 h afterwards. **B** Cell cycle analysis of LN229 (TMZ-sensitive) after CAP application. **C** T98G (TMZ-resistant) cells were CAP treated and cell cycle distribution was detected 48 h afterwards. **D** Mean proportion of cells in G2/ M phase after CAP application in three independent experiments (P-value*** < 0.001) of LN229 cells and **E** of T98G cells.

Supplementary figure S31: Concomitant therapy with CAP and TMZ features synergistic effects in glioma cells

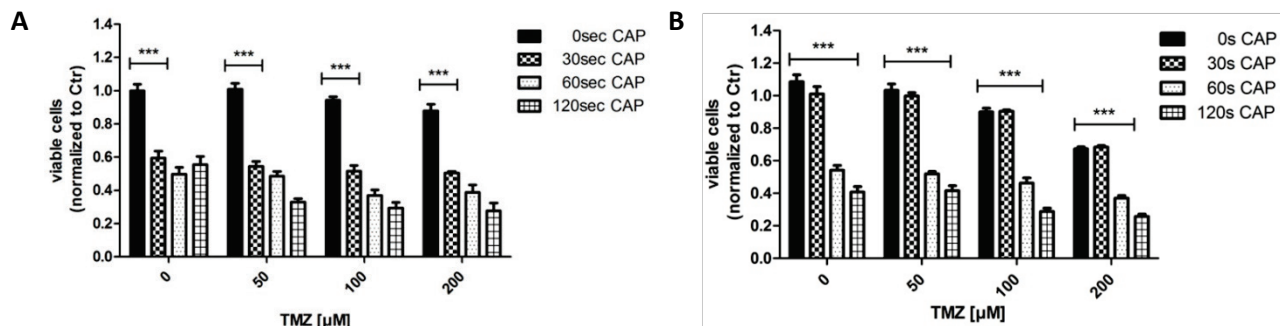


Figure S31: A T98G cells were first CAP treated once and TMZ was applied three days consecutively later. Viability was measured using MTT assay. **B** Viability of the LN229 cells after a single CAP treatment followed by three days of consecutive TMZ application.

Supplementary figure S32: Resistant glioma cells were re-sensitized of towards therapy with TMZ by CAP

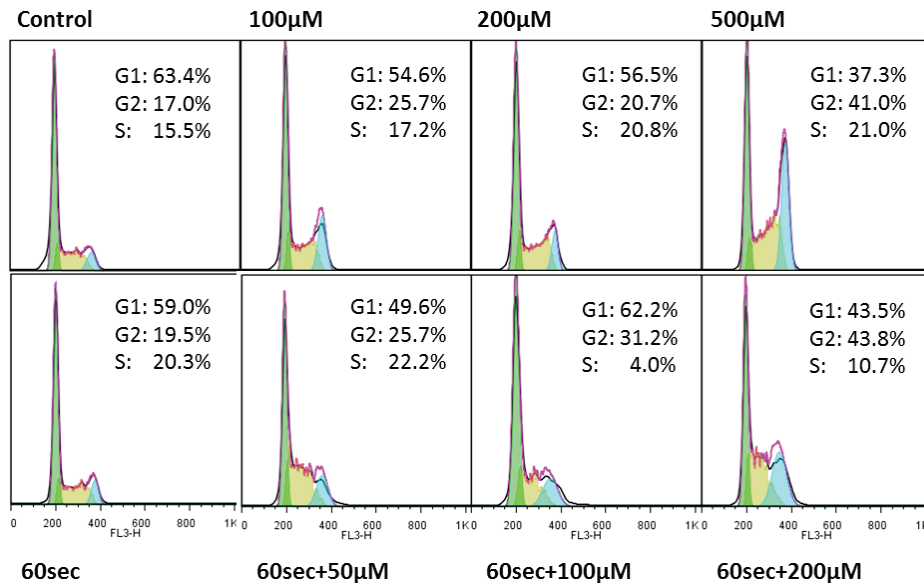


Figure S32: Combined treatment of CAP and TMZ was able to induce cell cycle arrest in resistant T98G cells. Cell cycle distribution of T98G cells after either TMZ alone (up to 500 µM) or concomitant treatment with CAP and TMZ (60 seconds plus TMZ).

Supplementary figure S33: CAP revealed similar effects on proliferation of LN18pEGFP compared to LN18 wt cells

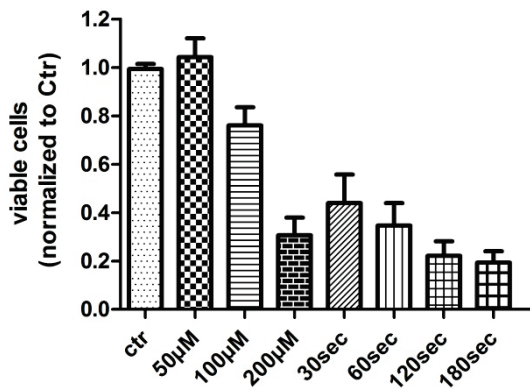


Figure S33: LN18pEGFP cells respond to treatment with CAP and TMZ similar to LN18 wt cells. LN18pEGFP cells were either CAP or TMZ (three days consecutively) treated and cell proliferation was measured afterwards.

Supplementary figure S34: Orthotopic brain slides cultures as a model for CAP selectivity

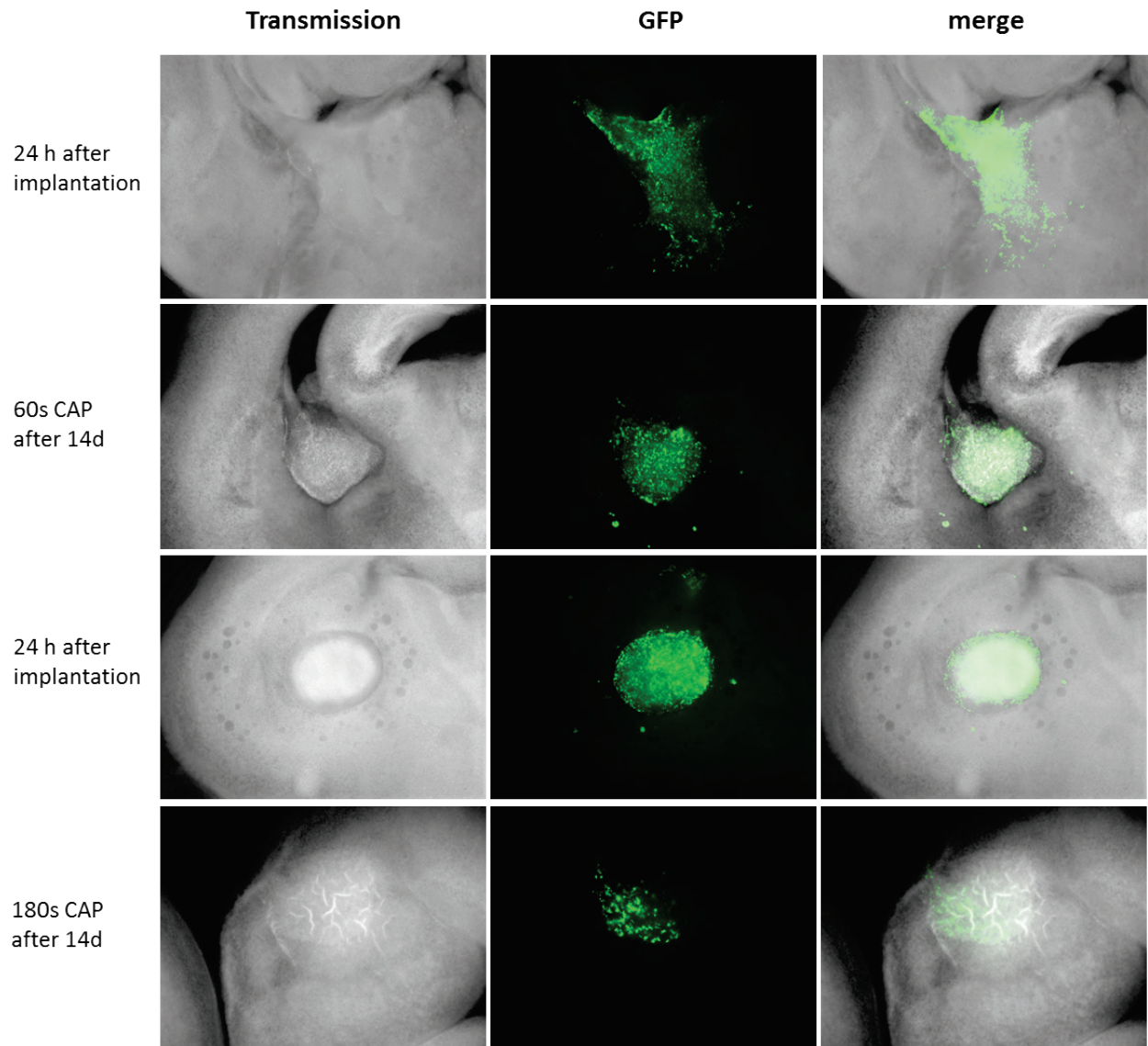


Figure S34: CAP displays cell selective properties. LN18pEGFP cells were transplanted onto orthotopic murine brain slices and allow settling for 24 h before CAP was applied onto the slices. Slices containing fluorescence expressing LN18 cells were monitored before and 14 days after CAP application.

Supplementary figure S35: ALDH1A1 knock down in glioma cells does not influence the effects of CAP on these cells

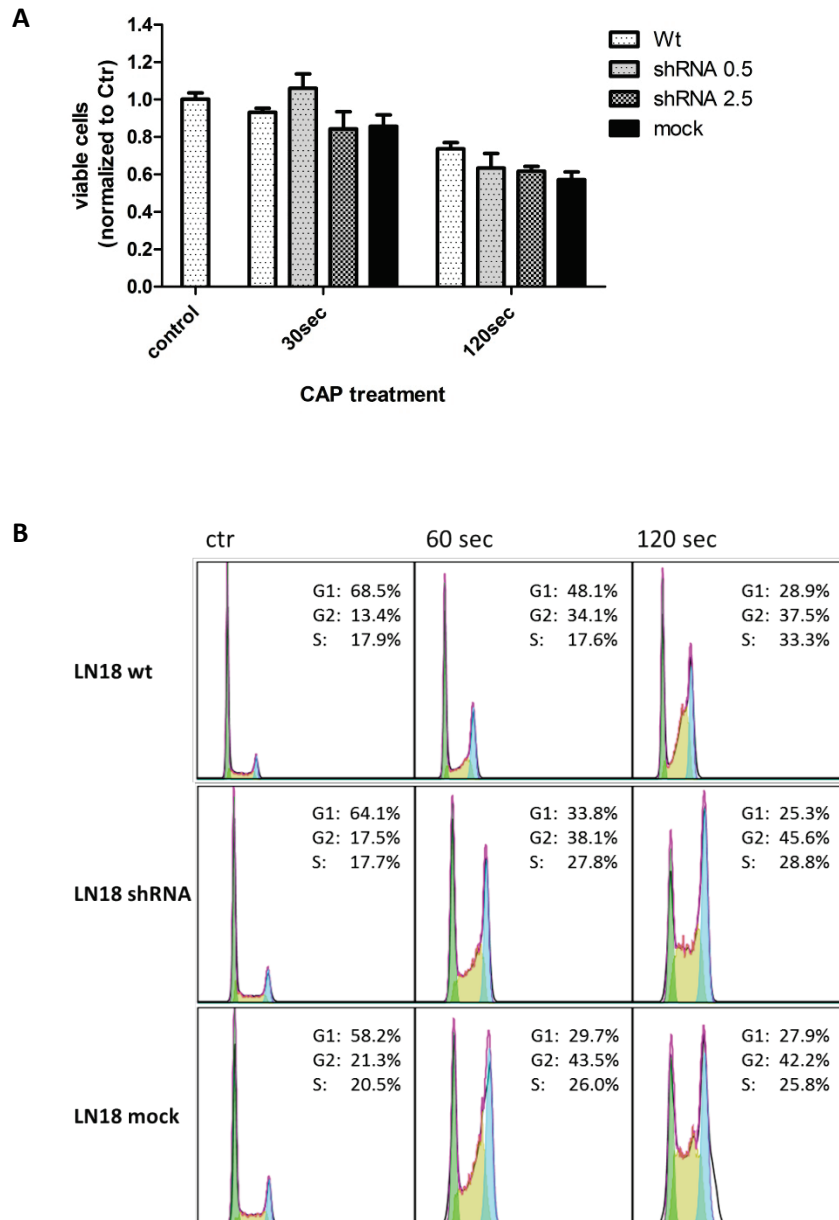


Figure S35: Lipid peroxidation induced by CAP might not be responsible for DNA damage in ALDH1A1 depleted glioma cells. ALDH1A1 was knocked down in LN18 cells and shRNA, mock and control cells were CAP treated. **A** Proliferation after CAP treatment for 30 seconds and 120 seconds was detected in LN18shRNA, LN18 mock and LN18 wt cells. **B** Cell cycle distribution 48 h after CAP treatment was analyzed in LN18 wt, LN18 ALDH1shRNA depleted and LN18 mock cells.

I. References

1. Langmuir I (1929) The interaction of electron and positive ion space charges in cathode sheaths. *Physical Review* 33: 0954-0989.
2. Isbary G, Heinlin J, Shimizu T, Zimmermann JL, Morfill G, et al. (2012) Successful and Safe Use of 2 Min Cold Atmospheric Argon Plasma in Chronic Wounds: Results of A Randomized Controlled Trial. *Br J Dermatol*.
3. Fridman G, Friedman G, Gutsol A, Shekhter AB, Vasilets VN, et al. (2008) Applied plasma medicine. *Plasma Processes and Polymers* 5: 503-533.
4. Dobrynin D, Fridman G, Friedman G, Fridman A (2009) Physical and biological mechanisms of direct plasma interaction with living tissue. *New Journal of Physics* 11.
5. Joshi SG, Cooper M, Yost A, Paff M, Ercan UK, et al. (2011) Nonthermal Dielectric-Barrier Discharge Plasma-Induced Inactivation Involves Oxidative DNA Damage and Membrane Lipid Peroxidation in *Escherichia coli*. *Antimicrobial Agents and Chemotherapy* 55: 1053-1062.
6. Fridman G, Peddinghaus M, Ayan H, Fridman A, Balasubramanian M, et al. (2006) Blood coagulation and living tissue sterilization by floating-electrode dielectric barrier discharge in air. *Plasma Chemistry and Plasma Processing* 26: 425-442.
7. Fridman G, Shereshevsky A, Jost MM, Brooks AD, Fridman A, et al. (2007) Floating electrode dielectric barrier discharge plasma in air promoting apoptotic behavior in melanoma skin cancer cell lines. *Plasma Chemistry and Plasma Processing* 27: 163-176.
8. Stoffels E, Flikweert AJ, Stoffels WW, Kroesen GMW (2002) Plasma needle: a non-destructive atmospheric plasma source for fine surface treatment of (bio)materials. *Plasma Sources Science & Technology* 11: 383-388.
9. Goree J, Liu B, Drake D, Stoffels E (2006) Killing of S-mutans bacteria using a plasma needle at atmospheric pressure. *Ieee Transactions on Plasma Science* 34: 1317-1324.
10. Walsh JL, Shi JJ, Kong MG (2006) Contrasting characteristics of pulsed and sinusoidal cold atmospheric plasma jets. *Appl Phys Lett* 88.
11. Laroussi M, Lu X (2005) Room-temperature atmospheric pressure plasma plume for biomedical applications. *Appl Phys Lett* 87.
12. Laroussi M, Hynes W, Akan T, Lu XP, Tendero C (2008) The plasma pencil: A source of hypersonic cold plasma bullets for biomedical applications. *Ieee Transactions on Plasma Science* 36: 1298-1299.
13. Shimizu T, Steffes B, Pompl R, Jamitzky F, Bunk W, et al. (2008) Characterization of microwave plasma torch for decontamination. *Plasma Processes and Polymers* 5: 577-582.
14. Morfill GE, Shimizu T, Steffes B, Schmidt HU (2009) Nosocomial infections-a new approach towards preventive medicine using plasmas. *New Journal of Physics* 11.
15. Kogelschatz U (2003) Dielectric-barrier discharges: Their history, discharge physics, and industrial applications. *Plasma Chemistry and Plasma Processing* 23: 1-46.
16. Sakiyama Y, Graves DB, Chang HW, Shimizu T, Morfill GE (2012) Plasma chemistry model of surface microdischarge in humid air and dynamics of reactive neutral species. *Journal of Physics D- Applied Physics* 45.
17. Shimizu T, Sakiyama Y, Graves DB, Zimmermann JL, Morfill GE (2012) The dynamics of ozone generation and mode transition in air surface micro-discharge plasma at atmospheric pressure. *New Journal of Physics* 14.
18. Pavlovich MJ, Chang HW, Sakiyama Y, Clark DS, Graves DB (2013) Ozone correlates with antibacterial effects from indirect air dielectric barrier discharge treatment of water. *Journal of Physics D- Applied Physics* 46.

19. Maisch T, Shimizu T, Isbary G, Heinlin J, Karrer S, et al. (2012) Contact-free inactivation of *Candida albicans* biofilms by cold atmospheric air plasma. *Appl Environ Microbiol* 78: 4242-4247.
20. Zimmermann JL, Dumler K, Shimizu T, Morfill GE, Wolf A, et al. (2011) Effects of cold atmospheric plasmas on adenoviruses in solution. *Journal of Physics D-Applied Physics* 44.
21. Hahnel M, von Woedtke T, Weltmann KD (2010) Influence of the Air Humidity on the Reduction of *Bacillus* Spores in a Defined Environment at Atmospheric Pressure Using a Dielectric Barrier Surface Discharge. *Plasma Processes and Polymers* 7: 244-249.
22. Klampfl TG, Isbary G, Shimizu T, Li YF, Zimmermann JL, et al. (2012) Cold atmospheric air plasma sterilization against spores and other microorganisms of clinical interest. *Appl Environ Microbiol*.
23. Maisch T, Shimizu T, Li YF, Heinlin J, Karrer S, et al. (2012) Decolonisation of MRSA, *S. aureus* and *E. coli* by cold-atmospheric plasma using a porcine skin model in vitro. *PLoS One* 7: e34610.
24. Lademann O, Kramer A, Richter H, Patzelt A, Meinke MC, et al. (2011) Skin Disinfection by Plasma-Tissue Interaction: Comparison of the Effectivity of Tissue-Tolerable Plasma and a Standard Antiseptic. *Skin Pharmacology and Physiology* 24: 284-288.
25. Isbary G, Morfill G, Schmidt HU, Georgi M, Ramrath K, et al. (2010) A first prospective randomized controlled trial to decrease bacterial load using cold atmospheric argon plasma on chronic wounds in patients. *Br J Dermatol* 163: 78-82.
26. Lupu AR, Georgescu N, Calugaru A, Cremer L, Szegli G, et al. (2009) The effects of cold atmospheric plasma jets on B16 and COLO320 tumoral cells. *Roum Arch Microbiol Immunol* 68: 136-144.
27. Kim G-CLHJ, Shon C.-H. (2009) The Effects of Micro plasma on Melanoma (G361) Cancer Cells. *Journal of the Korean Physical Society* 54: 625-632.
28. Kim CH, Bahn JH, Lee SH, Kim GY, Jun SI, et al. (2010) Induction of cell growth arrest by atmospheric non-thermal plasma in colorectal cancer cells. *Journal of Biotechnology* 150: 530-538.
29. Lupu AR, Georgescu N (2010) Cold atmospheric plasma jet effects on V79-4 cells. *Roum Arch Microbiol Immunol* 69: 67-74.
30. Kim CH, Kwon S, Bahn JH, Lee K, Jun SI, et al. (2010) Effects of atmospheric nonthermal plasma on invasion of colorectal cancer cells. *Appl Phys Lett* 96: 243701.
31. Vandamme M, Robert E, Lerondel S, Sarron V, Ries D, et al. (2011) ROS implication in a new antitumor strategy based on non-thermal plasma. *Int J Cancer*.
32. Volotskova O, Hawley TS, Stepp MA, Keidar M (2012) Targeting the cancer cell cycle by cold atmospheric plasma. *Sci Rep* 2: 636.
33. Kim JY, Ballato J, Foy P, Hawkins T, Wei Y, et al. (2011) Apoptosis of lung carcinoma cells induced by a flexible optical fiber-based cold microplasma. *Biosens Bioelectron* 28: 333-338.
34. Vandamme M, Robert E, Lerondel S, Sarron V, Ries D, et al. (2012) ROS implication in a new antitumor strategy based on non-thermal plasma. *Int J Cancer* 130: 2185-2194.
35. Keidar M, Walk R, Shashurin A, Srinivasan P, Sandler A, et al. (2011) Cold plasma selectivity and the possibility of a paradigm shift in cancer therapy. *Br J Cancer* 105: 1295-1301.
36. Ahn HJ, Kim KI, Kim G, Moon E, Yang SS, et al. (2011) Atmospheric-pressure plasma jet induces apoptosis involving mitochondria via generation of free radicals. *PLoS One* 6: e28154.
37. Thiyagarajan M, Waldbeser L, Whitmill A (2012) THP-1 leukemia cancer treatment using a portable plasma device. *Stud Health Technol Inform* 173: 515-517.
38. Barezki N, Laroussi M (2012) Dose-dependent killing of leukemia cells by low-temperature plasma. *Journal of Physics D-Applied Physics* 45.
39. Partecke LI, Evert K, Haugk J, Doering F, Normann L, et al. (2012) Tissue tolerable plasma (TTP) induces apoptosis in pancreatic cancer cells in vitro and in vivo. *BMC Cancer* 12: 473.
40. Arndt S, Wacker E, Li YF, Shimizu T, Thomas HM, et al. (2013) Cold atmospheric plasma, a new strategy to induce senescence in melanoma cells. *Exp Dermatol* 22: 284-289.

41. Vandamme M, Robert E, Pesnel S, Barbosa E, Dozias S, et al. (2010) Antitumor Effect of Plasma Treatment on U87 Glioma Xenografts: Preliminary Results. *Plasma Processes and Polymers* 7: 264-273.
42. Brulle L, Vandamme M, Ries D, Martel E, Robert E, et al. (2012) Effects of a non thermal plasma treatment alone or in combination with gemcitabine in a MIA PaCa2-luc orthotopic pancreatic carcinoma model. *PLoS One* 7: e52653.
43. Walk RM, Snyder JA, Srinivasan P, Kirsch J, Diaz SO, et al. (2013) Cold atmospheric plasma for the ablative treatment of neuroblastoma. *J Pediatr Surg* 48: 67-73.
44. Dolecek TA, Propp JM, Stroup NE, Kruchko C (2012) CBTRUS statistical report: primary brain and central nervous system tumors diagnosed in the United States in 2005-2009. *Neuro Oncol* 14 Suppl 5: v1-49.
45. Louis DN, Ohgaki H, Wiestler OD, Cavenee WK, Burger PC, et al. (2007) The 2007 WHO classification of tumours of the central nervous system. *Acta Neuropathol* 114: 97-109.
46. Schwartzbaum JA, Fisher JL, Aldape KD, Wrensch M (2006) Epidemiology and molecular pathology of glioma. *Nat Clin Pract Neurol* 2: 494-503; quiz 491 p following 516.
47. Stupp R, Hegi ME, Mason WP, van den Bent MJ, Taphoorn MJ, et al. (2009) Effects of radiotherapy with concomitant and adjuvant temozolomide versus radiotherapy alone on survival in glioblastoma in a randomised phase III study: 5-year analysis of the EORTC-NCIC trial. *Lancet Oncol* 10: 459-466.
48. Ohgaki H, Kleihues P (2011) Genetic profile of astrocytic and oligodendroglial gliomas. *Brain Tumor Pathol* 28: 177-183.
49. Ohgaki H, Dessen P, Jourde B, Horstmann S, Nishikawa T, et al. (2004) Genetic pathways to glioblastoma: a population-based study. *Cancer Res* 64: 6892-6899.
50. Weller M (2011) Novel diagnostic and therapeutic approaches to malignant glioma. *Swiss Medical Weekly* 141.
51. Stupp R, Mason WP, van den Bent MJ, Weller M, Fisher B, et al. (2005) Radiotherapy plus concomitant and adjuvant temozolomide for glioblastoma. *N Engl J Med* 352: 987-996.
52. Hickman JA, Stevens MF, Gibson NW, Langdon SP, Fizames C, et al. (1985) Experimental antitumor activity against murine tumor model systems of 8-carbamoyl-3-(2-chloroethyl)imidazo[5,1-d]-1,2,3,5-tetrazin-4(3H)-one (mitozolomide), a novel broad-spectrum agent. *Cancer Res* 45: 3008-3013.
53. Stevens MF, Hickman JA, Langdon SP, Chubb D, Vickers L, et al. (1987) Antitumor activity and pharmacokinetics in mice of 8-carbamoyl-3-methyl-imidazo[5,1-d]-1,2,3,5-tetrazin-4(3H)-one (CCRG 81045; M & B 39831), a novel drug with potential as an alternative to dacarbazine. *Cancer Res* 47: 5846-5852.
54. Newlands ES, Blackledge GR, Slack JA, Rustin GJ, Smith DB, et al. (1992) Phase I trial of temozolomide (CCRG 81045; M&B 39831; NSC 362856). *Br J Cancer* 65: 287-291.
55. Karran P, Macpherson P, Ceccotti S, Dogliotti E, Griffin S, et al. (1993) O6-methylguanine residues elicit DNA repair synthesis by human cell extracts. *J Biol Chem* 268: 15878-15886.
56. Karran P, Bignami M (1994) DNA damage tolerance, mismatch repair and genome instability. *Bioessays* 16: 833-839.
57. Friedman HS, Kerby T, Calvert H (2000) Temozolomide and treatment of malignant glioma. *Clin Cancer Res* 6: 2585-2597.
58. Dumenco LL, Warman B, Hatzoglou M, Lim IK, Abboud SL, et al. (1989) Increase in nitrosourea resistance in mammalian cells by retrovirally mediated gene transfer of bacterial O6-alkylguanine-DNA alkyltransferase. *Cancer Res* 49: 6044-6051.
59. Tano K, Shiota S, Collier J, Foote RS, Mitra S (1990) Isolation and structural characterization of a cDNA clone encoding the human DNA repair protein for O6-alkylguanine. *Proc Natl Acad Sci U S A* 87: 686-690.

60. Jaeckle KA, Eyre HJ, Townsend JJ, Schulman S, Knudson HM, et al. (1998) Correlation of tumor O6 methylguanine-DNA methyltransferase levels with survival of malignant astrocytoma patients treated with bis-chloroethylnitrosourea: a Southwest Oncology Group study. *J Clin Oncol* 16: 3310-3315.
61. Esteller M, Garcia-Foncillas J, Andion E, Goodman SN, Hidalgo OF, et al. (2000) Inactivation of the DNA-repair gene MGMT and the clinical response of gliomas to alkylating agents. *N Engl J Med* 343: 1350-1354.
62. Hegi ME, Liu L, Herman JG, Stupp R, Wick W, et al. (2008) Correlation of O6-methylguanine methyltransferase (MGMT) promoter methylation with clinical outcomes in glioblastoma and clinical strategies to modulate MGMT activity. *J Clin Oncol* 26: 4189-4199.
63. Weller M, Felsberg J, Hartmann C, Berger H, Steinbach JP, et al. (2009) Molecular predictors of progression-free and overall survival in patients with newly diagnosed glioblastoma: a prospective translational study of the German Glioma Network. *J Clin Oncol* 27: 5743-5750.
64. Melguizo C, Prados J, Gonzalez B, Ortiz R, Concha A, et al. (2012) MGMT promoter methylation status and MGMT and CD133 immunohistochemical expression as prognostic markers in glioblastoma patients treated with temozolomide plus radiotherapy. *J Transl Med* 10: 250.
65. Weiler M, Hartmann C, Wiewrodt D, Herrlinger U, Gorlia T, et al. (2010) Chemoradiotherapy of newly diagnosed glioblastoma with intensified temozolomide. *Int J Radiat Oncol Biol Phys* 77: 670-676.
66. Gaspar N, Marshall L, Perryman L, Bax DA, Little SE, et al. (2010) MGMT-independent temozolomide resistance in pediatric glioblastoma cells associated with a PI3-kinase-mediated HOX/stem cell gene signature. *Cancer Res* 70: 9243-9252.
67. Mirimanoff RO, Gorlia T, Mason W, Van den Bent MJ, Kortmann RD, et al. (2006) Radiotherapy and temozolomide for newly diagnosed glioblastoma: recursive partitioning analysis of the EORTC 26981/22981-NCIC CE3 phase III randomized trial. *J Clin Oncol* 24: 2563-2569.
68. Felsberg J, Thon N, Eigenbrod S, Hentschel B, Sabel MC, et al. (2011) Promoter methylation and expression of MGMT and the DNA mismatch repair genes MLH1, MSH2, MSH6 and PMS2 in paired primary and recurrent glioblastomas. *Int J Cancer* 129: 659-670.
69. Brandes AA, Franceschi E, Tosoni A, Bartolini S, Bacci A, et al. (2010) O(6)-methylguanine DNA-methyltransferase methylation status can change between first surgery for newly diagnosed glioblastoma and second surgery for recurrence: clinical implications. *Neuro Oncol* 12: 283-288.
70. Beier D, Schriefer B, Brawanski K, Hau P, Weis J, et al. (2012) Efficacy of clinically relevant temozolomide dosing schemes in glioblastoma cancer stem cell lines. *J Neurooncol* 109: 45-52.
71. Dahlrot RH, Hermansen SK, Hansen S, Kristensen BW (2013) What is the clinical value of cancer stem cell markers in gliomas? *Int J Clin Exp Pathol* 6: 334-348.
72. Ishii N, Maier D, Merlo A, Tada M, Sawamura Y, et al. (1999) Frequent co-alterations of TP53, p16/CDKN2A, p14ARF, PTEN tumor suppressor genes in human glioma cell lines. *Brain Pathol* 9: 469-479.
73. Ponten J, Macintyre EH (1968) Long term culture of normal and neoplastic human glia. *Acta Pathol Microbiol Scand* 74: 465-486.
74. Stein GH (1979) T98G: an anchorage-independent human tumor cell line that exhibits stationary phase G1 arrest in vitro. *J Cell Physiol* 99: 43-54.
75. Heins N, Malatesta P, Cecconi F, Nakafuku M, Tucker KL, et al. (2002) Glial cells generate neurons: the role of the transcription factor Pax6. *Nat Neurosci* 5: 308-315.
76. Silber JR, Bobola MS, Blank A, Chamberlain MC (2012) O(6)-methylguanine-DNA methyltransferase in glioma therapy: promise and problems. *Biochim Biophys Acta* 1826: 71-82.
77. Stoffels E, Roks AJM, Deelmm LE (2008) Delayed effects of cold atmospheric plasma on vascular cells. *Plasma Processes and Polymers* 5: 599-605.
78. Kieft IE, Broers JLV, Caubet-Hilloutou V, Slaaf DW, Ramaekers FCS, et al. (2004) Electric discharge plasmas influence attachment of cultured CHO k1 cells. *Bioelectromagnetics* 25: 362-368.

79. Yonson S, Coulombe S, Leveille V, Leask RL (2006) Cell treatment and surface functionalization using a miniature atmospheric pressure glow discharge plasma torch. *Journal of Physics D-Applied Physics* 39: 3508-3513.
80. Kim GJ, Kim W, Kim KT, Lee JK (2010) DNA damage and mitochondria dysfunction in cell apoptosis induced by nonthermal air plasma. *Appl Phys Lett* 96.
81. Yamazaki H, Ohshima T, Tsubota Y, Yamaguchi H, Jayawardena JA, et al. (2011) Microbicidal activities of low frequency atmospheric pressure plasma jets on oral pathogens. *Dental Materials Journal* 30: 384-391.
82. Nosenko T, Shimizu T, Morfill GE (2009) Designing plasmas for chronic wound disinfection. *New Journal of Physics* 11.
83. Staehelin J, Buhler RE, Hoigne J (1984) Ozone Decomposition in Water Studied by Pulse-Radiolysis .2. Oh and Ho4 as Chain Intermediates. *Journal of Physical Chemistry* 88: 5999-6004.
84. Martindale JL, Holbrook NJ (2002) Cellular response to oxidative stress: signaling for suicide and survival. *J Cell Physiol* 192: 1-15.
85. Bedard K, Krause KH (2007) The NOX family of ROS-generating NADPH oxidases: physiology and pathophysiology. *Physiol Rev* 87: 245-313.
86. Jackson AL, Loeb LA (2001) The contribution of endogenous sources of DNA damage to the multiple mutations in cancer. *Mutat Res* 477: 7-21.
87. Vandamme M, Robert E, Lerondel S, Pouvesle JM, Le Pape A (2012) [Non thermal plasmas, a new strategy in oncology?]. *Med Sci (Paris)* 28: 154-156.
88. Hegi ME, Diserens AC, Gorlia T, Hamou MF, de Tribolet N, et al. (2005) MGMT gene silencing and benefit from temozolomide in glioblastoma. *N Engl J Med* 352: 997-1003.
89. Kim JY, Wei Y, Li J, Kim SO (2010) 15- μ m-sized single-cellular-level and cell-manipulatable microplasma jet in cancer therapies. *Biosens Bioelectron* 26: 555-559.
90. Chalmers AJ, Ruff EM, Martindale C, Lovegrove N, Short SC (2009) Cytotoxic effects of temozolomide and radiation are additive- and schedule-dependent. *Int J Radiat Oncol Biol Phys* 75: 1511-1519.
91. Schafer A, Teufel J, Ringel F, Bettstetter M, Hoepner I, et al. (2012) Aldehyde dehydrogenase 1A1--a new mediator of resistance to temozolomide in glioblastoma. *Neuro Oncol* 14: 1452-1464.
92. Hirose Y, Berger MS, Pieper RO (2001) Abrogation of the Chk1-mediated G(2) checkpoint pathway potentiates temozolomide-induced toxicity in a p53-independent manner in human glioblastoma cells. *Cancer Res* 61: 5843-5849.
93. Hirose Y, Berger MS, Pieper RO (2001) p53 effects both the duration of G2/M arrest and the fate of temozolomide-treated human glioblastoma cells. *Cancer Res* 61: 1957-1963.
94. Harris LC, Remack JS, Houghton PJ, Brent TP (1996) Wild-type p53 suppresses transcription of the human O6-methylguanine-DNA methyltransferase gene. *Cancer Res* 56: 2029-2032.
95. Srivenugopal KS, Shou J, Mullapudi SR, Lang FF, Jr., Rao JS, et al. (2001) Enforced expression of wild-type p53 curtails the transcription of the O(6)-methylguanine-DNA methyltransferase gene in human tumor cells and enhances their sensitivity to alkylating agents. *Clin Cancer Res* 7: 1398-1409.
96. Vandamme M, Robert E, Dozias S, Sobilo J, Lerondel S, et al. (2011) Response of Human Glioma U87 Xenografted on Mice to Non Thermal Plasma Treatment. 1: 27-43.
97. Lefranc F, Brotchi J, Kiss R (2005) Possible future issues in the treatment of glioblastomas: special emphasis on cell migration and the resistance of migrating glioblastoma cells to apoptosis. *J Clin Oncol* 23: 2411-2422.
98. Hoentsch M, von Woedtke T, Weltmann KD, Nebe JB (2012) Time-dependent effects of low-temperature atmospheric-pressure argon plasma on epithelial cell attachment, viability and tight junction formation in vitro. *Journal of Physics D-Applied Physics* 45.
99. Stoffels E, Kieft IE, Sladek REJ (2003) Superficial treatment of mammalian cells using plasma needle. *Journal of Physics D-Applied Physics* 36: 2908-2913.

100. Stoffels E, Kieft IE, Sladek REJ, van den Bedem LJM, van der Laan EP, et al. (2006) Plasma needle for in vivo medical treatment: recent developments and perspectives. *Plasma Sources Science & Technology* 15: S169-S180.
101. Ostermann S, Csajka C, Buclin T, Leyvraz S, Lejeune F, et al. (2004) Plasma and cerebrospinal fluid population pharmacokinetics of temozolomide in malignant glioma patients. *Clin Cancer Res* 10: 3728-3736.
102. Portnow J, Badie B, Chen M, Liu A, Blanchard S, et al. (2009) The neuropharmacokinetics of temozolomide in patients with resectable brain tumors: potential implications for the current approach to chemoradiation. *Clin Cancer Res* 15: 7092-7098.
103. Mihaliak AM, Gilbert CA, Li L, Daou MC, Moser RP, et al. (2010) Clinically relevant doses of chemotherapy agents reversibly block formation of glioblastoma neurospheres. *Cancer Lett* 296: 168-177.
104. Hermisson M, Klumpp A, Wick W, Wischhusen J, Nagel G, et al. (2006) O6-methylguanine DNA methyltransferase and p53 status predict temozolomide sensitivity in human malignant glioma cells. *J Neurochem* 96: 766-776.
105. van Rijn J, Heimans JJ, van den Berg J, van der Valk P, Slotman BJ (2000) Survival of human glioma cells treated with various combination of temozolomide and X-rays. *Int J Radiat Oncol Biol Phys* 47: 779-784.
106. Laval F, Wink DA (1994) Inhibition by nitric oxide of the repair protein, O6-methylguanine-DNA-methyltransferase. *Carcinogenesis* 15: 443-447.
107. Georgescu N, Lupu AR (2010) Tumoral and Normal Cells Treatment With High-Voltage Pulsed Cold Atmospheric Plasma Jets. *Ieee Transactions on Plasma Science* 38: 1949-1955.
108. Zucker SN, Zirnheld J, Bagati A, Disanto TM, Des Soye B, et al. (2012) Preferential induction of apoptotic cell death in melanoma cells as compared with normal keratinocytes using a non-thermal plasma torch. *Cancer Biol Ther* 13: 1299-1306.
109. Iseki S, Nakamura K, Hayashi M, Tanaka H, Kondo H, et al. (2012) Selective killing of ovarian cancer cells through induction of apoptosis by nonequilibrium atmospheric pressure plasma. *Appl Phys Lett* 100.
110. Pangom K, Baik KY, Nam MK, Han JH, Rhim H, et al. (2013) Preferential killing of human lung cancer cell lines with mitochondrial dysfunction by nonthermal dielectric barrier discharge plasma. *Cell Death & Disease* 4.
111. Kaushik NK, Attri P, Kaushik N, Choi EH (2013) A Preliminary Study of the Effect of DBD Plasma and Osmolytes on T98G Brain Cancer and HEK Non-Malignant Cells. *Molecules* 18: 4917-4928.
112. Babaeva NY, Kushner MJ (2010) Intracellular electric fields produced by dielectric barrier discharge treatment of skin. *Journal of Physics D-Applied Physics* 43.
113. de Bouard S, Christov C, Guillamo JS, Kassab-Duchossoy L, Palfi S, et al. (2002) Invasion of human glioma biopsy specimens in cultures of rodent brain slices: a quantitative analysis. *J Neurosurg* 97: 169-176.
114. Ohnishi T, Matsumura H, Izumoto S, Hiraga S, Hayakawa T (1998) A novel model of glioma cell invasion using organotypic brain slice culture. *Cancer Res* 58: 2935-2940.
115. Ashwell S, Zabudoff S (2008) DNA damage detection and repair pathways--recent advances with inhibitors of checkpoint kinases in cancer therapy. *Clin Cancer Res* 14: 4032-4037.
116. Yamaura M, Mitsushita J, Furuta S, Kuniwa Y, Ashida A, et al. (2009) NADPH oxidase 4 contributes to transformation phenotype of melanoma cells by regulating G2-M cell cycle progression. *Cancer Res* 69: 2647-2654.
117. Boonstra J, Post JA (2004) Molecular events associated with reactive oxygen species and cell cycle progression in mammalian cells. *Gene* 337: 1-13.
118. Brisson M, Nguyen T, Wipf P, Joo B, Day BW, et al. (2005) Redox regulation of Cdc25B by cell-active quinolinediones. *Mol Pharmacol* 68: 1810-1820.

119. Kalghatgi S, Kelly CM, Cerchar E, Torabi B, Alekseev O, et al. (2011) Effects of non-thermal plasma on mammalian cells. *PLoS One* 6: e16270.
120. Lassen N, Pappa A, Black WJ, Jester JV, Day BJ, et al. (2006) Antioxidant function of corneal ALDH3A1 in cultured stromal fibroblasts. *Free Radic Biol Med* 41: 1459-1469.
121. Warburg O, Wind F, Negelein E (1927) The Metabolism of Tumors in the Body. *J Gen Physiol* 8: 519-530.
122. Vander Heiden MG, Cantley LC, Thompson CB (2009) Understanding the Warburg effect: the metabolic requirements of cell proliferation. *Science* 324: 1029-1033.
123. Oliva CR, Moellering DR, Gillespie GY, Griguer CE (2011) Acquisition of chemoresistance in gliomas is associated with increased mitochondrial coupling and decreased ROS production. *PLoS One* 6: e24665.
124. Kim GC, Kim GJ, Park SR, Jeon SM, Seo HJ, et al. (2009) Air plasma coupled with antibody-conjugated nanoparticles: a new weapon against cancer. *Journal of Physics D-Applied Physics* 42.
125. Leduc M, Guay D, Leask RL, Coulombe S (2009) Cell permeabilization using a non-thermal plasma. *New Journal of Physics* 11.
126. Kleinberg LR, Weingart J, Burger P, Carson K, Grossman SA, et al. (2004) Clinical course and pathologic findings after Gliadel and radiotherapy for newly diagnosed malignant glioma: implications for patient management. *Cancer Invest* 22: 1-9.

J. Abbreviations

ALDH1A1	Aldehyde dehydrogenase 1 A1
ATM	ataxia telangiectasia mutated
ATR	ATM and Rad3-related
BSA	Bovine serum albumin
bTSC	brain Tumor Stem Cells
CAP	Cold Atmospheric Plasma
CDK	Cyclin-dependent kinase
ChK1/ ChK2	cell cycle checkpoint kinase 1/ 2
DBD	Dielectric Barrier Discharge
DMSO	Dimethyl sulfoxide
DSB	double strand break
EGF	Epidermal Growth Factor
EGFR	Epidermal Growth Factor Receptor
ETC	Electron transport chain
FBS	Fetal Bovine Serum
FE-DBD	Floating Electrode DBD
GBM	Glioblastoma
GFAP	Glial fibrillary acidic protein
GFP	Green fluorescence protein
HE	Hämatoxylin-Eosin
HNE	4-Hydroxynonenal
HRP	Horse radish peroxidase
IDH1/2	Isocitrate dehydrogenase 1 and 2
LOH	Loss of heterozygosity
luc	Luciferase
MDA	malondialdehyde
MGMT	O-6-methylguanine-DNA methyltransferase
MMR	Mismatch repair
MTIC	MTIC (3-methyl-(triazen-1-yl) imidazole-4-carboxamide).

Abbreviations

MTT	(3-(4,5-Dimethylthiazol-2-yl)-2,5-diphenyltetrazolium bromide)
NAC	N-Acetyl-L-cysteine
O6-MG	O6-methylguanine
OSC	Organotypic slice culture
PARP1	Poly(ADP-ribose) polymerase 1
PBS	Phosphate buffered saline
PI	Propidiumiodid
PTEN	Phosphatase and tensin homolog
RNS	Reactive nitrogen species
RONs	Reactive oxygen and nitrogen species
ROS	Reactive oxygen species
SDS-PAGE	Sodium dodecyl sulfatepolyacrylamidegel electrophoresis
Ser	Serine
shRNA	short hairpin RNA
SMD	Surface Micro Discharge
SSB	single strand break
TMZ	Temozolomide
TP53	Tumor protein p53
TUNEL	Terminal deoxynucleotidyl transferase-mediated dUTP-biotin nick end labeling
Wt	Wild-type

K. List of publications

Ex vivo human skin experiments for the evaluation of safety of new cold atmospheric plasma devices

G. Isbary¹, J. Koeritzer¹, A. Mitra, Y.-F. Li, T. Shimizu, J. Schroeder, J. Schlegel, G.E. Morfill, W. Stolz, J.L. Zimmermann

¹ authors contributed equally

Clinical Plasma Medicine, June 2013

Restoration of Sensitivity in Chemo - Resistant Glioma Cells by Cold Atmospheric Plasma

J. Köritzer, V. Boxhammer, A. Schäfer, T. Shimizu, T.G. Klämpfl, Y.-F. Li, C. Welz, S. Schwenk-Zieger, G.E. Morfill, J.L. Zimmermann and J. Schlegel

PLoS ONE, May 2013

Investigation of the Mutagenic Potential of Cold Atmospheric Plasma at Bactericidal Dosages

V. Boxhammer, Y.-F. Li, J. Köritzer, T. Shimizu, T. Maisch, H. M. Thomas, J. Schlegel, G. E. Morfill and J. L. Zimmermann

Mutat Research, April 2013

Aldehyde dehydrogenase 1A1--a new mediator of resistance to temozolomide in glioblastoma

A. Schäfer, J. Teufel, F. Ringel, M. Bettstetter, I. Hoepner, M. Rasper, J. Gempt, J. Koeritzer, F. Schmidt-Graf, B. Meyer, C.P. Beier, J. Schlegel

Neuro-Oncology, December 2012

Bactericidal action of cold atmospheric plasma in solution

V. Boxhammer, G.E. Morfill, J.R. Jokipii, T. Shimizu, T.G. Klämpfl, Y.-F. Li, J. Köritzer, J. Schlegel and J.L. Zimmermann

New Journal of Physics, November 2012